ILMATIETEEN LAITOS
METEOROLOGISKA INSTITUTET
FINNISH METEOROLOGICAL INSTITUTE

140
CONTRIBUTIONS

CLIMATIC EFFECT OF LIGHT-ABSORBING IMPURITIES ON SNOW: EXPERIMENTAL AND FIELD OBSERVATIONS

JONAS SVENSSON

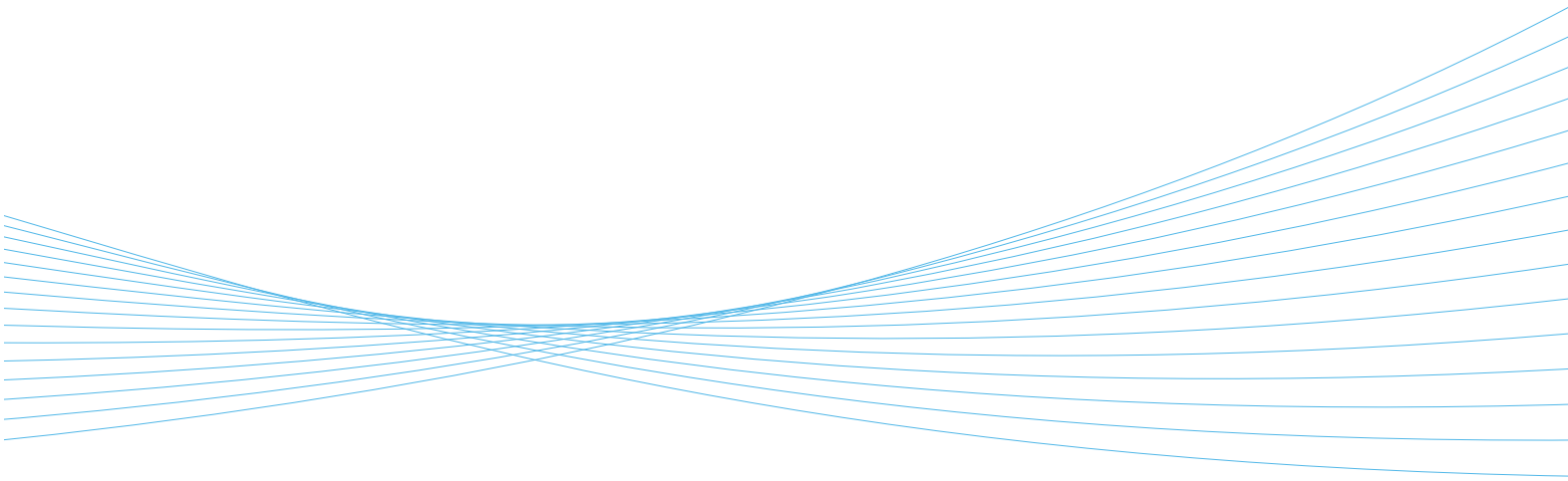

FINNISH METEOROLOGICAL INSTITUTE
CONTRIBUTIONS

No. 140

CLIMATIC EFFECT OF LIGHT-ABSORBING IMPURITIES ON SNOW: EXPERIMENTAL AND FIELD OBSERVATIONS

JONAS SVENSSON

Finnish Meteorological Institute
Helsinki, Finland

Doctoral Programme in Atmospheric Sciences
Department of Environmental Sciences
Faculty of Biological and Environmental Sciences
University of Helsinki, Finland

Academic Dissertation in Environmental Sciences
To be presented for public examination with the permission of the Faculty of Biological and Environmental Sciences of the University of Helsinki in the Auditorium Brainstorm at the Finnish Meteorological Institute, Helsinki, on December 8, 2017, at 12 o'clock noon.
Helsinki, 2017

Supervisors:	Professor Heikki Lihavainen, Ph.D. Atmospheric Composition Research Finnish Meteorological Institute, Helsinki, Finland
	Professor Atte Korhola, Ph.D. Environmental Change Research Unit, Department of Environmental Sciences, University of Helsinki, Finland
Thesis advisory committee:	Docent Aki Virkkula, Ph.D. Atmospheric Composition Research Finnish Meteorological Institute, Helsinki, Finland
	Professor Johan Ström, Ph.D. Atmospheric Science Unit, Department of Environmental Science and Analytical Chemistry, Stockholm University, Sweden
Pre-examiners:	Professor Jarkko Koskinen, Ph.D. Finnish Geospatial Research Institute, Masala, Finland
	Julia Schmale, Ph.D. Laboratory of Atmospheric Chemistry Paul Scherrer Institute, Villigen, Switzerland
Opponent:	Hans-Werner Jacobi, Research Director, Ph.D. Institute for Geosciences and Environmental Research, University Grenoble Alpes/CNRS/Grenoble INP/IRD, France
Custos:	Professor Pekka Kauppi, Ph.D. Department of Environmental Sciences, University of Helsinki, Finland

ISBN: 978-952-336-038-9 (paperback)
ISSN: 0782-6117
Erweko Oy
Helsinki 2017

ISBN: 978-952-336-039-6 (pdf)
http://ethesis.helsinki.fi
University of Helsinki, Unigrafia Oy
Helsinki 2017

FINNISH METEOROLOGICAL INSTITUTE

Published by	Finnish Meteorological Institute (Erik Palménin aukio 1), P.O. Box 503 FIN-00101 Helsinki, Finland	Series title, number and report code of publication Finnish Meteorological Institute Contributions 140
Author Jonas Svensson		Date November 2017

Title
Climatic effect of light-absorbing impurities on snow: experimental and field observations

Abstract
Snow and ice are essential components of the Earth system, modulating the energy budget by reflecting sunlight back into the atmosphere, and through its importance in the hydrological cycle by being a reservoir for fresh water. Light-absorbing impurities (LAI), such as black carbon (BC) and mineral dust (MD), have a unique role in influencing the reflectance of the cryosphere. Deposition of the anthropogenic and natural LAI constituents onto these bright surfaces initiates powerful albedo feedbacks that will accelerate melt. This is important globally, but especially for regions such as the Arctic and the Himalaya.
In this thesis, observations from both ambient and laboratory experiments are presented. The overarching research goal has been to better understand the climatic effect of LAI on snow. More specifically, an emphasis has been placed on exploring the process-level interactions between LAI and snow, which will enable better comprehension of LAI affecting the cryosphere.
Key findings in this thesis involves the investigations on the horizontal variability of BC concentrations in the surface snow that indicate a larger variability on the order of meter scale at a pristine Arctic site compared to a polluted site nearby a major urban area. In outdoor experiments, where LAI were used to artificially dope natural snow surfaces, the snow albedo was observed to decrease following LAI deposition. The albedo decrease was on the same order as in situ measurements of LAI and albedo conducted elsewhere. As snow melted during the experiment, the snow density was observed to decrease with increasing LAI concentration, while this effect was not observed in non-melting snow. The water retention capacity in melting snow is likely to be decreased by the presence of LAI. Measurements examining the absorption of BC indicate that BC particles in the snow have less absorbing potential compared to BC particles generated in the laboratory. The LAI content of snow pit investigations from two glaciers in the Sunderdhunga valley, northern India, an area not previously examined for LAI, presented high BC and MD content, affecting the radiative balance of the glacier snow. At different points, MD may be greater than BC in absorbing light at the snow surface. A continued monitoring of LAI in the cryosphere, both on the detailed scale explored here, as well as on the larger modelling perspective is needed in order to understand the overall response of the cryosphere to climate change.

Publishing unit
Atmospheric Composition Research

Classification (UDC)	Keywords
502.3/.7, 665.777.2, 613.32	Snow, light-absorbing impurities, black carbon, mineral dust, albedo, Arctic, Himalaya

ISSN and series title
0782-6117 Finnish Meteorological Institute Contributions

ISBN	Language	Pages
978-952-336-038-9 (paperback), 978-952-336-039-6 (pdf)	English	108

ACKNOWLEDGEMENTS

Diving into and exploring the world of science with this thesis has given me opportunities to work in some uniquely beautiful locations. From having the chance to experience a small portion of the majestic and humbling mountains of the Himalaya to the vast stillness of the Finnish north, I am most thankful.

Along this non-linear path leading up to this thesis I have been fortunate to have met some extraordinary people and some intellectual giants, all of which have shaped this thesis in one way or another. Here is a modest attempt at thanking some of you.

Since day one at FMI I have been supported by my supervisor Heikki, and not just scientifically, but also in many other areas. Having shared a tent with you at almost 5000 meters above sea-level a few times now in India I can say that it has been an interesting and fun ride. I have always been able to depend on you and your door has continually been open for discussions, thanks for everything. For my current research group leader, Eija, I also want to express gratitude for all of the support. Your positive attitude and enthusiasm around the office (and in the field) have been most encouraging and helpful.

From the University of Helsinki I thank Atte for taking me in as a PhD-student at a time when the bureaucracy seemed endless.

Aki, also known as the mad scientist of FMI, spreading soot all over the Arctic in the SoS experiments, I want to gratefully acknowledge. Your enthusiasm is contagious, and my work has greatly benefited from our various exchanges. Other SoS-members I want to thank for help and sticking with it. Outi, you have been most helpful with various things and several discussions with you have been very constructive for my work. Looking further in-house, I want to convey my appreciation to David, who assisted and guided me on so many things, especially in the beginning of my work, and that I today consider a good friend. In my mind, with your skills, a better man for the laboratory is hard to find, although nowadays you are mostly into UAVs. Antti, you were a great support in the beginning as well, and you brought me into the India AAFIG-project, which enabled me to venture back into what interests me most: studying glaciers. My office-mate, John, I also want to thank for numerous helpful discussions and positive encouragement. Other FMI colleagues, as well as the higher management I want to thank for shaping FMI into the respectable institute it is.

Other colleagues, Meri, I'm most glad that our paths crossed and to have worked with you. I believe you are a good scientist and hope to continue to work alongside you. At NPI, Elisabeth and J-C are acknowledged for fruitful collaboration (with some work on my end still left to be done). Back home in Sweden at SU I want to thank Johan for his expert tutelage. Your contribution to all of this is far from small. You are the one who got me into this whole mess in the first place. But, here we are, and since day one I have always appreciated our encouraging and stimulating exchanges. You have a way of making science interesting and simple. In case it has not been obvious, I have thoroughly enjoyed working with you and have learned a lot from you.

From my parents I have received the best of support. Det blev inte mycket till hockey karriär utan något helt annat. I vilket fall har jag alltid haft erat stöd och det är jag tacksam för, även om ett tack känns i underkant. Nu när jag själv har grabbarna hemma har jag fått en ny dimension av uppskattning till allt som ni gjort och ställt upp med under alla dessa år. My sons, Owen, Jasper, and Tobias are most entangled in this work. In a myriad of ways, you continually make me aware of what really matters. You are most incredible and I cannot wait to see the men you will become in the future. Don't you ever forget that I believe in you and that you have what it takes. To my amazing wife, Kate, who would have thought that we would be led here? Your sacrifice, support, and love is beyond my understanding. Without you I would not be here today. Grow old with me, the best is yet to be.

CONTENTS

LIST OF PUBLICATIONS

This thesis contains an introductory review, followed by four research articles. In the introductory part, the articles are referred to by their roman numerals. Papers I, III, and IV are reprinted under the Creative Commons License. Paper II is reproduced with permission from the publisher.

I Svensson, J., Ström, J., Hansson, M., Lihavainen, H., and Kerminen, V.-M.: Observed metre scale horizontal variability of elemental carbon in surface snow. Environmental Research Letters, 8, 034012, doi:10.1088/1748-9326/8/3/034012, 2013.

II Svensson, J., Virkkula, A., Meinander, O., Kivekäs, N., Hannula, H.-R., Järvinen, O., Peltoniemi, J.I., Gritsevich, M., Heikkilä, A., Kontu, A., Neitola, K., Brus, D., Dagsson-Waldhauserova, P., Anttila, K., Vehkamäki, M., Hienola, A., de Leeuw, G., and Lihavainen, H.: Soot-doped natural snow and its albedo — results from field experiments. Boreal Environment Research, 21, 481-503, 2016.

III Meinander, O., Kontu, A., Virkkula, A., Arola, A., Backman, L., Dagsson-Waldhauserová, P., Järvinen, O., Manninen, T., Svensson, J., de Leeuw, G., and Leppäranta, M.: Brief communication: Light-absorbing impurities can reduce the density of melting snow, The Cryosphere, 8, 991-995, doi:10.5194/tc-8-991-2014, 2014.

IV Svensson, J., Ström, J., Kivekäs, N., Dkhar, N. B., Tayal, S., Sharma, V. P., Jutila, A., Backman, J., Virkkula, A., Ruppel, M., Hyvärinen, A., Kontu, A., Hannula, H.-R., Leppäranta, M., Hooda, R. K., Korhola, A., Asmi, E., and Lihavainen, H.: Contribution of dust and elemental carbon to the reduction of snow albedo in the Indian Himalaya and the Finnish Arctic, Atmospheric Measurements Techniques Discussion, in review, 2017.

AUTHORS' CONTRIBUTION TO THE PUBLICATIONS

I J. Svensson planned the study with J. Ström and M. Hansson. J. Svensson conducted the field measurements and the laboratory analysis. The results were interpreted by J. Svensson with supervision from J. Ström and M. Hansson. The manuscript was written by J. Svensson with contributions from other coauthors.

II A. Virkkula led the experiments with input from others. J. Svensson participated in the field experiments and analyzed data. J. Svensson prepared the manuscript with contributions from coauthors.

III O. Meinander formed the hypothesis presented in the paper, and wrote the manuscript. J. Svensson participated in collection of experimental data and analyzing field data, and contributed to the writing of the manuscript.

IV J. Svensson planned the study with J. Ström. Laboratory and field measurements were mainly conducted by J. Svensson. The results were interpreted by J. Svensson with supervision from J. Ström and input from others. The writing of the manuscript was led by J. Svensson with contributions from coauthors.

ABBREVIATIONS

BC	Black Carbon
eBC	Equivalent Black Carbon
BrC	Brown Carbon
CC	Carbonate Carbon
CCN	Cloud Condensation Nuclei
EC	Elemental Carbon
FMI ARC	Finnish Meteorological Institute
GAW	Global Atmosphere Watch
GrIS	Greenland Ice Sheet
IN	Ice nuclei
ISSW	Integrating Sphere Integrating Sandwich Spectrophotometer
LAHM	Light-Absorption Heating Method
LAI	Light-Absorbing Impurities
MAC	Mass Absorption Cross Section
MD	Mineral Dust
NIR	Near-Infra Red Region
OC	Organic Carbon
PSAP	Particle Soot Absorption Photometer
rBC	Refractory Black Carbon
SP2	Single Particle Soot Photometer
SoS	Soot on Snow
SZA	Solar Zenith Angle
TOM	Thermal-Optical Method

1. INTRODUCTION

Snow and ice are vital components in the Earth's spheres, interacting closely with the atmosphere, hydrosphere, and the biosphere. If snow is accumulated over a longer time span and the accumulation exceeds melting, the snow transforms into ice and a glacier begins to form. Glaciers have reshaped the modern world throughout the geological timescale with great mass fluctuations during glacial and interglacial periods. Today, most of the globe's frozen water is stored at the poles. Referred to as the third pole, the Hindu Kush-Himalayan and Tibetan plateau contains the most snow and ice outside of the Arctic and Antarctica. The water stored in glacier reservoirs worldwide accounts for about 70% of Earth's freshwater. With the vast amount of fresh water stored in the cryosphere, melting plays an integral part in regulating the water cycle. Melted glacier ice contributes to the current sea-level rise, while also some regions risk increased potential of natural hazards, such as landslides and glacial lake outburst floods.

Snow and glacier meltwater at mid latitudes and equatorial regions (e.g. South and North America and south and central Asia) provide a crucial fresh water source, necessary for agriculture, hydropower, and public health in many nations (e.g. Barnett et al., 2005; Immerzel et al., 2010; Kaser et al., 2010; Bolch et al., 2012). Meltwater delivers water during periods of drought. Water availability is, however, currently at risk due to climatic shifts. Additional climate changes could further strain water availability by changing the quantity and timing of melt. Such added stress, in regions with preexisting severe water scarcity, has the potential to create political instability and population migrations. Glaciers respond to climatic changes either through increased or decreased glacier volume, leading to an advancing or retreating glacier, respectively. But, since glacier changes are delayed by flow dynamics, there is a time lag between climatic changes and the response at the glacier terminus. In a warming climate the glacier mass balance typically will be negative, but the glacier runoff will increase and downstream areas have increased water availability. On the other hand, a continued shrinking and negative mass balance will affect glacier volume and eventually lead to less meltwater becoming available. The interactions between climate, cryosphere, and hydrosphere are complex and show dissimilar patterns world-wide. Thus, different areas face divergent fates. While some regions will experience a decrease in meltwater availability, others will confront the opposite, with increased water availability, depending on the stage of glacier change (Ragettli et al., 2016).

Fresh snow is a medium that reflects solar radiation more effectively than any other natural surface. This attribute is fundamental for Earth's climate. Covering immense land and sea areas in the northern hemisphere during parts of the year, snow and ice have an essential role in modulating the surface reflectance of incoming solar radiation. In this regard, the term albedo is of importance: defined as the amount of reflecting light divided by the incoming light. For visible light, this fraction of reflected light can exceed 90% (Warren, 1982). The rate and timing of snow and ice melt in the northern hemisphere have an important climatic role since uncovered ground or sea will have a significantly lower albedo than snow. This is most significant in the spring when snow extent is at its maximum and is also exposed to high solar insolation (e.g. Hall and Qu, 2006; Flanner et al., 2011). In the Arctic, the northern hemisphere snow albedo feedback has been observed and reported to be partially responsible for the Arctic amplification, where recent warming has been more pronounced than elsewhere globally (e.g. Déry and Brown, 2007; Serreze et al., 2007; AMAP, 2011).

While temperature increase is the main global driver of melting snow and glaciers, additional processes are also important (e.g. Barnett et al., 2005). Albedo depends on several factors for snow, but the primary agents are snow grain size and the presence of light-absorbing impurities (LAI)

(Warren and Wiscombe, 1980). A collective term for particulates that absorb light, LAI includes insoluble organic carbon (OC), mineral dust (MD), and the broadly defined black carbon (BC). Both OC and BC are derived from the incomplete combustion of carbonaceous matter, while MD originates from the crustal surface of the Earth. The tiny particles can be transported in the atmosphere over long distances before they are deposited onto snow and ice. Of the different impurities, BC is the material with the strongest climatic warming potential.

Once LAI decrease the snow albedo, several processes are set into motion which eventually cause a greater negative climatic effect. Snow with a lower albedo increases the amount of solar radiation absorbed, thus trapping even more heat in the snow. Warmer temperatures facilitates more rapid snow aging and a subsequent snow grain growth (Wiscombe and Warren, 1980). In larger grained snow BC has a more pronounced negative effect on the albedo compared to smaller grains (Warren and Wiscombe, 1980; Hadley and Kirchstetter, 2012; Dang et al., 2015). This positive feedback supplies itself with faster snow aging with higher temperatures, further reducing the albedo. Ultimately, this leads to an earlier onset of snowpack melt, uncovering the underlying surface with a significantly lower albedo, further hastening snow melt. During snow melt, LAI have a tendency to remain at the surface (e.g. Conway et al., 1996; Xu et al., 2012; Doherty et al., 2013), further concentrating their warming potential towards the surface of the snow, contributing to additional lowering of the albedo and speeding up melt (Flanner et al., 2007). Diminishing snow cover and increased thawing further influences the exchange between atmosphere and the ground, as well as the microbiology.

The overarching objective of this thesis is to investigate LAI in snow through field measurements and laboratory experiments in order to better understand and constrain the climatic impacts of LAI in snow. For this thesis, BC is emphasized, but other constituents are evaluated as well. Per unit mass, BC is the material with the largest potential impact on snow albedo, but anthropogenic and natural LAI must be studied jointly for a complete understanding. Further, the research conducted in this thesis focuses on the upper layers of the snowpack, where the albedo reduction from LAI is most applicable. While the negative effects of LAI on the cryosphere are clear, additional measurements and experiments are still needed. Measurements are sparse in some regions, and many of the process-level dynamics remain unresolved. An increased understanding will enable the scientific community to better constrain the effect of LAI on snow albedo and melt. For this purpose, different specific small-scale measurements and experiments have been conducted. The aim of this thesis is to examine the following questions:

1. What is the variability of black carbon in surface snow on spatial scales on the order of meters, and is there any difference in variability between polluted and clean sites?

Addressed in Paper I, this detail of small scale variability appeared to be overlooked in the pre-existing literature, thus Paper I aimed at contributing to this lack of knowledge.

2. What are the microphysical and radiative properties of an artificially perturbed snow surface using black carbon as light-absorbing impurity?

Dedicated experiments examining the relationship between LAI and the physical and radiative properties of snow are very limited. This is studied in Papers II and III.

3. How will light-absorbing impurities deposited during early spring affect the microphysical properties of the snowpack during the melting season?

Since BC has a tendency to remain in the top layers of the snowpack, it was hypothesized in Paper III that BC could influence snow melting properties.

4. Is it possible to deconvolute a laboratory liquid-based mixture of mineral dust and black carbon based on their respective optical properties, and how do the optical properties of the laboratory sample particles compare to ambient snow sample particles?

The optical properties of BC in snow have an effect on absorption, and it has been suggested that BC may be less absorbing than current estimates. This subject is investigated in Paper IV.

5. What is the relative contribution of mineral dust and black carbon to the light absorption of impurities at the high altitude glacier snow surface in Sunderdhunga valley, Himalayan India, and how does this contribution compare to the snowpack of the Finnish Arctic?

The current cryospheric changes occurring in the Himalaya are complex, and the role of the different LAI need to be scrutinized through measurements (e.g. Gertler et al., 2016). This is investigated in Paper IV.

2. BACKGROUND

2.1 Snow and interaction with radiation

Snowmelt is a product of the heat exchange between the snow and its surrounding environment. At the snow surface, temperature and the absorption of shortwave radiation mainly controls melt. Absorption depends on the incident radiation and the albedo. The albedo varies greatly with wavelength over the solar spectrum and depends on the physical properties of snow, such as grain size, depth, density, liquid water content, LAI, as well as cloud cover, and solar zenith angle (SZA) (Warren and Wiscombe, 1980). In the visible light spectra solar irradiance peak at the Earth's surface (most energy), and snow scatters visible light very efficiently and is basically non-absorptive. The deposition of nearly all aerosols on a snowpack therefore, apart from sulfate and sea-salt, will absorb sunlight producing a positive radiative forcing. In the near infra-red region (NIR), however, the effect of impurities is negligible as snow is dark and practically black, and the albedo is more sensitive to snow grain size (Warren, 1982). With time snow grains metamorphose, resulting in larger grains, enabling photons to travel deeper into the snowpack (Colbeck, 1982). With deeper penetration the photons are more likely to encounter a LAI, accounting for the greater negative effect LAI have in larger snow grains (Warren and Wiscombe, 1980; Hadley and Kirchstetter, 2012; Dang et al., 2015). The spectral properties of the snowpack have been used to deduce information about the surface properties using remote sensing techniques (e.g. Nolin and Dozier, 2000).

2.2 Light-absorbing impurities in snow

2.2.1 Carbonaceous aerosol

Aerosols refer to particles consisting of liquids or solids suspended in a gas. In the atmosphere, aerosols exists as a diverse combination of particles with different shapes, sizes, and chemical compositions. On an individual basis, a single particle can further consist of different constituents, with varying shapes and forms. Primary particles are directly emitted into the atmosphere, while secondary particles are formed in the atmosphere through gas to particle conversion. Emission sources for both types of aerosol can be either anthropogenic or natural, or a combination of both. An aerosol population usually encompass a wide size range, as aerosols exists in the range from a few nm up to tens of µm. The chemical and physical properties of an aerosol governs its interaction with surrounding media. Once in the atmosphere, the particles interact with light through reflection and absorption, contributing to what is known as the direct climate effect of aerosols. Aerosols also act as seeds to form cloud particles, so called cloud condensation nuclei (CCN) or ice nuclei (IN)

(Andreae and Rosenfeld, 2008). By altering the amount or properties of these nuclei particles, the microphysical properties of clouds may be perturbed. This may modify the optical properties or lifetime of clouds, known as the indirect climate effect of aerosols (Rosenfeld, 2000).

One aerosol species with a special relevance to the climatic impact of aerosols is the broadly defined BC. Black by nature, BC is the aerosol with the greatest absorption of light per unit mass. On a global scale, BC is estimated as second only to carbon dioxide as a climate warming agent (Jacobson, 2001; Hansen and Nazarenko, 2004; Ramanathan and Carmichael, 2008; Bond et al., 2013). It is produced during the combustion of carbon-based materials, largely fossil fuels and biomass burning. Depending on the specific carbon fuel used, temperature and pressure where the combustion occurs, an array of different particles produced can be classified as BC (Andreae and Gelencsér, 2006; Bond and Bergström, 2006; Bond et al., 2013; Petzold et al., 2013). Quantifying and characterizing the variety of BC particles is, therefore, not straightforward. The ideal analytical technique would determine several different properties of the particles simultaneously; currently this is not possible with a single instrument. As a consequence, different properties of BC are operationally defined dependent on measuring technique. Using the atmospheric research terminology, the different operational definitions proposed by Petzold et al. (2013) are: elemental carbon (EC) referring to methods that specifically measure carbon content of carbonaceous matter; refractory BC (rBC) is measured with incandescence methods; equivalent BC (eBC) when an optical absorption method has been used. Further, the term soot, refers to the process by which the particles are formed.

Black carbon does not only enhance climate warming, but is also detrimental to air quality and human health. Exposure to particles has been proven to have harmful health effects on humans (e.g. Janssen et al., 2011; Shindell et al., 2012). Determining emission sources and temporal variability of BC is therefore crucial from both a climate mitigation and air quality standpoint. Currently, global emissions estimates indicate an increasing trend, most probably due to expanding economies in Asian countries, whereas most other regions globally are decreasing their emissions (Bond et al., 2013). After a BC particle has been emitted it usually is hydrophobic (repels water molecules), but will rather quickly interact with other particles and condensable vapors to form a hydrophilic state (onto which water can adhere) (e.g. Jiao et al., 2014). Aerosol particulate mass has an average atmospheric residence time of one week in the lower troposphere, before it is scavenged, either through wet or dry deposition possibly far from its original emission source (Raes et al., 2000). Falling snowflakes are very efficient in scavenging aerosols (Paramonov et al., 2011). Microscopic studies of snowflakes have found thousands of aerosol particles inside or attached to snowflakes in Japan, and a large fraction of the aerosols were believed to be of carbonaceous origin (Magono et al., 1979). In instances when BC particles are mixed and rise to high altitudes their lifetime may be prolonged, which can transport them globally (Stohl, 2006). An aerosol co-emitted with BC during combustion and mainly biomass burning is OC, which may or may not absorb light. It is defined as brown carbon (BrC) when it absorbs light in the shorter wavelength ranges (Andreae and Gelencsér, 2006).

The mass absorption cross section (MAC) describes the efficiency by which aerosol particles absorb light. It is the light absorption coefficient divided by the mass concentration of the particles, usually expressed in $m^2\ g^{-1}$ (e.g. Seinfeld and Pandis, 2006; Moosmüller et al., 2009). This value depends mainly on the size of the particles. For airborne BC particles, MAC commonly has higher values for smaller particles (up to 100 nm), with a peaking MAC value in the range 100-200 nm, after which there is a sharp drop off in MAC with BC particle size (greater than 300 nm). This relates to smaller particles being volume absorbers of light, while the absorption of light not penetrating to the

core of the particle for larger particles. Measurements of MAC have been studied in detail in atmospheric aerosols (e.g. see review of Moosmüller et al., 2009), whereas the absorptivity of BC in snow is largely unresolved. Recently, an attempt was made to quantify LAI absorption in the seasonal snow of northern China, with the particulates collected on Nuclepore filters. This study made extensive use of the spectral response of different substances (Zhou et al., 2017). This method relied on filter techniques, which may cause different optical properties in ambient snow compared to filters conditions. Thus, the MAC inferred from filters may not accurately reflect values in snow conditions.

2.2.2 Mineral dust and other light-absorbing impurities

While BC is the particle with the most light-absorbing potential by mass in snow, other impurities existing in the snow also contribute to an albedo reduction and enhanced melt. The extent to which the impurity influence the snow is dependent of its absorptivity and concentration. Although the specific absorption by MD is less than BC, given enough MD concentration, the two can be of equal magnitude. Spectrally, the albedo reduction from BC is the greatest in the visible spectrum, while MD have a greater decrease in the Ultraviolet (UV) range (Warren and Wiscombe, 1980). Particles associated with MD originate from semi-arid regions where the soil is easily eroded and sparse vegetation can contain the particles from being suspended into the atmosphere. For global atmospheric aerosol mass and aerosol optical depth MD accounts for one of the most significant fractions (Tegen et al., 1997). It has the potential to be transported over great distances before depositing at Earth's surface and act as an important nutrient in the tropical rain forest, or perturb snow surfaces at the poles or even the Himalayas. Globally, there exists many areas that supply the atmosphere with MD, thus there are many different species of MD found world-wide in mixed variations in snowpacks and glaciers.

The significance of MD affecting snow albedo and melt has been investigated for some regions globally. It has been most extensively studied in the snowpacks of western United States, where it has been identified as the dominating LAI, shortening the duration of snow cover by weeks, as well as shifting the timing and intensity of runoff (e.g. Painter et al., 2007; Painter et al., 2010). In the Nepalese Himalaya, snow pit observations have shown that MD sometimes appear in such concentrations that it may be a greater than BC in disturbing snow albedo of Mera glacier (Kaspari et al., 2014). Likewise, glaciers of the European Alps have shown to be affected by MD originating from the Saharan desert (e.g. Lavanchy et al., 1999; Di Mauro et al., 2015; Gabbi et al., 2015). In the Arctic, Doherty et al. (2010) points out that 20-50 % of the light absorption by LAI in the seasonal snowpack is due to non-BC particles, although part of the fraction also includes BrC. Icelandic MD has been identified as a large source for the Arctic cryospehere (Meinander et al., 2016 and references therein), with the possibility of being distributed to the Greenland Ice Sheet (GrIS) (Groot Zwaaftink et al., 2016).

The term cryoconite is defined as granular sediment consisting of mineral and biological matter (Cook et al., 2015). Dark in appearance, cryoconite absorbs solar radiation, and is usually visible in centimeter deep meltwater holes on glacier and ice sheets world-wide. The role of microbiology and snow algae affecting snow albedo has recently been highlighted through measurements (e.g. Takeuchi et al., 2006; Lutz et al., 2014), and it appears that it can be significant for some regions. In the Arctic, for example, Lutz et al. (2016) estimated that 13% of the snow albedo decrease over one melt season was due to snow algae blooms.

2.2.3 Studies of light-absorbing impurities in snow

The effect of LAI on snow albedo was first outlined in detail through the modelling work of Warren and Wiscombe (1980). The work is based on Wiscombe and Warren (1980), where snow

reflectance modelling was over-estimated in the visible spectrum compared to observations. By incorporating small concentrations of LAI in the modelling, the model-measurement bias was eliminated (Warren and Wiscombe, 1980). More contemporary work, include the work of Hansen and Nazarenko (2004), which further raised awareness on BC in snow, by arguing that BC in snow may be responsible for 25% of the observed global warming. Additionally highlighted in Flanner et al. (2007), world-wide simulations showed the third pole as especially vulnerable, with an exceptionally high radiative forcing due to high deposition of LAI in snow.

To measure BC in snow with remote sensing techniques has been shown to be difficult, with surface properties introducing noise on the same magnitude as the actual BC reduction on albedo, making attribution of BC on albedo difficult (Warren, 2013). In-field measurements are therefore a crucial component of studying LAI effect on snow. The observational record of LAI in snow actually dates back prior to the remote sensing era. During the age of polar exploration, over a century ago, explorers such as Nordenskiöld and Nansen made the first recorded observations of impurities (Nordenskiöld actually first used the term cryoconite) in snow and ice on the GrIS. The modern day observational research on LAI in snow was outlined in the work of Clarke and Noone (1985). In their study concentrations of LAI in snow of the North American and European Arctic were found to be substantial enough to perturb the radiative balance of the snowpack. The spatial coverage was further updated in Doherty et al. (2010), extending with samples from many locations across the Arctic. This large spatial variability of BC in snow survey indicated that Greenland snow had the lowest concentrations, while the highest concentrations were in northeastern Siberia.

Spatial studies are good to obtain an overview representation of typical BC mixing ratios that can be observed on a large scale. However, it makes comparison difficult temporally since details concerning recent snowing and deposition of BC events are lost, which can have a large impact on the BC mixing ratios locally. For this purpose, ice cores are environmental archives that can provide deposition trends of LAI, even including pre-industrial times. In the Arctic the few existing records have indicated a peak in BC around 1910, coinciding with the period of industrialization (McConnell et al., 2007; Keegan et al., 2014; Ruppel et al., 2014). Since the 1970s, though, contrasting patterns for BC deposition has been observed (Ruppel et al., 2014). In the recent year of 2012, when the GrIS experienced exceptional wide-spread melt, BC has been suggested as significant contributor to this unusual melt (Keegan et al., 2014). The extent to which BC, as well as other LAI, is affecting the current albedo decay and melt increase of the GrIS is debated and complicated by many involved parameters and processes (e.g. Box et al., 2012; Dumont et al., 2014; Polachenski et al., 2015; Tedesco et al., 2016).

Long term records of LAI in snow from the Himalaya are also rather limited. The few records to-date have indicated contrasting patterns on the temporal progress of LAI in snow (e.g. Ming et al., 2008; Xu et al., 2009; Kaspari et al., 2011; Ginot et al., 2014; Jenkins et al., 2016). Snow pit studies investigating LAI, covering possibly a few annual deposition years, on the other hand, have provided spatial coverage of LAI in snow on the third pole (e.g. Xu et al., 2006, Ming et al., 2009; Kaspari et al., 2014; Jacobi et al., 2015; Yang et al., 2015; Li et al., 2016; Schmale et al., 2017). Most studies have shown an enriching of LAI at certain layers and that the LAI content decreases with altitude. The more recent work (e.g. studies of Li et al. and Schmale et al.) includes source apportionment, which provide indications on the origin sources for BC. Additionally, crude estimates on glacier melt from the LAI in the snow has been made (in Kaspari et al. and Schmale et al.). Contrasting patterns in the dominating impurity for albedo reduction has also been estimated, with MD in Nepal (Kaspari et al., 2014), while BC is more governing the snow albedo in central Asia and parts of Tibet (Schmale et al., 2017; Li et al., 2017).

Our current understanding of the effects of LAI on snow is largely based on models. Field experiments can help to better understand the interaction between LAI and snow. For BC on snow this has been done in outdoor conditions (Conway et al., 1996; Brandt et al., 2011), and in laboratory conditions (Hadley and Kirchstetter, 2012). In Conway et al. (1996) BC particles mixed in snow were spread over glacier snow surfaces in Washington State, U.S. followed by monitoring of the subsequent changes, with an emphasis on the movement of LAI within the snow with melt. In another outdoor experiment, artificial snow was produced with a snow-gun while BC was mixed with the freezing water (Brandt et al., 2011). With a highly contaminated snow this experiment confirmed radiative transfer calculations of the negative effect of BC on snow albedo. In a laboratory-based experiment Hadley and Kirchstetter (2012) showed that with increasing snow grain size the negative effect of BC on albedo was enhanced, compared to model predictions.

More detailed observations, on a process level in the snow, have suggested that BC particles have a tendency to be larger sized in snow compare to air (Schwarz et al., 2013). Information on the size of the particles is crucial for the absorptivity and the MAC of the BC. It also seems as if the larger airborne BC particles are more efficiently removed by precipitation (Schwarz et al., 2013; Mori et al., 2016). Once in the snow, the particle size appears to be further affected, with growth due to melt-freezing activities in the snow (Schwarz et al., 2013).

2.2.4 Measurement methods of light-absorbing impurities in snow

To measure all of the different LAI constituents in snow can be a complex task that requires more than one analytical technique. Ambient measurements are further challenged by the fact that the snow samples should be in a frozen state prior to analysis to avoid contamination (growth of biological material) or uncontrolled losses of particles. Maintaining the samples frozen is particularly challenging when snow samples are collected in remote environments, which they often are. Traditionally, as with airborne aerosols, LAI in snow have been collected on filters through filtering of melted samples. This approach eliminates the challenge of maintaining the sample frozen, since filtering can be done in field-like conditions. The filters can thereafter be analyzed optically, which has been done using an integrating sphere integrating sandwich spectrophotometer (ISSW) (Doherty et al., 2010; Grenfell et al., 2011). Using this measurement set-up an optical spectral absorption by impurities on the filter is obtained. It is not specific to the different constituents, instead it requires an interpretation of the spectral response. Another, less utilized method to analyze filters is the light absorption heating method (LAHM). It consists of exposing the particle-laden filters to visible light and measuring their absorptive response by monitoring the particle temperature increase, and has been used in the Andes of Peru (Schmitt et al., 2015). Another analysis technique for filters involves the thermal-optical method (TOM) (e.g. Forsström et al., 2009; Hagler et al., 2007; Cachier et al., 1989), and it is based on the different volatilization temperatures for different carbon species (OC and EC).

There is one existing non-filter based method, and it uses laser-induced incandescence of particles. The instrument used is the single particle soot photometer (SP2), (not explored in this thesis) which was originally made for atmospheric aerosols measurements. Particles contained in melted snow samples are needed to be aerosolized with a nebulizer before detection with the instrument, introducing uncertainties with this method (e.g. Schwarz et al., 2012). Nevertheless, the SP2 can provide actual size estimates of the BC particles, which is of great benefit for accurately calculating the absorption, and consequently, the radiative forcing in the snow.

Traditionally MD in snow has been measured by weighing filters before and after liquid samples has been filtered, applicable in regions where dust is believed to be the dominating LAI in

the snow occurring in higher concentrations (e.g. Aoki et al., 2006; Painter et al., 2012). Microscopy has also been used (Thevenon et al., 2009), as well as microparticle counters (Ginot et al., 2014) and mass spectrometry (Kaspari et al., 2014).

3. RESEARCH AREAS AND METHODOLOGY

3.1 Research areas

The geographical areas of research in this thesis consisted of different sites in Fennoscandia, resulting in the basis of the data for Paper I, III, IV, and the Indian Himalaya, constituting the data for Paper IV. Each site is characterized by different demographics and climatology, thus setting the stage for different investigations on LAI in snow. The Arctic and the Himalaya are two areas where LAI have been identified as having crucial roles in affecting the cryosphere (e.g. Hansen and Nazarenko, 2004; Flanner et al., 2007; Xu et al., 2009). Experimental campaigns in outdoor conditions on the seasonal snowpack at different locations in Finland are another part of this thesis, contributing with the measurements in Paper II and III.

3.1.1 Pallas and Sodankylä, Finland

The measurements originating from northern Finland are in the vicinity of the Pallas-Sodankylä Global Atmosphere Watch (GAW) station. Consisting of two main sites; the Pallas Atmosphere-Ecosystem Supersite and the Finnish Meteorological Institute's Arctic Research Centre in Sodankylä (FMI ARC). The former is located in northwestern Finland inside the Pallas-Yllästunturi national park, and the latter is situated 120 km southeast of Pallas. Both are north of the Arctic Circle. Snow samples from Pallas, used in Paper I and IV, were collected above the tree line in close proximity to the atmospheric measurement station that is positioned on top of the small fell, Sammaltunturi. Local emissions are minimal, but some influence from regional and long range transported particles exists. The snow at Pallas and Sodankylä is characterized as the northern boreal forest zone with a typical taiga snow type. Typically, snow cover lasts for about 200 days in the year (Oct-May), with maximum snow depth around 80-100 cm. At Sodankylä, weekly surface snow samples for LAI content have been collected since 2009. Parts of this data set has been used in this thesis. Sodankylä was also one of the experimental sites in the soot on snow (SoS) experiments, further explained in section 3.2. The snow at Sodankylä was investigated for Papers II, III, and IV.

3.1.2 Tyresta, Sweden

The Tyresta sampling site is located in Tyresta national park, about 25 km south-west of Stockholm, Sweden. With its close proximity to metropolitan Stockholm, and significant regional emissions, it served to compare the clean Arctic site with a polluted location in Paper I. Collection of snow samples was done from an open section of a mire in the spring of 2010, inside a larger forested zone with no known local emissions over a 5 km radius.

3.1.3 Sunderdhunga, India

The Sunderdhunga valley is located in the western Himalaya, in the state of Uttarakhand, India. Several glaciers are situated in the valley, but the chosen glaciers investigated in Paper IV were Bhanolti and Durga Kot glaciers (N 30° 12', E 79° 51'). Facing northeast they cover an elevation of 4400-5500 m a.s.l. The glaciers in the area contribute to the Ganges river basin, and there is no known local pollution. On a regional scale the closest towns are Bageshwar and Almora, 40 and 70 km southwards, with populations of 9 000 and 34 000, respectively. Otherwise the larger scale emission of particulates originate from the Indo-gangetic plain (IGP). Airborne measurements at Mukteshwar, 90

km southwards, have identified BC and dust to peak during the pre-monsoon season (Hyvärinen et al., 2011; Raatikainen et al., 2017).

3.2 Soot on snow experiments

Soot on snow (SoS) experiments were a series of outdoor experiments where soot was spread onto a natural snow surface and its effect on snow properties were monitored. The outcome from the experiments are presented Paper II and III. The first SoS experiment was on a farming field in southern Finland in Nurmijärvi, 30 km north of Helsinki. Soot was produced by burning wood and rubber pellets from used tires in a wood-burning stove. The smoke from combustion followed a pipe surrounded with snow for cooling into a rectangular experimental chamber placed on top of the snowpack where the particles were deposited. Next to the contaminated snow area a reference site was set-up. The following winters experiment was conducted at Jokioinen, in southern Finland about 100 km northwest of Helsinki. For this campaign a different approach to put impurities onto the snow surface was taken. Soot collected by chimney cleaners in Helsinki from wood and oil burning was deposited to the snow surface by a blowing system into a tent standing on top of the snow surface. Once the soot had been placed on the snow surface in circular spots of 4 m, unfavorable weather conditions seem to have masked the effect of soot on snow. With new snowfall and high winds our conclusion is that the top layer of the snow containing the soot was redistributed in the surrounding areas. Since this experiment did not provide quantitative data it will not be discussed in any further detail. The last experiment was made at the Sodankylä airfield, nearby the FMI ARC in Sodankylä, Arctic Finland. For this experiment several contaminant snow spots were made with different amounts of soot, and other LAI consisting of Icelandic volcanic ash and glaciogenic silt. The blowing system from 2012 was modified, otherwise contaminant spots were produced in the same way as in 2012.

3.3 Snow sample collection and filtering

From each location the collection of snow samples followed a similar working scheme. In field, snow layers were visually inspected, after which snow samples were usually collected with a stainless steel spatula into Nasco whirl-pak bags that had been tested not to contaminate samples. Subsequent melting and filtering of the sample is based largely upon the procedures from Forsström et al. (2009). Melting was conducted in a microwave oven, although a different melting procedure was utilized for part of the samples in Paper IV (details given below). The meltwater was filtered through glassware, with the impurities collected onto a micro quartz fiber filter (Munktell, 55 or 47 mm diameter, grade T 293). Filters were thereafter dried and stored in cold conditions before analysis.

Some site specific sampling were conducted and are worth mentioning in this context. For Paper I, snow samples were collected in different square grid-nets with 5 m or 2.5 m between each sampling point. This was done for surface snow samples (0-5 cm). For the experimental Papers II and III, snow surface samples were collected after the soot had been spread over the snow surface. In Paper IV, snow pits from two Indian glaciers were sampled in intervals, and the comparison snow from Finland contained surface snow samples from a seasonal snowpack. Due to the remoteness and high altitude of the samples obtained on glaciers in Paper IV, a different approach to the post-sampling handling was conducted. The location did not allow snow samples to remain frozen until melting and filtering in the laboratory. Therefore, the samples were melted over a camping stove in an enclosed glass container at the expedition base camp, after which they were filtered.

3.4 Light-absorbing impurities analysis

In this thesis the carbonaceous fraction of the LAI in snow was measured using TOM in Paper I, II, II, and IV. Thus, EC is the operationally defined constituent that has been measured. The Sunset laboratory OCEC-analyzer (Sunset Laboratory Inc. USA; Birch and Cary, 1996) was used. From the filter substrates a punch (usually either 1 or 1.5 cm^2) is taken and analyzed in two stages. During the first stage, in a helium atmosphere, the temperature is increased stepwise and OC and carbonate carbon (CC) is volatilized and detected by a flame ionization detector. In the second stepwise heating of the filter, oxygen is incorporated, and EC is measured. Since pyrolysis is likely to occur to some degree, a laser is used to measure the transmittance (and/or reflectance depending on instrument model) of the filter during analysis to account for potential charring. Different measurement protocols have been used, most notably NIOSH and EUSAAR_2 (Cavalli et al., 2010). The uncertainties with measuring LAI with TOM derive from inefficiency of the filters to capture all of the impurities, an uneven filter loading, as well as loss of particles to filtering equipment, most of which has been addressed to some degree in the different manuscripts and references within. Further, during filter analysis, filters containing a high MD loading can interfere with an accurate split point (Wang et al., 2012), and samples containing a high fraction of pyrolyzed OC can cause an artifact (Lim et al., 2014).

In Paper II electron microscopy study was added to investigate the LAI on a particle basis. For this purpose a sample of contaminated snow was melted onto a silicone disk. The remaining particles were thereafter observed with a Hitachi Hi-tech S-4800 field-emission electron microscope fitted with an Oxford Instruments Inca 350 energy-dispersive X-ray microanalysis system. Soot particles were identified as such by EDS measurements with both 5 kV and 20 kV acceleration voltages. The 5 kV measurements were used for detecting carbon and oxygen in the soot particles, and the 20 kV measurements were used to check for metals present in mineral dust, such as Na, Al, Ca, Fe.

To estimate the fraction of non-EC refractory impurities a custom built PSAP was added to the TOM analysis in Paper IV. Using this procedure has been reported previously by Lavanchy et al. (1999). However, as a different set of instruments were used here, a few laboratory procedure tests were conducted to verify the method, which are presented in Paper IV. The laboratory test included filters with different mixtures of LAI, which were generated in the laboratory by mixing different content of MD and BC with water followed by filtering the liquid mixture. Filter sets containing soot only, as well as dust only, and a mixture of the two were generated. The soot filters were made with two different kinds of soot: NIST and soot collected by chimney cleaners in Helsinki (same soot used in SoS experiments). For the mineral-containing samples two different minerals (Silicone carbide (SiC) and granite) were tested. The filters containing a mix of impurities were made with SiC and soot. The filters were analyzed according to the following procedure: from a dried filter a 1 cm^2 filter punch was measured with the PSAP, followed by OCEC-analysis. Thereafter it was again measured in the PSAP (while being compared to particle free filter). With this approach the change in transmission before and after burning off the carbonaceous impurities was obtained. This allowed fractions of MD to be estimated from the filters, since the light absorption from the carbonaceous constituents were made, leaving the remaining fraction to MD.

3.5 Albedo and physical properties of snow

In the SoS experiments measurements started immediately following soot deposition to the snow. In terms of albedo a set of pyranometers (manufactured by Kipp & Zonen) were employed for

this purpose by measuring the downwelling and upwelling irradiance at wavelengths 285 (or 310 depending on sensor) to 2800 nm. The albedo was the ratio between the two irradiances. Pyranometers measuring the upwelling irradiance were set 30 cm above the snow surface to measure throughout most of the day. The expanded standard uncertainty (2σ) was determined to ±2.8 % or ±6.1 %, depending on the sensor. Broadband albedo raw data had a time resolution of 1 min, but was reduced to a 1 h average (solar noon ±30 min) when presented in results and discussion section. This consistent approach also relived the measurement for any correction needed from shadows casted by the infrastructure for the pyranometers.

In the SoS experiments the snow physical properties observed consisted of thickness, density, hardness, grain size and shape. The measurements were made according to the International Classification for Seasonal Snow on the Ground (Fierz et al., 2009). In addition to these measurements, the last experiment had the additional snow grain size determined through macro-photography of each snow layer against a 1 mm grid.

4. RESULTS AND DISCUSSION

The main results of the research from the four papers encompassed in this thesis are presented and discussed in this chapter. The outline is as follows: section 4.1 presents the result from Paper I where the small scale variability of EC in surface snow was studied at both a clean and a polluted site; section 4.2 includes results from Paper II and III where a natural snowpack was experimentally contaminated with LAI. Specifically, section 4.2.1 focus on the albedo results, while section 4.2.2 highlights observations on the snow density made during the experiment. The results from Paper IV, where the contribution from different LAI constituents is investigated in snow from the Indian Himalaya and the Finnish Arctic, is presented in section 4.3; while the light absorption of EC from the laboratory and natural snow is assessed in section 4.4.

4.1 Small scale spatial variability of elemental carbon in surface snow

The investigated surface snow of Pallas displayed large varying EC concentrations on a horizontal meter scale of 2.5 and 5 m. The EC concentration had a range of 13 and 31 μg L^{-1} (25^{th} and 75^{th} percentile, respectively), and a standard deviation of 60% of the mean. At the comparison site near to urbanization, Tyresta, Sweden, with major regional emission sources (metropolitan of Stockholm), there was less relative spatial variability in the EC concentration in the snow surface with a range of 174 and 505 μg L^{-1} (25^{th} and 75^{th} percentile), and standard deviation of 20% of the mean. At Pallas, post-depositional processes in the snow are likely to be one main reason for the difference in small scale variability. The area sampled is above the tree line and snow drift is a common process with a key role in redistributing snow. Snowpacks near each other may, therefore, vertically represent very different EC depositional histories (i.e. EC concentration). This can create vertical gradients of EC in the snowpack, translating into horizontal spatial variability if wind erodes the surface and transports it to a different place. This may be especially evident when studying upper snow layers (top 5 cm of the snow in our case). Additionally, differences in the proximity to sources of BC can impact variability. Observations of airborne eBC have revealed polluted air masses originating from Central and Eastern Europe reaching Pallas, interceded with periods of clean air masses from the north, thus resulting in a heterogeneous temporal pattern of BC (Hyvärinen et al., 2011). On the contrary, at Tyresta, the sampling site receives higher EC concentrations in air on a more constant basis, which leads to greater dry and wet deposition on the snow surface, which may

mask any heterogeneity of EC in the snow. It is also very likely that the snowpack of Tyresta does not experience snowdrift to the same extent as Pallas.

Based on measurements conducted on the size of rBC particles in the snow, there are indications that there can be significant variability in the size distribution of rBC particles in snow. This seems to be due to the presence of exceptionally large rBC particles (Schwarz et al., 2012). The rate at which BC particles aggregate into larger particles is likely to be dependent on ambient meteorological conditions and the amount of BC deposited. Here, more frequent melt cycles and higher atmospheric BC concentrations are expected to lead to larger particles. As all the measurement techniques used today to characterize BC in snow have various size—dependent sampling efficiencies, this may introduce uncertainties. For the filter technique used in our study, there is an underestimation of small BC particles, which could attribute to the variability seen in the Pallas observations. The spatial variability of LAI in snow horizontally has been reported elsewhere (Forsström et al., 2013; Delaney et al., 2015; Lazarik et al., 2017), which further emphasizes the importance of collecting multiple samples from a measurement site to obtain a representative value.

4.2 Effect of soot on the physical properties of snow

4.2.1 Broadband albedo

After deposition of soot onto snow surfaces, the change in albedo was monitored and the temporal evolution could be compared between the different experiments. In 2011, the contaminated surface snow with an EC concentration of 20 000 µg L^{-1} had a general albedo decrease for the first week. Whereas in 2013, the snow spot containing the highest EC concentration (6 000 µg L^{-1}) first lowered the albedo when deposited on the snow, but during the subsequent two days the albedo recovered from approximately 0.4 to 0.65. A plausible reason for the different temporal evolutions of the albedo in the two experiment years could be that the decrease in 2011 was amplified by snow grain growth caused by the added soot particles. With larger grained snow, BC has an enlarged reduction of the albedo (Warren and Wiscombe, 1980; Hadley and Kirchstetter, 2012; Dang et al., 2015). The observed rising of albedo in 2013, on the other hand, could possibly be explained by soot particles sinking into the snow surface. This was on a millimeter to centimeter vertical scale and the particles sunk within minutes of deposition, during daytime when elevated solar radiation occurred. The daily maximum temperature was above 0°C during that time, while during the night it was -10°C (or below). The cold night temperatures possibly stopped further vertical motion of the absorbing particles within the snow. This process has further effects on the bidirectional reflectance factor (BRF), studied during the experiment (reported in detail in Peltoniemi et al., 2015). After the particles had depressed into the snow, the difference in surface reflectance between the contaminated snow and the clean snow is largest when measured at nadir, while it is smallest at larger zenith angles (where it is mostly pure snow one sees). This applies to higher impurity concentrations and implies that, for a ground observer, the albedo of contaminated snow could be overestimated, while the nadir angle (used for example by satellites) will underestimate the albedo (Peltoniemi et al., 2015).

After the first few days, the ensuing weeks showed similar patterns of albedo evolution for both experiments. New snowfall events covered the soot layer in the snow, increasing the albedo of the contaminated snow to a similar value as the albedo of the reference snow. The albedo of the snowpack containing soot particles was thereafter observed to decrease faster than the reference snow's albedo (e.g. during one event in 2011 the albedo was 0.83 and 0.82 after snow for the reference and contaminated snow, respectively. After two days the albedo was 0.66 and 0.36 for the reference

and contaminated snow, respectively). The buried soot layer therefore affected the new snow by increasing solar radiation and melting the new snow.

The observed albedo decrease during both the 2011 and 2013 experiments caused by increased BC concentration generally agrees with the previous laboratory study of Hadley and Kirchstetter (2012). In more detail, the SoS results show that the BC reduction on albedo in natural snow is not as pronounced as the laboratory conditions used in Hadley and Kirchstetter (2012). This is probably due to different light conditions used in each study (Hadley and Kirchstetter (2012) used a SZA of 0°). From the experimental data, a parameterization for albedo decrease with EC concentration was shown to be nearly identical to a similar function provided in Pedersen et al. (2015), which is based on extensive *in situ* measurements of spectral surface albedo and EC concentrations. The SoS data based parametrization was further used as input in the modelling work of Hienola et al. (2016), where the radiative impact of Nordic anthropogenic BC was estimated.

4.2.2 Snow density

Snow density is generally understood to increase with time and especially during melt season. Counterintuitive to this notion, the snow density was observed to decrease during snowmelt in the SoS experiment. Based on the concurrent measured LAI content in the snow, it appeared to be linked to the LAI concentration, as higher LAI content was associated with lower snow densities. The same relationship between increasing LAI content and decreasing density was not observed in non-melting snow. During the snowmelt period, a rain event on snow occurred. However, the same conditions where maintained with lower densities for increasing LAI concentration. Based on this observation, it was hypothesized that LAI decrease the water retention capacity of melting snow. Additional, independent, small scale experiments on the meltwater release confirmed that LAI contaminated snow discharge water faster than clean snow. Plausible processes explanations for the decrease in snow density could be that LAI:

1. Increase melting or evaporation or both of the snow surrounding the impurities, allowing air pockets around the impurities to be formed, leading to less dense snow
2. Reduce the adhesion of water to the snow grains. The decrease of liquid water holding capacity will result in decreased snow density.
3. Increase snow metamorphism, and consequently increasing grain size, which has a lower water retention capacity, creating a reduced density.

In natural snow melting conditions at Sodankylä, following the experiments, analogous snow density decrease with increasing LAI has been observed to occur (Meinander et al., 2016). Recently, Skiles and Painter (2017), reported from measurements in the seasonal snowpack of Colorado, U.S., a similar lowering of surface snow density in the presence of a heavy dust loading. Before robust conclusions can be made on this density effect, additional measurements are needed.

4.3 Contribution of different light-absorbing impurities in snow

The investigated glacier area in the Indian Himalaya, Sunderdhunga (an area previously unexplored with respect to LAI in snow) displayed higher EC concentrations than previous measurements of EC from inside the Chinese boarder to the northeast. Although direct comparisons are difficult due to different sets of measurement techniques and surrounding geography, Sunderdhunga may have a greater amount of LAI in the snow, due to its lower altitude and location on the southern flank of the Himalaya.

The fraction of MD responsible for the light absorption on the filter was very high for the Indian originating filters. The majority of surface snow samples had MD contributions exceeding

56%, thereby indicating an abundance of dust in the snow on the two sampled glaciers. Hence, MD probably plays an important role in reducing the snow albedo on glaciers in this area of the Himalaya. On the contrary, the two investigated sites in the Finnish Arctic displayed a much smaller fraction of MD for the LAI in the snow. Most MD fractions were smaller than 20%, which is on the same scale as estimates reported from other Arctic locations (Doherty et al., 2010). In this part of the Arctic, MD is likely to affect the snow radiative balance to a much lesser extent than the Himalayan samples. Other studies have highlighted the importance and abundance of MD in other regions of the Himalaya, where in some cases dust has been measured at such high concentrations that it may be exceeding BC in the snow albedo reduction as the most dominant particulate (Kaspari et al., 2014; Qu et al., 2014). Contrasting observations have been made in other third pole regions however, with BC being the dominant light absorber in the snow (Ming et al., 2016; Li et al. 2017; Schmale et al., 2017; Zhang et al., 2017). A broader picture of MD versus BC in reducing snow albedo is still needed in high mountain Asia.

4.4 Optical properties of elemental carbon in snow

The measurement obtained MAC EC for the ambient samples from Arctic Finland and Himalayan India is roughly half of the MAC for laboratory EC particles treated with the same liquid-filtering procedure. This indicates a less absorbing efficiency for the same amount of mass EC for the snow originating particles. Hypothetical speculations for the difference include a possible difference in the size of EC particles, with the laboratory filters containing a higher amount of smaller sized EC particles compared to the ambient samples. A higher frequency of smaller particles will result in a greater MAC. Another hypothesis to explain the difference in MAC is that a higher content of OC was measured in the snow originating EC particles. Elevated OC content, combined with the EC particles being further embedded in the filter medium due to liquid-filtering, could have the effect of masking the EC particles, making them less efficient absorbers in this particular matrix. This is inconsistent with results from air samples (e.g. Jacobson, 2001; Cappa et al., 2012; Bond et al., 2013). In a snow albedo context, EC particles with less absorptive efficiency have implications on the snow albedo reduction, which has also been suggested in Schwarz et al. (2013). Based on their observations of the size of rBC particles in snow, Schwarz et al. calculate that the BC absorption in snow is overestimated by 40%.

5. CONCLUSIONS

In this thesis a set of different measurements and experiments were conducted to increase our understanding of LAI interaction with snow and its role in the climate system. In conformance with the aforementioned scientific questions, the main conclusions of this thesis are:

1. The BC concentration in surface snow presented large horizontal variability, significant down to the meter scale. It was clear that the pristine Finnish Arctic presented a relatively larger variability compared to the more polluted site near Stockholm. Differences in post-depositional processes of BC and distance to emission sources are pointed out as main reasons for the differences in variability.
2. Following BC doping of a snow surface, the albedo of a natural snowpack is reduced. With higher BC concentrations, on the order of >1 000 μg L^{-1}, the decrease in albedo and change in snow properties can be attributed to the added LAI. At smaller concentrations, the BC effect may be masked by other influences (external such a meteorological conditions or other

micro-processes in the snowpack). The importance of observation at very high temporal frequency cannot be overstated.

3. The density of surface snow decreases with increasing LAI concentration during melt. No such relationship was observed in non-melting conditions. The LAI likely reduce the water retention capacity of the melting snow, thereby decreasing the density.
4. Through optical measurements of particle-laden filters combined with mass estimates, the respective fractions of MD and BC can be assessed, when combining thermal-optical and strictly optical methods. The light absorption of BC particles originating from snow has half of the light absorbing efficiency of laboratory based BC particles. In order to more accurately estimate the BC forcing in snow, the site-specific optical properties of BC should be considered.
5. Deposited LAI to the Himalayan glacier surface at an elevation of 5000 m exists in highly concentrated annual layers that affect the radiative balance of the glacier surface. At a higher elevation the contribution of LAI is unknown. The fraction of MD absorbing light can sometimes exceed that of BC, suggesting that the snow radiative balance in the sampled area may at times be more affected by MD than BC.

6. FUTURE OUTLOOK

The conducted measurements and experiments in this thesis have underlined areas where further research is needed. One suggested topic is the process of LAI deposition from the atmosphere to the snow surface. Measurements of deposition and the removal of LAI from the atmosphere to the snow would allow new perspectives on this process, and would improve our understanding of LAI interaction with the snow surface. Once the particulates are at the snow surface, it is vital to investigate LAI migration through the snowpack. Traditionally, LAI has been observed to remain at the surface during melt. However, this process appears required to be re-evaluated (Lazarcik et al., 2017). Additional post-depositional processes in the snow, such as BC growth in size by agglomeration is another subject that would benefit additional studies. The light absorption of BC in snow (as well as other LAI), a parameter very influential for the reduction in albedo, needs to be further addressed. This will enable more accurate estimates on the LAI reduction of snow albedo. Ideally the MAC would be measured while the LAI particles are in the snowpack, since the light condition will change in other measuring environments (e.g. particles collected on filter). Although the task to measure in the snow is challenging, as ideally non-intrusive measurement techniques would be desirable to investigate LAI and snow interaction on a micro scale.

A geographical area, where LAI and the different constituents are affecting the cryosphere, needing further attention is the Himalaya and the other parts of the third pole. This vast region has divergent patterns for both glacier change and LAI deposition, and in order to assess the role of LAI affecting the area, supplementary research is necessary. Likewise, the Andes of South America has not been explored in terms of LAI affecting the ongoing negative cryospheric changes.

In the future the relative contribution between natural and anthropogenic LAI in snow is not very clear. Climate change may increase natural deposition of MD and biomass BC from forest fires, whereas political incentives may reduce the BC from fossil fuels. Any scenario requires detailed knowledge about the processes acting on the snow at the grain size level in order to understand the big picture about the cryosphere and the hydrological cycle. More process research is needed in order to provide climate models with the best available understanding. Our prediction skills about our future environment will never be better than the knowledge we feed into the models.

REFERENCES

AMAP: Snow, water, ice and permafrost in the Arctic: Climate change and the cryosphere, Arctic Monitoring and Assessment Programme, Oslo, Norway, 2011.

Andreae, M.O. and Gelencsér, A.: Black carbon or brown carbon? The nature of light-absorbing carbonaceous aerosols, Atmos. Chem. Phys., 6, 3131–3148, doi:10.5194/acp-6-3131-2006, 2006.

Andreae, M.O. and Rosenfeld, D.: Aerosol–cloud–precipitation interactions. Part 1. The nature and sources of cloud-active aerosols, Earth-Sci. Rev., 89, 13–41, doi:10.1016/j.earscirev.2008.03.001, 2008.

Aoki, T., Motoyoshi, H., Kodama, Y., Yasunari, T. J., Sugiura, K., and Kobayashi, H.: Atmospheric aerosol deposition on snow surfaces and its effect on albedo. SOLA, 2, 13–16, doi: 10.2151/sola.2006-004, 2006.

Barnett, T. P., Adam, J. C., and Lettenmaier, D. P.: Potential impacts of a warming climate on water availability in snow-dominated regions, Nature, 438, 303–309, doi:10.1038/nature04141, 2005.

Birch, M. E. and Cary, R. A.: Elemental carbon-based method for monitoring occupational exposures to particulate diesel exhaust, Aerosol Sci. Technol., 25, 221–241, 1996.

Bolch, T., Kulkarni, A., Kääb, A., Huggel, C., Paul, F., Cogley, J.G., Frey, H., Kargel, J.S., Fujita, K., Scheel, M., Bajracharya, S., and Stoffel, M.: The State and Fate of Himalayan Glaciers, Science, 336, 310–314, 2012.

Bond, T. and Bergstrom, R.: Light Absorption by Carbonaceous Particles: An Investigative Review, Aerosol Sci. Tech., 40, 27– 67, 2006.

Bond, T.C., Doherty, S.J., Fahey, D.W., Forster, P.M., Berntsen, T., DeAngelo, B.J., Flanner, M.G., Ghan, S., Kärcher, B., Koch, D., Kinne, S., Kondo, Y., Quinn, P.K., Sarofim, M.C., Schultz, M.G., Schulz, M., Venkataraman, C., Zhang, H., Zhang, S., Bellouin, N., Guttikunda, S.K., Hopke, P.K., Jacobson, M.Z., Kaiser, J.W., Klimont, Z., Lohmann, U., Schwarz, J.P., Shindell, D., Storelvmo, T., Warren, S.G., and Zender, C.S.: Bounding the role of black carbon in the climate system: A scientific assessment, J. Geophys. Res.-Atmos., 118, 5380–5552, doi:10.1002/jgrd.50171, 2013.

Box, J. E., Fettweis, X., Stroeve, J. C., Tedesco, M., Hall, D. K. & Steffen, K.: Greenland ice sheet albedo feedback: thermodynamics and atmospheric drivers, The Cryosphere, 6, 821-839, doi:10.5194/tc-6-821-2012, 2012.

Brandt, R. E., Warren, S. G., and Clarke, A. D.: A controlled snow- making experiment testing the relation between black carbon content and reduction of snow albedo, J. Geophys. Res.-Atmos., 116, D08109, doi:10.1029/2010jd015330, 2011.

Cachier, H., Bremond, M.P., and Buat-Ménard, P.: Determination of atmospheric soot carbon with a simple thermal method, Tellus Ser.B, 41B, 379-390, 1989.

Cappa, C., Onasch, T., Massoli, P., Worsnop, D., Bates, T., Cross, E., Davidovits, P., Hakala, J., Hayden, K., Jobson, B., Kolesar, K., Lack, D., Lerner, B., Li, S., Mellon, D., Nuaaman, I., Olfert, J., Petäja, T., Quinn, P., Song, C., Subramanian, R., Williams, E., and Zaveri, R.: Radiative absorption enhancements due to the mixing state of atmospheric black carbon, Science, 337, 1078–1081, doi:10.1126/science.1223447, 2012.

Cavalli, F., Viana, M., Yttri, K.E., Genberg, J., and Putaud, J-P.: Toward a standardised thermal-optical protocol for measuring atmospheric organic and elemental carbon: the EUSAAR protocol, Atmos. Meas. Tech. 3, 79–89, doi:10.5194/amt-3-79-2010, 2010.

Clarke, A. D. and Noone, K. J.: Soot in the Arctic snowpack—a cause for perturbations in radiative transfer, Atmos. Environ. 19, 2045–2053, 1985.

Colbeck, S.C.: An overview of seasonal snow metamorphism, Rev. Geophys., 20(1), 45–61, doi:10.1029/RG020i001p00045, 1982.

Conway, H., Gades, A., and Raymond, C. F.: Albedo of dirty snow during conditions of melt, Water Resour. Res., 32, 1713–1718, 1996.

Cook, J., Edwards, A., Takeuchi, N., and Irvine-Fynn, T.: Cryoconite: the dark biological secret of the cryosphere. Prog. Phys. Geog. 40, 66–111, doi.org/10.1177/0309133315616574, 2015.

Dang, C., Brandt, R. E., and Warren, S.G.: Parameterizations for narrowband and broadband albedo of pure snow and snow containing mineral dust and black carbon, J. Geophys. Res.-Atmos., 120, 5446–5468, doi:10.1002/2014JD022646, 2015.

Delaney, I., S. Kaspari, S., and Jenkins, M.: Black carbon concentrations in snow at Tronsen Meadow in Central Washington from 2012 to 2013: Temporal and spatial variations and the role of local forest fire activity, J. Geophys. Res.-Atmos., 120, 9160–9172, doi:10.1002/2015JD023762, 2015.

Déry, S. J., and Brown, R.D.: Recent Northern Hemisphere snow cover extent trends and implications for the snow-albedo feedback, Geophys. Res. Lett., 34, L22504, doi:10.1029/2007GL031474, 2007.

Di Mauro, B., Fava, F., Ferrero, L., Garzonio, R., Baccolo, G., Delmonte, B. & Colombo, R.: Mineral dust impact on snow radiative properties in the European Alps combining ground, UAV, and satellite observations, J. Geophys. Res.-Atmos., 120, 6080–6097. doi:10.1002/2015JD023287, 2015.

Doherty, S. J., Warren, S. G., Grenfell, T. C., Clarke, A. D. & Brandt, R. E.: Light-absorbing impurities in Arctic snow, Atmos. Chem. Phys., 10, 11647-11680, doi:10.5194/acp-10-11647-2010, 2010.

Doherty, S. J., Grenfell, T.C., Forsström, S., Hegg, D.L., Brandt, R.E. & Warren, S.G.: Observed vertical redistribution of black carbon and other insoluble light-absorbing particles in melting snow, J. Geophys. Res.-Atmos.,118, doi:10.1002/jgrd.50235, 2013.

Doherty, S. J., Hegg, D.A., Johnson, J.E., Quinn, P.K., Schwarz, J.P., Dang, C. & Warren, S.G.: Causes of variability in light absorption by particles in snow at sites in Idaho and Utah, J. Geophys. Res.-Atmos., 121, doi:10.1002/2015JD024375, 2016.

Dumont, M., Brun, E., Picard, G., Michou, M., Libois, Q., Petit, J.-R., Geyer, M., Morin, S. & Josse, B.: Contribution of light-absorbing impurities in snow to Greenland's darkening since 2009, Nat. Geosci., 7, 509–512, doi:10.1038/ngeo2180, 2014.

Fierz, C., Armstrong, R., Durand, Y., Etchevers, P., Greene, E., McClung, D., Nishimura, K., Satyawali, P., and Sokratov, S.: The International Classification for Seasonal Snow on the Ground, no. 83 in IHP-VII Technical Documents in Hydrology, IACS Contribution No. 1, UNESCO-IHP, Paris, 2009.

Flanner, M.G., Zender, C. S., Randerson, J. T., and Rasch, P. J.: Present day climate forcing and response from black carbon in snow, J. Geophys. Res.-Atmos, 112, D11202, doi:10.1029/2006JD008003, 2007.

Flanner, M.G., Shell, K.M., Barlage, M., Perovich, D.K., and Tschudi, M.A.: Radiative forcing and albedo feedback from the Northern Hemisphere cryosphere between 1979 and 2008, Nat. Geosci., 4, 151-155, doi:10.1038/ngeo1062, 2011.

Forsström, S., Ström, J., Pedersen, C.A., Isaksson, E., and Gerland, S.: Elemental carbon distribution in Svalbard snow, J. Geophys. Res.-Atmos., 114, D19112, doi:10.1029/2008JD011480, 2009.

Forsström, S., Isaksson, E., Skeie, R.B., Ström, J., Pedersen, C.A., Hudson, S.R., Berntsen, T.K., Lihavainen, H., Godtliebsen, F. & Gerland, S.: Elemental carbon measurements in European Arctic snow packs, J. Geophys. Res.-Atmos., 118, 13,614–13, 627, doi:10.1002/2013JD019886.2013, 2013.

Gabbi, J., Huss, M., Bauder, A., Cao, F. & Schwikowski, M. The impact of Saharan dust and black carbon on albedo and long-term mass balance of an Alpine glacier, The Cryosphere, 9, 1385-1400, doi:10.5194/tc-9-1385-2015, 2015.

Gertler, C.G., Puppala, S.P., Panday, A., Stumm, D., Shea, J.: Black carbon and the Himalayan cryosphere: a review. Atmos. Environ. 125, 404–417, doi.org/10.1016/j.atmosenv.2015.08.078, 2016.

Ginot, P., Dumont, M., Lim, S., Patris, N., Taupin, J.-D., Wagnon, P., Gilbert, A., Arnaud, Y., Marinoni, A., Bonasoni, P., and Laj, P.: A 10 year record of black carbon and dust from a Mera Peak ice core (Nepal): variability and potential impact on melting of Himalayan glaciers, The Cryosphere, 8, 1479–1496, doi:10.5194/tc-8-1479-2014, 2014.

Grenfell, T.C., Doherty, S.J., Clarke, A. D., and Warren, S.G.: Spectrophotometric determination of absorptive impurities in snow, Appl. Opt., 50(14), 2037–2048, 2011.

Groot Zwaaftink, C. D., Grythe, H., Skov, H., and Stohl, A.: Substantial contribution of northern high-latitude sources to mineral dust in the Arctic, J. Geophys. Res.-Atmos., 121, 13678–13697, doi:10.1002/2016JD025482, 2016.

Hadley, O.L. and Kirchstetter, T.W.: Black carbon reduction of snow albedo, Nature Clim. Change, 2, 437–440, 2012.

Hagler, G. S.W., Bergin, M.H., Smith, E.A., Dibb, J.E., Anderson, C., and Steig, E.J.: Particulate and water-soluble carbon measured in recent snow at Summit, Greenland, Geophys. Res. Lett., 34, L16505, doi:10.1029/2007GL030110, 2007.

Hansen, J. and Nazarenko, L.: Soot climate forcing via snow and ice albedos, P. Natl. Acad. Sci. USA, 101, 423–428, 2004

Hall, A. and Qu, X.: Using the current seasonal cycle to constrain snow albedo feedback in future climate change, Geophys. Res. Lett., 33, L03502, doi:10.1029/2005GL025127, 2006.

Hyvärinen, A.P., Kolmonen, P., Kerminen, V.M., Virkkula, A., Leskinen, A., Komppula, M., Hatakka, J., Burkhart, J. Stohl, A., Aalto, P., Kulmala, M., Lehtinen, K.E., Viisanen, Y., Lihavainen, H.: Aerosol black carbon at five background measurement sites over Finland, A gateway to the Arctic. Atmos. Environ. 45 (24), 4042-4050. doi.org/10.1016/j.atmosenv.2011.04.026, 2011.

Hyvärinen, A.-P., Raatikainen, T., Brus, D., Komppula, M., Panwar, T. S., Hooda, R. K., Sharma, V.P., and Lihavainen, H.: Effect of the summer monsoon on aerosols at two measurement stations in Northern India – Part 1: PM and BC concentrations, Atmos. Chem. Phys., 11, 8271-8282, doi:10.5194/acp-11-8271-2011, 2011.

Immerzeel, W.W., van Beek, L.P.H., and Bierkens, M.F.P.: Climate Change Will Affect the Asian Water Towers, Science, 328, 1382–1385, doi:10.1126/science.1183188, 2010.

Jacobson, M.Z.: Strong radiative heating due to the mixing state of black carbon in atmospheric aerosols, Nature, 409, 695–697, 2001.

Janssen, N.A.H., Hoek, G., Simic-Lawson, M., Fischer, P., van Bree, L., ten Brink, H., Keuken, M., Atkinson, R.W., Anderson, H.R., Brunekreef, B., and Cassee, F.R.: Black Carbon as an Additional Indicator of the Adverse Health Effects of Airborne Particles Compared with PM10 and PM2.5, Environ. Health Perspect., 119, 1691-1699, doi:10.1289/ehp.1003369, 2011.

Jacobi, H.-W., Lim, S., Ménégoz, M., Ginot, P., Laj, P., Bonasoni, P., Stocchi, P., Marinoni, A., and Arnaud, Y.: Black carbon in snow in the upper Himalayan Khumbu Valley, Nepal: observations and modeling of the impact on snow albedo, melting, and radiative forcing, The Cryosphere, 9, 1685-1699, doi.org/10.5194/tc-9-1685-2015, 2015.

Jiao, C., Flanner, M.G., Balkanski, Y., Bauer, S.E., Bellouin, N., Berntsen, T.K., Bian, H., Carslaw, K.S., Chin, M., De Luca, N., Diehl, T., Ghan, S.J., Iversen, T., Kirkevåg, A., Koch, D., Liu, X., Mann, G.W., Penner, J.E., Pitari, G., Schulz, M., Seland, Ø., Skeie, R. B., Steenrod, S.D., Stier, P., Takemura, T., Tsigaridis, K., van Noije, T., Yun, Y., and Zhang, K.: An AeroCom assessment of black carbon in Arctic snow and sea ice, Atmos. Chem. Phys., 14, 2399-2417, https://doi.org/10.5194/acp-14-2399-2014, 2014.

Jenkins, M., Kaspari, S., Shi-Chang, K., Grigholm, B., Mayewski, P.A.: Geladaindong black carbon ice core record (1843–1982): Recent increases due to higher emissions and lower snow accumulation, Adv. Clim. Change Res., 7, 132-138, doi.org/10.1016/j.accre.2016.07.002, 2016.

Kaser, G., Grosshauser, M., and Marzeion, B.: Contribution of glaciers to water availability in different climate regimes, P. Natl. Acad. Sci. USA, 107, 20223–20227, doi:10.1073/pnas.1008162107, 2010.

Kaspari, S., Painter, T.H., Gysel, M., Skiles, S.M., and Schwikowski, M.: Seasonal and elevational variations of black carbon and dust in snow and ice in the Solu-Khumbu, Nepal and estimated radiative forcings, Atmos. Chem. Phys., 14, 8089–8103, doi:10.5194/acp-14-8089-2014, 2014.

Kaspari, S., Schwikowski, M., Gysel, M., Flanner, M.G., Kang, S., Hou, S., and Mayewski, P.A.: Recent increase in black carbon concentrations from a Mt. Everest ice core spanning 1860–2000AD, Geophys. Res. Lett., 38, L04703, doi:10.1029/2010GL046096, 2011.

Keegan, K. M., Albert, M. R., McConnell, J. R., Baker, I.: Climate change and forest fires synergistically drive widespread melt events of the Greenland Ice Sheet, Proc. Natl. Acad. Sci. USA, 111, 7964–7967, doi:10.1073/pnas.1405397111, 2014.

Lavanchy, V.M.H., Gäggler, H.W., Schotterer, U., Schwikowski, M., and Baltensperger, U.: Historical record of carbonaceous particle concentrations from a European high-alpine glacier (Colle Gnifetti, Switzerland), J. Geophys. Res., 104, 21227–21236, doi:10.1029/1999JD900408, 1999.

Lazarcik, J., Dibb, J.E., Adolph, A.C., Amante, J.M., Wake, C.P., Scheuer, E., Mineau, M.M., and Albert, M.R.: Major fraction of black carbon is flushed from the melting New Hampshire snowpack nearly as quickly as soluble impurities, J. Geophys. Res.-Atmos., 122, 537–553, doi:10.1002/2016JD025351, 2017.

Li, C.L., Bosch, C., Kang, S.C., Andersson, A., Chen, P.F., Zhang, Q.G., Cong, Z.Y., Chen, B., Qin, D.H., and Gustafsson, Ö.: Sources of black carbon to the Himalayan-Tibetan Plateau glaciers, Nat. Commun., 7, 12574, doi:10.1038/Ncomms12574, 2016.

Li, X., Kang, S., He, X., Qu, B., Tripathee, L., Jing, Z., Paudyal, R., Li, Y., Zhang, Y., Yan, F., Li, G., Li, C.: Light-absorbing impurities accelerate glacier melt in the Central Tibetan Plateau, Sci. Total Environ., 587-588, 482-490, doi.org/10.1016/j.scitotenv.2017.02.169, 2017.

Lim, S., Faïn, X., Zanatta, M., Cozic, J., Jaffrezo, J.-L., Ginot, P., and Laj, P.: Refractory black carbon mass concentrations in snow and ice: method evaluation and inter-comparison with elemental carbon measurement, Atmos. Meas. Tech., 7, 3307-3324, doi:10.5194/amt-7-3307-2014.

Lutz, S., Anesio, A.M., Jorge Villar, S.E., and Benning, L.G.: Variations of algal communities cause darkening of a Greenland glacier, FEMS Microbiol. Ecol. 89, 402–414. doi: 10.1111/1574-6941.12351, 2014.

Lutz, S., Anesio, A.M., Raiswell, R., Edwards, A., Newton, R.J., Gill, F., and Benning, L.G.: The biogeography of red snow microbiomes and their role in melting arctic glaciers. Nat. Commun. 7: 11968, doi:10.1038/ncomms11968, 2016.

Magono, C., Endoh, T., Ueno, F., Kubota, S., and Itasaka, M.: Direct observations of aerosols attached to falling snow crystals, Tellus, 31, 102–114, 1979.

McConnell, J.R., Edwards, R., Kok, G.L., Flanner, M.G., Zender, C.S., Saltzman, E.S., Banta, J.R., Pasteris, D.R., Carter, M.M. & Kahl, J.D.W.: 20th century industrial black carbon emissions altered Arctic climate forcing, Science, 317, 1381-1384, doi: 10.1126/science.1144856, 2007.

Meinander, O., Dagsson-Waldhauserova, P., and Arnalds, O.: Icelandic volcanic dust can have a significant influence on the cryosphere in Greenland and elsewhere. Polar Research, 35, 31313, doi:10.3402/polar.v35.31313, 2016.

Meinander, O., Virkkula, A., Kontu, A., Svensson, J., Hannula, H.-R. Dagsson-Waldhauserova, P., Arola, A., Backman, L., Manninen, T., De Leeuw, G., and Leppäranta, M.: Light Absorbing Particles and Density of Melting Snow, Reports Series in Aerosol Science, 180, Proceedings of the 2nd Pan-Eurasian Experiment (PEEX) Conference and the 6th PEEX Meeting, 2016.

Ming, J., Cachier, H., Xiao, C., Qin, D., Kang, S., Hou, S., and Xu, J.: Black carbon record based on a shallow Himalayan ice core and its climatic implications, Atmos. Chem. Phys., 8, 1343– 1352, doi:10.5194/acp-8-1343-2008, 2008.

Ming, J., Xiao, C., Cachier, H., Qin, D., Qin, X., Li, Z., and Pu, J.: Black Carbon (BC) in the snow of glaciers in west China and its potential effects on albedos, Atmos. Res., 92, 114–123, 2009.

Ming, J., Xiao, C., Wang, F., Li, Z., and Li, Y.: Grey Tienshan Urumqi glacier No.1 and light-absorbing impurities, Environ. Sci. Poll. Res., 23, 9549-9558, doi:10.1007/s11356-016-6182-7, 2016.

Mori, T., Moteki, N., Ohata, S., Koike, M., Goto-Azuma, K., Miyazaki, Y., and Kondo, Y.: Improved technique for measuring the size distribution of black carbon particles in liquid water, Aerosol Sci. Tech., 50, 242–254, doi:10.1080/02786826.2016.1147644, 2016.

Moosmüller, H., Chakrabarty, R.K. and Arnott, W.P.: Aerosol light absorption and its measurement: A review, J. Quant. Spectrosc. Radiat. Transfer, 110, 844–878, doi:10.1016/j.jqsrt.2009.02.035, 2009

Nolin, A.W. and Dozier, J.: A hyperspectral method for remotely sensing the grain size of snow, Remote Sens. Environ., 74, 207-216, 2000.

Painter, T. H., Barrett, A. P., Landry, C. C., Neff, J. C., Cassidy, M. P., Lawrence, C. R., McBride, K.E., and Farmer, G. L.: Impact of disturbed desert soils on duration of mountain snow cover, Geophys. Res. Lett., 34, L12502, doi:10.1029/2007GL030284, 2007.

Painter, T. H., Deems, J. S., Belnap, J., Hamlet, A. F., Landry, C. C., and Udall, B.: Response of Colorado River runoff to dust radiative forcing in snow, Proc. Natl. Acad. Sci. USA, 107, 17125–17130, doi: 10.1073/pnas.0913139107, 2010.

Painter, T. H., Skiles, S. M., Deems, J. S., Bryant, A. C., and Landry C.C.: Dust radiative forcing in snow of the Upper Colorado River Basin: 1. A 6 year record of energy balance, radiation, and dust concentrations. Water Resour. Res., 48, doi: 10.1029/2012wr011985, 2012.

Paramonov, M., Grönholm, T., and Virkkula, A.: Below-cloud scavenging of aerosol particles by snow at an urban site in Finland, Boreal Environ. Res., 16, 304–320, 2011.

Pedersen, C. A., Gallet, J. C., Ström, J., Gerland, S., Hudson, S. R., Forsström, S., Isaksson, E., and Berntsen, T. K.: In situ observations of black carbon in snow and the corresponding spectral surface albedo reduction, J. Geophys. Res.-Atmos., 120, 1476–1489, doi: 10.1002/2014JD022407, 2015.

Peltoniemi, J. I., Gritsevich, M., Hakala, T., Dagsson-Waldhauserová, P., Arnalds, Ó., Anttila, K., Hannula, H.-R., Kivekäs, N., Lihavainen, H., Meinander, O., Svensson, J., Virkkula, A. & de Leeuw, G.: Soot on Snow experiment: bidirectional reflectance factor measurements of contaminated snow, The Cryosphere, 9, 2323-2337, doi:10.5194/tc-9-2323-2015, 2015.

Petzold, A., Ogren, J.A., Fiebig, M., Laj, P., Li, S., Baltensperger, U., Holzer-Popp, T., Kinne, S., Pappalardo, G., Sugimoto, N., Wehrli, C., Wiedensohler, A. and Zhang, X.: Recommendations for reporting black carbon measurements, Atmos. Chem. Phys., 13, 8365–8379, 10.5194/acp-13-8365-2013, 2013.

Polashenski, C.M., Dibb, J.E., Flanner, M.G., Chen, J.Y., Courville, Z.R., Lai, A.M., Schauer, J.J., Shafer M.M. & Bergin, M. Neither dust nor black carbon causing apparent albedo decline in Greenland's dry snow zone; implications for MODIS C5 surface reflectance, Geophys. Res. Lett., 42, 9319–9327, doi:10.1002/2015GL065912, 2015.

Qu, B., Ming, J., Kang, S.-C., Zhang, G.-S., Li, Y.-W., Li, C.-D., Zhao, S.-Y., Ji, Z.-M., and Cao, J.-J.: The decreasing albedo of the Zhadang glacier on western Nyainqentanglha and the role of light absorbing impurities, Atmos. Chem. Phys., 14, 11117-11128, doi:10.5194/acp-14-11117-2014, 2014.

Raatikainen, T., Brus, D., Hooda, R. K., Hyvärinen, A.-P., Asmi, E., Sharma, V. P., Arola, A., and Lihavainen, H.: Size selected black carbon mass distributions and mixing state in polluted and clean environments of northern India, Atmos. Chem. Phys., 17, 371-383, doi:10.5194/acp-17-371-2017, 2017.

Rosenfeld, D.: Suppression of rain and snow by urban and industrial air pollution, Science, 287, 1793–1796, doi:10.1126/science.287.5459.1793, 2000.

Raes, F., Dingenen, R. V., Vignati, E., Wilson, J., Putaud, J., Seinfeld, J. H. and Adams, P.: Formation and cycling of aerosols in the global troposphere, Atmos. Environ., 34, 4215–4240, doi:10.1016/S1352-2310(00)00239-9, 2000.

Ragettli, S., Immerzeel, W. W., and Pellicciotti, F.: Contrasting climate change impact on river flows from high-altitude catchments in the 35 Himalayan and Andes Mountains, P. Natl. Acad. Sci. USA, 113, 9222–9227, doi:10.1073/pnas.1606526113, 2016.

Ramanathan, V. & Carmichael, G. Global and regional climate changes due to black carbon, Nat. Geosci., 1, 221-227, doi:10.1038/ngeo156, 2008.

Ruppel, M. M., Isaksson, I., Ström, J., Beaudon, E., Svensson, J., Pedersen, C. A., and Korhola, A.: Increase in elemental carbon values between 1970 and 2004 observed in a 300-year ice core from Holtedahlfonna (Svalbard), Atmos. Chem. Phys., 14, 11447–11460, doi:10.5194/acp-14-11447-2014, 2014.

Schmale, J., Flanner, M., Kang, S., Sprenger, M., Zhang, Q., Guo, J., Li, Y., Schwikowski, A., Farinotti, D.: Modulation of snow reflectance and snowmelt from Central Asian glaciers by anthropogenic black carbon, Nat. Sci. Reports, 7, 40501, doi:10.1038/srep40501, 2017.

Schmitt, C. G., All, J. D., Schwarz, J. P., Arnott, W. P., Cole, R. J., Lapham, E., and Celestian, A.: Measurements of light-absorbing particles on the glaciers in the Cordillera Blanca, Peru, The Cryosphere, 9, 331-340, doi:10.5194/tc-9-331-2015, 2015.

Schwarz, J. P., Doherty, S. J., Li, F., Ruggiero, S. T., Tanner, C. E., Perring, A. E., Gao, R. S., and Fahey, D. W.: Assessing Single Particle Soot Photometer and Integrating Sphere/Integrating Sandwich Spectrophotometer measurement techniques for quantifying black carbon concentration in snow, Atmos. Meas. Tech., 5, 2581–2592, doi:10.5194/amt-5-2581-2012, 2012.

Schwarz, J. P., Gao, R. S., Perring, A. E., Spackman, J. R., and Fahey, D.W.: Black carbon aerosol size in snow, Nat. Sci. Reports, 3, 1356, doi:10.1038/srep01356, 2013.

Seinfeld, J. H. and Pandis, S. N.: Atmospheric chemistry and physics - from air pollution to climate change (2nd Edition), John Wiley & Sons, 2006.

Serreze, M.C., Holland, M.M., Stroeve, J.: Perspectives on the Arctic's shrinking sea ice cover, Science, 315, 1533–1536, doi:10.1126/science.1139426, 2007.

Shindell, D., Kuylenstierna, J.C. I., Vignati, E., van Dingenen, R., Amann, M., Klimont, Z., Anenberg, S.C., Muller, N., JanssensMaenhout, G., Raes, F., Schwartz, J., Faluvegi, G., Pozzoli, L., Kupiainen, K., Höglund-Isaksson, L., Emberson, L., Streets, D., Ramanathan, V., Hicks, K., Oanh, N.T.K., Milly, G., Williams, M., Demkine, V., and Fowler, D.: Simultaneously Mitigating Near-Term Climate Change and Improving Human Health and Food Security, Science, 335, 183–189, doi: 10.1126/science.1210026, 2012.

Skiles, S.M. and Painter T.H.: Daily evolution in dust and black carbon content, snow grain size, and snow albedo during snowmelt, Rocky Mountains, Colorado, Journal of Glaciology, doi: 10.1017/jog.2016.125, 2017.

Stohl, A.: Characteristics of atmospheric transport into the Arctic troposphere, J. Geophys. Res.-Atmos., 111, D11306, doi:10.1029/2005JD006888, 2006.

Takeuchi, N., Dial, R., Kohshima, S., Segawa, T., and Uetake J.: Spatial distribution and abundance of red snow algae on the Harding Icefield, Alaska derived from a satellite image, Geophys. Res. Lett., 33, L21502, 2006.

Tedesco, M., Doherty, S., Fettweis, X., Alexander, P., Jeyaratnam, J., and Stroeve, J.: The darkening of the Greenland ice sheet: trends, drivers, and projections (1981–2100), The Cryosphere, 10, 477-496, doi.org/10.5194/tc-10-477-2016, 2016.

Tegen, I., P. Hollrig, P., Chin, M., Fung, I., Jacob, D., and Penner, J.: Contribution of different aerosol species to the global aerosol extinction optical thickness: Estimates from model results, J. Geophys. Res., 102, 23895-23915, doi:10.1029/97JD01864, 1997.

Thevenon, F., Anselmetti, F. S., Bernasconi, S. M., and Schwikowski, M.: Mineral dust and elemental black carbon records from an Alpine ice core (Colle Gnifetti glacier) over the last millennium, J. Geophys. Res.-Atmos, 114, 102, doi: 10.1029/2008JD011490, 2009.

Wang, M., Xu, B., Zhao, H., Cao, J., Joswiak, D., Wu, G., and Lin, S.: The Influence of Dust on Quantitative Measurements of Black Carbon in Ice and Snow when Using a Thermal Optical Method, Aerosol Sci. Technol., 46, 60–69, doi:10.1080/02786826.2011.605815, 2012.

Warren, S. G.: Optical properties of snow, Rev. Geophys., 20(1), 67–89, doi:10.1029/RG020i001p00067, 1982.

Warren, S. G.: Can black carbon in snow be detected by remote sensing? J. Geophys. Res.-Atmos., 118, 779–786, doi:10.1029/2012JD018476, 2013.

Warren, S. and Wiscombe, W.: A model for the spectral albedo of snow II. Snow containing atmospheric aerosols, J. Atmos. Sci., 37, 2734–2745, 1980.

Wiscombe, W. and Warren, S.: A model for the spectral albedo of snow. I: Pure Snow, J. Atmos. Sci., 37, 2712–2733, 1980.

Xu, B., Yao, T., Liu, X., and Wang, N.: Elemental and organic carbon measurements with a two-step heating-gas chromatography system in snow samples from the Tibetan Plateau, Ann. Glaciol., 43, 257–262, 2006.

Xu, B., Cao, J., Hansen, J., Yao, T., Joswiak, D.R., Wang, N., Wu, G., Wang, M., Zhao, H., Yang, W., Liu, X., and He, J.: Black soot and the survival of Tibetan glaciers. Proc. Nat. Acad. Sci. USA, 106, 22114–22118, doi:10.1073/pnas.0910444106, 2009.

Xu, B., Cao, J., Joswiak, D., Liu, X., Zhao, H., and He, J.: Post depositional enrichment of black soot in snow-pack and acceler- ated melting of Tibetan glaciers, Environ. Res. Lett., 7, 014022, doi:10.1088/1748-9326/7/1/014022, 2012.

Yang, S., Xu, B., Cao, J., Zender, C. S., and Wang, M.: Climate effect of black carbon aerosol in a Tibetan Plateau glacier, Atmos. Environ., 111, 71–78, doi.org/10.1016/j.atmosenv.2015.03.016 1352-2310, 2015.

Zhang, Y., Kang, S., Cong, Z., Schmale, J., Sprenger, M., Li, C., Yang, W., Gao, T., Sillanpää, M., Li, X., Liu, Y., Chen, P., Zhang, X.: Light-absorbing impurities enhance glacier albedo reduction in the southeastern Tibetan plateau, J. Geophys. Res.-Atmos., 122, 6915–6933, doi:10.1002/2016JD026397, 2017.

Zhou, Y., Wang, X., Wu, X., Cong, Z., Wu, G., and Ji, M.: Quantifying Light Absorption of Iron Oxides and Carbonaceous Aerosol in Seasonal Snow across Northern China, Atmosphere, 8, doi:10.3390/atmos8040063, 2017.

PAPER I

Observed metre scale horizontal variability of elemental carbon in surface snow

OPEN ACCESS
IOP PUBLISHING ENVIRONMENTAL RESEARCH LETTERS
Environ. Res. Lett. **8** (2013) 034012 (7pp) doi:10.1088/1748-9326/8/3/034012

Observed metre scale horizontal variability of elemental carbon in surface snow

J Svensson[1], J Ström[2], M Hansson[3], H Lihavainen[1] and V-M Kerminen[4]

[1] Finnish Meteorological Institute, PO Box 503, FI-00101 Helsinki, Finland
[2] Department of Applied Environmental Science, Stockholm University, SE-10691 Stockholm, Sweden
[3] Department of Physical Geography and Quaternary Geology, Stockholm University, SE-10691 Stockholm, Sweden
[4] Department of Physics, University of Helsinki, PO Box 64, FI-00014 Helsinki, Finland

E-mail: jonas.svensson@fmi.fi

Received 5 June 2013
Accepted for publication 15 July 2013
Published 26 July 2013
Online at stacks.iop.org/ERL/8/034012

Abstract
Surface snow investigated for its elemental carbon (EC) concentration, based on a thermal–optical method, at two different sites during winter and spring of 2010 demonstrates metre scale horizontal variability in concentration. Based on the two sites sampled, a clean and a polluted site, the clean site (Arctic Finland) presents the greatest variability. In side-by-side ratios between neighbouring samples, 5 m apart, a ratio of around two was observed for the clean site. The median for the polluted site had a ratio of 1.2 between neighbouring samples. The results suggest that regions exposed to snowdrift may be more sensitive to horizontal variability in EC concentration. Furthermore, these results highlight the importance of carefully choosing sampling sites and timing, as each parameter will have some effect on EC variability. They also emphasize the importance of gathering multiple samples from a site to obtain a representative value for the area.

Keywords: black carbon, elemental carbon, surface snow, metre scale variability

1. Introduction

Cryospheric changes can provide good indications of climatic change (e.g. Lemke *et al* 2007). Examples of these are observations in changing sea ice cover, glacier mass balances, or the onset of snowmelt. It has been understood for some time that dark impurities in snow can potentially have large feedback effects on the rate of these changes (Warren and Wiscombe 1980, Clarke and Noone 1985, Hansen and Nazarenko 2004).

In the recent decade, black carbon (BC), has been a research area of increasing interest, especially its climatic impact on snow and ice albedo (e.g. Hansen and Nazarenko 2004, Flanner *et al* 2007, McConnell *et al* 2007, Xu *et al* 2009), but also its negative effects on human health (e.g. Anenberg *et al* 2010, Shindell *et al* 2012). Combustion from biomass and fossil fuels are sources of BC particles, hence BC may have both a natural and anthropogenic component.

In this study we will focus on rather small, metre scale, variability of elemental carbon (EC) concentrations in surface snow. For our snow impurity study here, the terms EC and BC are used synonymously, as EC is operationally defined by using a thermal–optical method, while BC and refractory black carbon (rBC) in snow are determined with an optical and a laser-induced incandescence method, respectively. Previous surveys of BC and EC in snow that mainly focused on regional

(Forsström *et al* 2009, Doherty *et al* 2010, Hadley *et al* 2010, Ye *et al* 2012) and local (Aamaas *et al* 2011) variability also briefly examined small scale horizontal variations in surface snow.

Here, two sites with very different ambient conditions are compared, representing a clean and a polluted environment (Pallas, northern Finland ∼68°N and Stockholm, Sweden ∼59°N). The comparison was conducted on observations made at two different times during the same snow season. The aim of this letter is to investigate the spatial variability of EC on a metre scale in surface snow (top 5 cm) from these different sites, and to analyse possible reasons for this variability.

2. Experiment

2.1. Measurement sites and analytical method

Investigations were carried out at two different sites in the winter and spring of 2010. Tyresta National Park (N 59°11′ E 18°18′), circa 25 km from the city centre of Stockholm, Sweden served as the polluted site. Its proximity to an urban area with a population of about 2 million people (metropolitan area), makes the site considerably affected by air pollution. The sampling site in Tyresta, which is an open section of a mire, is exposed to only limited local emissions within about a 5 km radius. Pallas-Yllästunturi National Park (N 67°58′ E 24°06′; 450 m a.s.l.), located in Arctic Finland, served as the clean site with no major city influencing the local and regional air.

Samples were collected on Sammaltunturi mountain slightly above the tree line where the terrain was quite flat. Samples from both sites were gathered during winter conditions, on 17 February in Tyresta (hereafter called TY1) and on 3 and 4 March in Pallas (PA1a and PA1b). Supplementary samples during the melting season in spring were collected on 21 March in Tyresta (TY2) and 7 May in Pallas (PA2). The sample strategy consisted of collecting individual surface snow (approximately the upper 5 cm) samples in different grids, with the most common grid-net consisting of a 20 m × 20 m square with samples taken every 5 m within the square (see figures 1(a)–(e)). Typical sample volumes (melted snow) were around 1 l for both sites.

Snow samples were melted in a glass jar using a microwave oven and filtered through a microquartz filter as in Forsström *et al* (2009) and Aamaas *et al* (2011). The dried microquartz filters containing the collected impurities were analysed in a thermal–optical carbon aerosol analyzer (Sunset Laboratory Inc., Forest Grove, USA) following the NIOSH 5040 protocol (Birch 2003) (see Birch and Cary (1996) for a detailed description of the thermal–optical method). In short, the thermal–optical carbon aerosol analyser first heats the filter (a 1.5 cm^2 punch) in a helium atmosphere, and organic carbon (OC) and carbonate carbon (CC) are released from the filter and detected by a flame ionization detector (FID). In a second step, the filter is again heated, but in an atmosphere containing oxygen. In the second step, EC is released. However, pyrolysis of the OC which occurred in the first step is detected as EC in the second step. To account for this, a laser is used to monitor the transmittance of the filter as the transmittance decreases during pyrolysis. The point in time when the transmittance returns to its original value during the second step determines the partitioning between OC and EC in the thermogram.

2.2. Measurement uncertainties

The NIOSH 5040 (Birch 2003) analysis protocol has been argued to underestimate EC content during analysis (Chow *et al* 2001, Reisinger *et al* 2008). Mineral oxides existing on the filter sample can produce oxygen during the first—oxygen free—stage of the analysis. Some of the EC is then incorrectly accounted for as OC during the second stage. In a recent study by Wang *et al* (2012), where they investigated the influence of dust on EC measurements in ice and snow using a thermal–optical method, similar results with a bias in the OC/EC split were found. Chow *et al* (2001) compared the NIOSH protocol with a different analysis protocol, IMPROVE (Chow *et al* 1993), on air samples and found that NIOSH values were typically less than half of IMPROVE values. Similarly, Aamaas *et al* (2011) examined the IMPROVE/NIOSH 5040 ratio on snow samples with the result of IMPROVE having higher EC estimates by a factor of two compared to NIOSH 5040. In this study, an evaluation of the different protocol procedures revealed an average corresponding ratio IMPROVE/NIOSH 5040 that corroborates this approximate factor of two (average values of 2.23, and median value of 1.73, when comparing 10 samples) and as a consequence, the samples analysed with NIOSH 5040 were multiplied by 2 to compensate for the underestimation of the NIOSH protocol.

An assessment of the representativeness of a filter punch (1.5 cm^2) for the entire filter (with 11.34 cm^2 area) was also evaluated. Four punches from each filter, instead of the ordinary one punch, were analysed from a subset of 12 filters (3 from each sampling episode) to observe the representativeness of single filter punches. As expected, greater variability was found for filters with low loading than for filters with high loading. In summary, samples with an EC filter loading of less than ∼0.35 $\mu g\ cm^{-2}$ generated a coefficient of variation (standard deviation as a fraction of the mean, expressed in %) of 40% or greater. Samples with EC filter content greater than ∼1 $\mu g\ cm^{-2}$ produced a coefficient of variation of 23% or less. The average EC content per filter from Pallas and Tyresta was 1.92 $\mu g\ cm^{-2}$ and 26.6 $\mu g\ cm^{-2}$, respectively.

A shortcoming of using the filter-based method is that some EC particles can potentially percolate through the filter (Ogren *et al* 1983). This filtration efficiency issue, known as undercatch, was investigated for a subset of filters. Two filter substrates where placed on top of each other in the filter setup, and the sample water was drawn through the filters at the same filtration event. The average and median values from 16 events (12 sub-Arctic snow and 4 Arctic snow samples) were 14% and 2%, respectively. On two additional occasions the melt water was recycled. In this

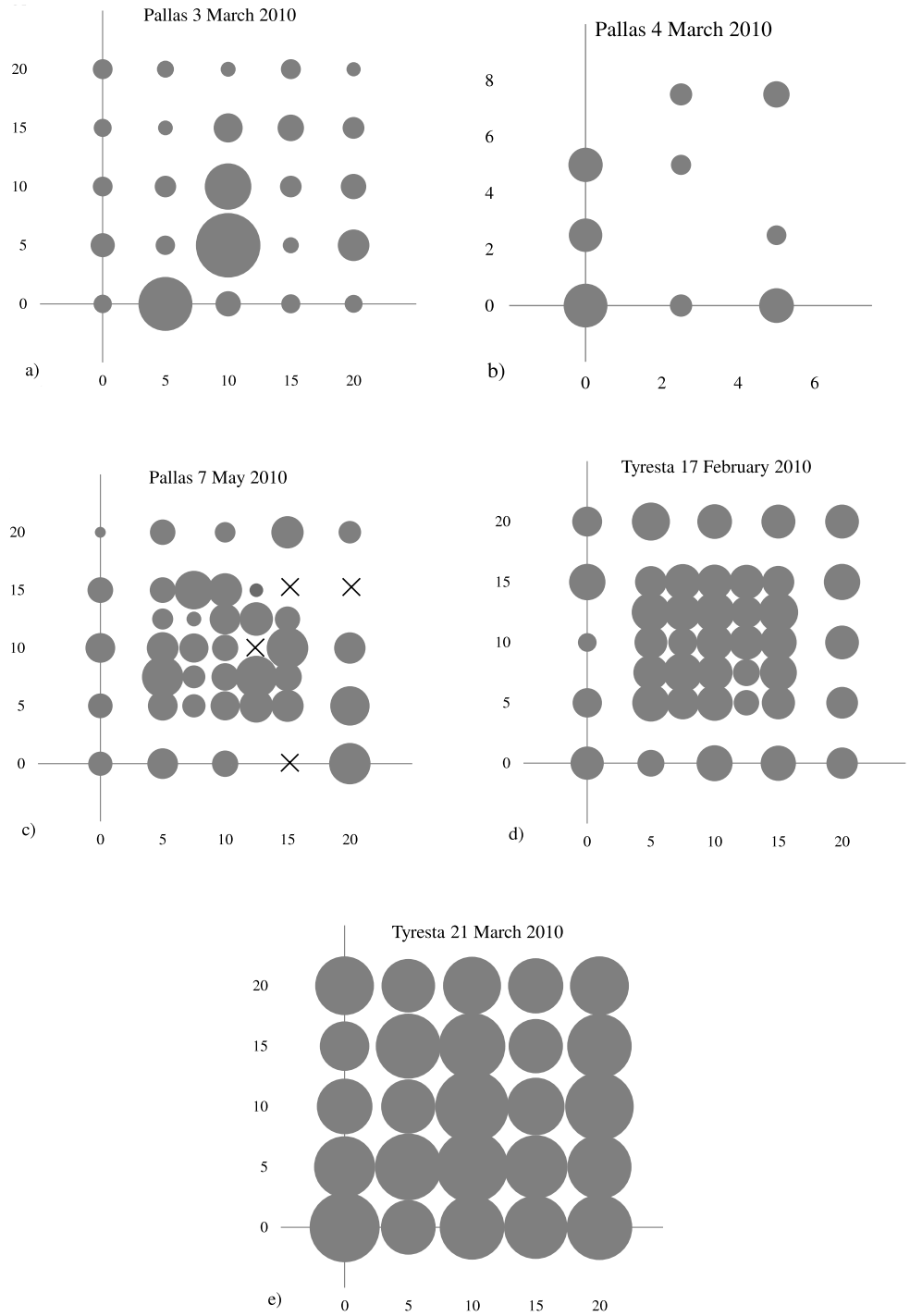

Figure 1. (a)–(e) Circle charts from each sampling event with the area of the circle representing the samples' corresponding EC concentration. The area of the circles are relative as Pallas concentrations are much lower than Tyresta (see table 1). Ordinate and coordinate scales are in metres. Crosses from Pallas 7 May 2010 correspond to samples below the detection limit.

procedure, a sample was filtered once and that collected water was filtered again on another filter. On one of those events, no EC was observed on the second filter and for the other event, an undercatch of as much as 50% compared to the first filtration was observed. Aamaas *et al* (2011) found similar differences when testing this way. Of three filters, two

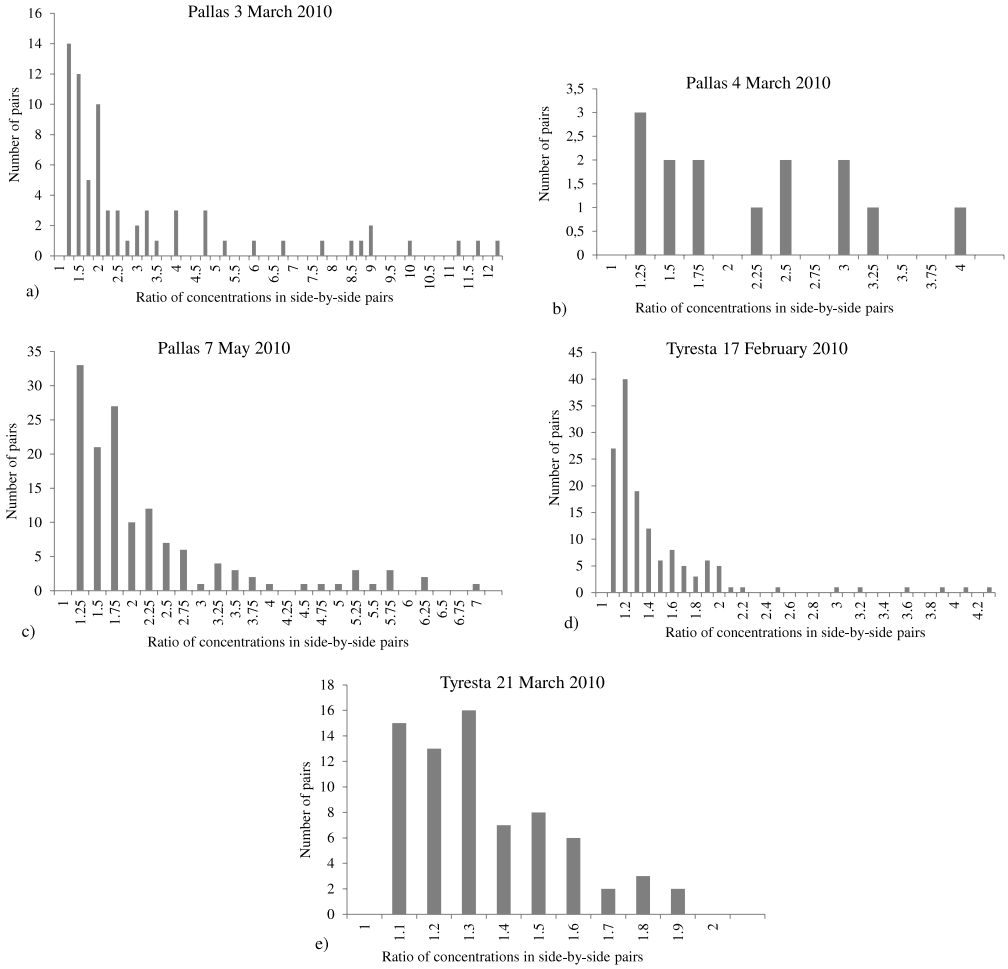

Figure 2. (a)–(e) Side-by-side ratios of neighbouring samples shown in histograms from each sampling event.

had undetectable amounts, while one had a 70% efficiency. These findings demonstrate that undercatch can influence the results and more systematic experiments are needed in the future. Using stacked filters reduces the risk of unwanted loss or contamination compared to recycling the water. For comparison, Nuclepore filters (0.4 μm) used in an optical method using the integrating-sandwich spectrophotometer (Clarke 1982, Grenfell *et al* 2011) have been proposed to have an undercatch of about 15% (Clarke and Noone 1985, Doherty *et al* 2010).

3. Results and discussion

As expected, the typical EC concentration observed at Tyresta was higher than in Pallas. In Tyresta, the measured EC mixing ratio typically ranged from 174 to 505 ppb (25th and 75th percentile, respectively) and in Pallas the range was between 13 and 31 ppb. The concentrations increased from winter to spring at both sampling sites, the median value being roughly threefold from TY1 to TY2 (182.7 versus 608.3 ppb) and twofold from PA1a to PA2 (from 13.0 versus 24.8 ppb). These increases corroborated the accumulation of EC particles occurring throughout the spring in the surface of the snowpack, which has been observed by others (e.g. Conway *et al* 1996, Doherty *et al* 2010, Aamaas *et al* 2011).

Aside from the similarity of a general increase in EC concentrations over the season, other indicators of variability were clearly larger in Pallas than in Tyresta. The variation of EC between samples is illustrated by histograms showing the side-by-side ratio existing between neighbouring samples (distance of 2.5 and 5 m) presented in figures 2(a)–(e). (Ratios presented here are always >1 because the higher concentration is divided by the lower in comparison to Doherty *et al* 2010, figure 6, where ratios below 1 are also presented. This was done here to display a more easily read histogram.) In Tyresta this ratio was typically <2 with a median of 1.2 for all the samples. In Pallas values >2 were common and the median for all samples from there was 1.7. For neither site could the observed variability be explained simply by uncertainties in the sampling procedure,

Table 1. Measured EC concentrations from each sampling event. (Note: coefficient of variation is expressed in percentage.)

Site	Sampling date	Number of samples	Corresponding figures in this letter	Average (ppb)	Median (ppb)	Min (ppb)	Max (ppb)	Standard deviation (ppb)	Coefficient of variation
PA1a	3 March 2010	25	1(a); 2(a)	25	13	6.6	140	30	120
PA1b	4 March 2010	9	1(b); 2(b)	20	15	8.6	42	11	59
PA2	7 May 2010	41	1(c); 2(c)	26	25	0.0	58	16	61
TY1	17 February 2010	41	1(d); 2(d)	180	180	53	250	40	22
TY2	21 March 2010	25	1(e); 2(e)	580	610	370	810	120	20

Table 2. Summary of the side-by-side ratios within each sampling event.

Site	Sampling date	Corresponding figures in this letter	Number of pairs	Max ratio	Average ratio	Median ratio
PA1a	3 March 2010	1(a); 2(a)	72	16	3.2	1.8
PA1b	4 March 2010	1(b); 2(b)	14	3.8	2.1	2.0
PA2	7 May 2010	1(c); 2(c)	140	6.8	2.1	1.6
TY1	17 February 2010	1(d); 2(d)	140	4.3	1.3	1.3
TY2	21 March 2010	1(e); 2(e)	72	1.8	1.4	1.2

reflecting an interesting difference in variability between these two sites. The expected median side-by-side ratio from analysis uncertainty was 1.27, assuming a coefficient of variation of 23% (taken from the representativeness of a filter punch), which is an upper level estimate since the average EC loading is typically higher than for the estimate made here (average loading for Pallas samples was 1.92 μg cm^{-2} compared to the 1 μg cm^{-2} used for this expected median side-by-side ratio). The samples from PA1a present the largest spatial variability of the data set. This is partially explained by the fact that the three samples with the highest concentrations from all of the Pallas samples were measured at this event (PA1a). The remaining samples at PA1a also differed significantly, indicated by a median side-by-side ratio of 1.81 for all of the samples in this grid-net (table 2). To assess the possibility of contamination in the three samples with the highest concentrations from Pallas (PA1a), the procedure of side-by-side ratios was repeated excluding these three samples. The resulting median side-by-side ratio for the remaining 22 samples in that dataset was 1.54, which demonstrates notable variation regardless of the excluded samples. Although the possibility of contamination cannot be ruled out, contaminating the filters to an EC loading equivalent of the highest concentrations observed requires considerable effort. Simple miss handling of the filter is not sufficient. Hence, it is unlikely that contamination has occurred at Pallas.

A notable variation was also displayed in the grid-net from PA1b, which was a smaller grid-net with a 2.5 m distance between the samples, collected at about the same location, but 24 h after the PA1a event. During the time between the two sampling events, snowdrift had erased all traces of the earlier snow sampling from the previous day. The median side-by-side ratio for this grid-net was 2.0 (figure 2(a), table 2). Wind-driven snowdrift is a common process in Pallas being especially prominent in areas above the tree line. Redistribution of snow from snowdrift has been proposed as an important mechanism creating variations of impurity concentrations in the snow in other regions of the Arctic (i.e. Svalbard) (Forsström *et al* 2009). The variations observed in Pallas support this view. The snowdrift can mix snow of different ages (with different depositional history) and impurity concentrations, thereby causing particle variability in the snow. This can, in turn, create vertical gradients in the snow that can be translated into horizontal variability when sampling a vertical layer of 5 cm. Doherty *et al* (2010) found that the largest variation between samples where observed in snow pits with strong vertical gradients of BC concentrations. Other recent work on BC in snow, utilizing a different analysis method (the single particle soot photometer), has proposed that there is a significant variability in the size distribution of BC particles in snow (Schwarz *et al* 2012). With the hypothesis that our filter-based method does not capture small EC particles well, as the undercatchment section has suggested potential losses of EC particles while filtering, some of the variation observed in our data could be attributed to the loss of smaller EC particles in our samples. This speculation remains to be further tested, however. It should also be noted that the key result of Schwarz *et al* (2012, 2013) is that BC particles tend to be larger in snow compared to the atmosphere, thus the question of how many small particles are lost in our method is yet to be thoroughly quantified.

The spatial variation in Tyresta was not as pronounced as in Pallas, as reflected by the median side-by-side ratio of 1.25 for TY1 and 1.22 for TY2 (figures 2(d) and (e), table 2). An important element that partially explains the difference in variation between Tyresta and Pallas was the relevant absence of wind and subsequent snowdrift at the former.

The overall variation within the samples from each sampling event was verified by the coefficient of variation from each event (table 1). The sampling events with high coefficients of variation were those from Pallas, especially PA1a (PA1a: 122%; PA1b: 59%; PA2: 61%), whereas the datasets from Tyresta showed much lower coefficients of variation (TY1: 22% and TY2: 20%). The coefficients of variation, together with the side-by-side ratio histograms,

demonstrate the existing variation of EC in the snow from the sites. A recent study conducted in the Sierra Nevada Mountains (CA, USA) by Sterle *et al* (2013) found a spatial variability of rBC in the upper sections of the snow pits during the accumulation season.

The variation presented by Forsström *et al* (2009) had an average relative root mean square deviation of 1.0 on a horizontal scale of 1 m. Thus, the observed variations by Forsström *et al* (2009) share the horizontal variability of EC in snow that is presented here, even though the samples from PA1a, PA1b and PA2 displayed even greater variations than observed by Forsström *et al* (2009). In our case at Pallas, what could set the stage for variability are the existing ambient air conditions. Observations in air have shown polluted air masses originating from Central and Eastern Europe migrating north, while clean air masses from the north also occur at Pallas (Hyvärinen *et al* 2011).

In the work of Doherty *et al* (2010), the variability of BC on a 50–100 cm scale was briefly examined to test the representativeness of a sampling location by individual samples. In a similar side-by-side ratio study carried out with samples from East and West Russia, the Canadian Arctic, and Tromsø, Norway, the concentrations of their samples were almost always within 50% of each other. In fact, most of their samples were typically within 20–30% of each other. Our Pallas samples showed greater variability being >100% from sample to sample. Our Tyresta samples had a variability that was comparable to that presented by Doherty *et al* (2010). Doherty *et al* (2010) does stress the need to gather multiple samples from one location or region in order to attain a representative value, which is also strongly emphasized by the results of this study.

Doherty *et al* (2010) suggested that a closer proximity to emission sources would result in greater depositional heterogeneity of BC. For plumes in the atmosphere this is often the case, but our results indicate that this is not necessary always the case in snow. Tyresta—which is closer to emission sources—showed greater homogeneity than the Pallas samples collected further away from emission sources. The two sites are very different, but post-deposition processes might be more important in a remote environment such as Pallas compared to Tyresta, where stronger dry and wet deposition of EC due to higher ambient air concentrations may help to mask variability caused by snow drift. This would result in a vertically more homogeneous snow pack with respect to EC concentration. This hypothesis remains to be tested.

In light of the results observed in this work, the following recommendations for future sampling of BC/EC in snow are suggested for optimizing measurements: (1) collect multiple vertical profiles a few metres apart to achieve a more representative value for the sampling location, especially during the earlier part of the snow season when the BC loading may be lower; (2) having consistency when sampling layers is of great importance, as well as conducting studies of the layering in the snowpack. Preferably, physical properties of the snow pack (e.g. density, snow grain size, etc) that were not observed in our study, but in light of our results, should be noted in future studies; (3) when choosing sampling site the local and regional contamination of BC should be taken into account. Areas especially prone to wind exposure should be avoided.

4. Conclusions

Using a comparatively simple filtering technique we observed a spatial variability of EC particles in surface snow on a metre scale. The surface snow displayed greater variability during the winter season and had a tendency towards a more homogeneous pattern during the spring. Greater variability was found for the remote site compared to the site closer to the emission sources.

Our study highlights the importance of carefully choosing the sampling site and timing of the sampling. It also underlines the importance of collecting several samples from a sampling site. EC variation can exist within a few metres in the surface snow. This is also something that needs to be considered when single observations represent large regions in climate models. Our work also argues for the need of studies on EC in snow that focus on both deposition and post-depositional processes taking place in the snow (e.g. microphysics, wind's effect, and metamorphism), as understanding these processes is necessary in order to understand the EC concentration in the snow.

Acknowledgments

This research was supported by Cryosphere–Atmosphere Interactions in a Changing Arctic Climate (CRAICC), part of the Nordic Top-level Research Initiative (TRI). The authors also acknowledge the support from the Swedish Research Council's Formas (svart och vit). We thank Professor Örjan Gustavsson and Martin Kruså, Stockholm University, for the use of the OCEC-instrument and valuable instruction of the instrument. Gustaf Peterson and Katherine Svensson are accredited for their assistance during snow sampling; and KS also for language editing.

References

Aamaas B, Bøggild C E, Stordal F, Berntsen T, Holmén K and Ström J 2011 Elemental carbon deposition to Svalbard snow from Norwegian settlements and long-range transport *Tellus* B **63** 340–51

Anenberg S C, Horowitz L W, Tong D Q and West J 2010 An estimate of the global burden of anthropogenic ozone and fine particulate matter on premature human mortality using atmospheric modeling *Environ. Health Perspect.* **118** 1189–95

Birch M E 2003 Diesel particulate matter (as elemental carbon) method 5040 *NIOSH Manual of Analytical Methods* (Cincinnati, OH: National Institute of Occupational Safety and Health)

Birch M E and Cary R A 1996 Elemental carbon-based method for monitoring occupational exposures to particulate diesel exhaust *Aerosol Sci. Technol.* **25** 221–41

Chow J C, Watson J G, Crow D, Lowenthal D H and Merrifield T 2001 Comparison of IMPROVE and NIOSH carbon measurements *Aerosol Sci. Technol.* **34** 23–34

Chow J C, Watson J G, Pritchett L C, Pierson W R, Frazier C A and Purcel R G 1993 The DRI thermal-optical reflectance carbon analysis system: description, evaluation and applications in US air quality studies *Atmos. Environ.* A **27** 1185–201

Clarke A D 1982 Integrating sandwich: a new method of measurement of the light absorption coefficient for atmospheric particles *Appl. Opt.* **21** 3011–20

Clarke A D and Noone K J 1985 Soot in the arctic snowpack: a cause for perturbations in radiative transfer *Atmos. Environ.* **19** 2045–53

Conway H, Gades A and Raymond C F 1996 Albedo of dirty snow during conditions of melt *Water Resour. Res.* **32** 1713–8

Doherty S J, Warren S G, Grenfell T C, Clarke A D and Brandt R E 2010 Light-absorbing impurities in Arctic snow *Atmos. Chem. Phys.* **10** 11647–80

Flanner M G, Zender C S, Randerson J T and Rasch P J 2007 Present day climate forcing and response from black carbon in snow *J. Geophys. Res.* **112** D11202

Forsström S, Ström J, Pedersen C A, Isaksson E and Gerland S 2009 Elemental carbon distribution in Svalbard snow *J. Geophys. Res.* **114** D19112

Grenfell T C, Doherty S J, Clarke A D and Warren S G 2011 Light absorption from particulate impurities in snow and ice determined by spectrophotometric analysis of filters *Appl. Opt.* **50** 2037–48

Hadley O L, Corrigan C E, Kirchstetter T W, Cliff S S and Ramanathan V 2010 Measured black carbon deposition on the Sierra Nevada snow pack and implication for snow pack retreat *Atmos. Chem. Phys.* **10** 7505–13

Hansen J and Nazarenko L 2004 Soot climate forcing via snow and ice albedos *Proc. Natl Acad. Sci. USA* **101** 423–8

Hyvärinen A-P *et al* 2011 Aerosol black carbon at five background measurement sites over Finland, a gateway to the Arctic *Atmos. Environ.* **45** 4042–50

Lemke P *et al* 2007 Observations: changes in snow, ice and frozen ground *Climate Change 2007: The Physical Science Basis. Contribution of Working Group I to the Fourth Assessment Report of the Intergovernmental Panel on Climate Change* (Cambridge: Cambridge University Press)

McConnell J, Edwards R L, Kok G L, Flanner M G, Zender C S, Saltzman E S, Banta J R, Pasteris D R, Carter M M and Kahl J D W 2007 20th century industrial black carbon emissions altered Arctic climate forcing *Science* **317** 1381–4

Ogren J A, Charlson R J and Grobllckl P J 1983 Determination of elemental carbon in rainwater *Anal. Chem.* **55** 1569–72

Reisinger P, Wonashütz A, Hitzenberger P, Petzold A, Bauer H, Jankowski N, Puxbaum H, Chi X and Maenhaut W 2008 Intercomparison of measurement techniques for black or elemental carbon under urban background conditions in wintertime: influence of biomass combustion *Environ. Sci. Technol.* **42** 884–9

Schwarz J P, Doherty S J, Li F, Ruggiero S T, Tanner C E, Perring A E, Gao R S and Fahey D W 2012 Assessing single particle soot photometer and integrating sphere/integrating sandwich spectrophotometer measurement techniques for quantifying black carbon concentration in snow *Atmos. Meas. Tech.* **5** 2581–92

Schwarz J P, Gao R S, Perring A E, Spackman J R and Fahey D W 2013 Black carbon aerosol size in snow *Sci. Rep.* **3** 1356

Shindell D *et al* 2012 Simultaneously mitigating near-term climate change and improving human health and food security *Science* **335** 183–9

Sterle K M, McConnell J R, Dozier J, Edwards R and Flanner M G 2013 Retention and radiative forcing of black carbon in eastern Sierra Nevada snow *Cryosphere* **7** 365–74

Wang M, Xu B, Zhao H, Cao J, Joswiak D, Wu G and Lin S 2012 The influence of dust on quantitative measurements of black carbon in ice and snow when using a thermal optical method *Aerosol Sci. Technol.* **46** 60–9

Warren S G and Wiscombe W J 1980 A model for the spectral albedo of snow. II: snow containing atmospheric aerosols *J. Atmos. Sci.* **37** 2734–45

Xu B *et al* 2009 Black soot and the survival of Tibetan glaciers *Proc. Natl Acad. Sci. USA* **106** 22114–8

Ye H, Zhang R, Shi J, Huang J, Warren S G and Fu Q 2012 Black carbon in seasonal snow across northern Xinjiang in northwestern China *Environ. Res. Lett.* **7** 044002

PAPER II

Soot-doped natural snow and its albedo — results from field experiments

BOREAL ENVIRONMENT RESEARCH 21: 481–503
ISSN 1239-6095 (print) ISSN 1797-2469 (online)

Helsinki 11 May 2016

Soot-doped natural snow and its albedo — results from field experiments

Jonas Svensson[1)]*, Aki Virkkula[1)2)3)], Outi Meinander[1)], Niku Kivekäs[1)4)], Henna-Reetta Hannula[5)], Onni Järvinen[3)], Jouni I. Peltoniemi[3)6)], Maria Gritsevich[6)3)7)], Anu Heikkilä[1)], Anna Kontu[5)], Kimmo Neitola[1)], David Brus[1)], Pavla Dagsson-Waldhauserova[8)9)10)], Kati Anttila[1)6)], Marko Vehkamäki[11)], Anca Hienola[1)], Gerrit de Leeuw[1)3)] and Heikki Lihavainen[1)]

[1)] *Finnish Meteorological Institute, P.O. Box 503, FI-00101 Helsinki, Finland (*corresponding author's e-mail: jonas.svensson@fmi.fi)*
[2)] *Institute for Climate and Global Change Research & School of Atmospheric Sciences, Nanjing University, 163 Xianlin Road, CN-210023 Nanjing, China*
[3)] *Department of Physics, P.O. Box 64, FI-00014 University of Helsinki, Finland*
[4)] *Department of Physics, Lund University, P.O. Box 118, SE-221 00 Lund, Sweden*
[5)] *Arctic Research Center, Finnish Meteorological Institute, Tähteläntie 62, FI-99600 Sodankylä, Finland*
[6)] *Finnish Geospatial Research Institute, Geodeetinrinne 2, FI-02430 Masala, Finland*
[7)] *Institute of Physics and Technology, Ural Federal University, RU-620002 Ekaterinburg, Russia*
[8)] *Faculty of Environment, Agricultural University of Iceland, Hvanneyri, IS-311 Borgarnes, Iceland*
[9)] *Departments of Physical and Earth Sciences, University of Iceland, Sæmundargata 2, IS-101 Reykjavik, Iceland*
[10)] *Czech University of Life Sciences Prague, Faculty of Environmental Sciences, Department of Ecology, Kamycka 1176, CZ-165 21, Prague, Czech Republic*
[11)] *Department of Chemistry, P.O. Box 55, FI-00014 University of Helsinki, Finland*

Received 23 Dec. 2015, final version received 6 Apr. 2016, accepted 7 Apr. 2016

Svensson J., Virkkula A., Meinander O., Kivekäs N., Hannula H.-R., Järvinen O., Peltoniemi J.I., Gritsevich M., Heikkilä A., Kontu A., Neitola K., Brus D., Dagsson-Waldhauserova P., Anttila K., Vehkamäki M., Hienola A., de Leeuw G. & Lihavainen H. 2016: Soot-doped natural snow and its albedo — results from field experiments. *Boreal Env. Res.* 21: 481–503.

Soot has a pronounced effect on the cryosphere and experiments are still needed to reduce the associated uncertainties. This work presents a series of experiments to address this issue, with soot being deposited onto a natural snow surface after which the albedo changes were monitored. The albedo reduction was the most pronounced for the snow with higher soot content, and it was observed immediately following soot deposition. Compared with a previous laboratory study the effects of soot on the snow were not as prominent in outdoor conditions. During snowmelt, about 50% of the originally deposited soot particles were observed to remain at the snow surface. More detailed experiments are however needed to better explain soot's effect on snow and to better quantify this effect. Our albedo *versus* soot parameterization agreed relatively well with previously published relationships.

Editor in charge of this article: Veli-Matti Kerminen

Introduction

Soot particles consist of black carbon (BC) and organics, originating from both anthropogenic and natural combustion sources. Once deposited onto snow surfaces, they increase absorption of solar radiation and reduce the snow's albedo (Warren and Wiscombe 1980). This leads to faster snow aging, resulting in further lowered reflectivity. With more aged snow, the effect of BC on snow and ice is further enhanced. This positive feedback leads to an earlier onset of snowmelt (Flanner *et al*. 2007).

Ambient measurements of BC in snow and ice have been conducted in different regions of the globe. For example, in the Arctic, BC concentrations in snow have been shown to be in the range of 0–100 ppb (Forsström *et al*. 2009, 2013, Doherty *et al*. 2010, Meinander *et al*. 2013, Svensson *et al*. 2013) and cause a perturbation to the radiative balance (Flanner *et al*. 2007). In Himalayan snow and ice, with a closer proximity to major emission sources, higher BC concentrations (> 100 ppb) have been measured and have been proposed to have a more pronounced negative effect on the cryosphere and the hydrological cycle (e.g., Xu *et al*. 2012, Kaspari *et al*. 2014, Qu *et al*. 2014). The same has also been observed in the snow of the European Alps (e.g. Fily *et al*. 1997, Lavanchy *et al*. 1999). However, there were only few experimental studies of the effect of BC on snow (Conway *et al*. 1996, Brandt *et al*. 2011, Hadley and Kirchstetter 2012).

Conway *et al*. (1996) mixed high amounts (0.003–0.03 kg m^{-2}) of soot (both of hydrophilic and hydrophobic character) and volcanic ash in 10 liters of snow and distributed these separate contaminant mixtures in a 2.5-cm-deep layer on top of the melting snow during the melt season on the Blue Glacier, WA, USA. Thereafter, the ablation and albedo were monitored and it was found that during the melt, the soot particles were more efficiently scavenged through the snow than the volcanic-ash particles. The soot particles were of submicron size while the volcanic ash particles were larger (> 5 μm), probably explaining the difference in scavenging efficiency. Additionally, the hydrophobic soot particles were less efficiently scavenged through the snow than the hydrophilic soot particles. Nonetheless, the remaining fraction of soot particles at the surface still caused a clear reduction in albedo (30% less for the contaminated snow compared to the natural snow) and an increase in ablation rate of 50% on the glacier surface, compared to the non-contaminated glacier surface.

The experimental approach used by Brandt *et al*. (2011) was based on two artificial snowpacks (with and without added soot) created with a snow gun on an open field. Snow samples were collected and analyzed for their BC concentration with a filter-based method (filters analyzed optically). With the combined BC concentration and the inferred snow grain size based on near-infrared albedo measurements, they calculated the albedo reduction of the snowpack in a radiative transfer model, confirming the negative effect of BC on the snowpack albedo.

Hadley and Kirchstetter (2012) produced pure and BC contaminated artificial snowpacks in a laboratory experiment to study the effects of BC on snow albedo. With BC concentrations in a wide range, BC was found to reduce snow albedo, with the BC effects amplified when the snow grain size was increased. This study also verified the widely used Snow, Ice and Aerosol Radiation (SNICAR) model (Flanner *et al*. 2007).

While Conway *et al*. (1996) focused on the mobility of soot and ash particles through the snowpack during glacier melt, using very high concentrations of impurities on the snow; Brandt *et al*. (2011) contaminated snow with 2500 ppb BC and had its albedo reduction verified in a radiative transfer model. Hadley and Kirchstetter (2012) used a range of different BC levels and snow grain sizes to confirm the reduction of BC on snow albedo in a controlled laboratory environment.

Here, we present a series of unique experiments, carried out during three consecutive winters in different regions of Finland, in which we deposited soot onto a natural snowpack. The idea was to deposit the soot in a controlled way and thereafter measure the snow albedo and monitor it throughout the melting season. Selected observations of the snow physical properties and the temporal progression of soot concentrations were also conducted. The first results of these

experiments were presented by Meinander *et al*. (2014) who showed that the BC affects the density of melting snow and by Peltoniemi *et al*. (2015) who showed that the reflectance of the soot-doped snow has a strong directional dependence. While these two papers presented selected, focused results from these experiments, the goal of the present paper is to give an overview of all the experiments, including time series of the observations, highlighting albedo and recommendations for planning future experiments based on the experiences gained.

Experiments and methods

Experiment sites

The experiments were conducted in three consecutive winters: 2011, 2012, and 2013. In 2011, they were undertaken from early March until April on a farming field in southern Finland (60°24´N, 24°42´E) near the town of Nurmijärvi, 30 km north of Helsinki. When the experiment commenced, the snowpack thickness was 50 cm and winter conditions with subzero temperatures prevailed in the area. The second experiment was conducted in another farming field at the Finnish Meteorological Institute (FMI) observatory (60°48´N, 23°30´E) in Jokioinen, southern Finland, ~100 km northwest of Helsinki, in February and March. At the start of the experiment, the snow depth at the site was 30 cm. The third experiment took place at the Sodankylä airfield (67°23´N, 26°36´E), located near the FMI Arctic Research Centre, in Sodankylä, northern Finland, in April and May 2013. The snow depth at the experimental site was 65 cm before the soot deposition started. Hereafter, the experiments in 2011, 2012, and 2013 will be referred to as SoS2011, SoS2012, and SoS2013, respectively.

Soot deposition onto the snow

Soot was deposited with different methods onto the snow surface (*see* Table 1). During SoS2011, soot particles were produced by burning various organic materials (wood and rubber pellets from used tires) in a wood-burning stove. The smoke was led through a pipe, cooled by snow surrounding the pipe, and into a rectangular chamber ($3.3 \times 7.5 \times 2.8$ m, W × L × H) standing on top of the snow (Fig. 1A). The air in the smoke was not cooled enough before entering the chamber, thus a majority of the particles escaped the chamber with the warmer air and were not deposited in the desired location on the snow. According to infrared images taken during the burning, the temperature of the surface snow inside the chamber remained below freezing (Fig. 1B), hence, melting did not occur during the soot deposition. Inside the chamber, the soot particles were deposited onto the snow surface in a heterogeneous pattern (Fig. 1C). An undisturbed reference site, with no impurities added, was established in close proximity (15 m) to the experimental chamber.

Because of the temperature gradient and the heterogeneous distribution pattern of the deposited soot particles in SoS2011, a different approach to deposit the soot was taken in SoS2012 and SoS2013. Soot was acquired beforehand from a chimney-sweeping company (Consti Talotekniikka) in Helsinki, which collected the soot from residential buildings with small-scale wood and oil burning. The soot was blown into a custom-made cylindrical chamber (diameter of 4 m) that was carefully placed on the snow surface. The blowing system consisted of a blower, a tube blowing air into a barrel filled with the soot, and a cyclone removing particles larger than about 3 μm (Fig. 2A). Since the flow did not remain constant during the blowing, the removal of larger particles with the cyclone was only achieved with moderate success, as was observed in the electron microscopic analyses (*see* section "Electron microscopic analyses").

After the deposition of soot in SoS2012, the three soot-contaminated spots were covered with 10 cm of new snow. The sensors had not even been set up to measure albedos of clean and soot-doped snow before the snowfall started. The following day high winds occurred as well. After these events all of the spots had very similar albedos and the melting time of the snow depended mostly on the amount of snow on each spot. The soot analysis of the snow samples revealed that samples collected one month later contained significantly four times less soot as

Table 1. General characteristics of SoS2011 and SoS2013 campaigns and the measurements performed. (**A**) SoS 2011, Nurmijärvi, southern Finland, 5 March 2011–12 April 2011: soot produced by burning organics in a stove was deposited onto snow surface in rectangular chamber; (**B**) SoS 2013, Sodankylä, northern Finland, 4 April 2013–2 May 2013: soot collected from a chimney was deposited onto several spots on the snow surface through a blowing system.

	Elemental carbon analysis of snow samples	Albedo	Snow stratigraphy, including: hardness, wetness, density, grain size, and shape, and temperature	Meteorological observations
A				
Date	5 March 2011	Broadband measurements continuous	1 April 2011	Continuous
Comments	Surface samples collected following soot deposition	–	Snow-pit measurements of reference snow and sooted snow area	–
Results presented in this paper	Table 2, section "Elemental carbon in SoS2013 surface snow"	Fig. 4a, section "SoS2011"	Appendixes 1–2, section "Physical snow characteristics"	Fig. 4a
B				
Date	4 April 2013–8 April 2013, 17 April 2013	Broadband measurements continuous	3 April 2013, 5 April 2013, 6 April 2013, 10 April 2013, 17 April 2013	Continuous
Comments	Sampling of all spots immediately following soot deposition; sampling of spots S5, S7, and reference area on 17 April	–	Reference snow-pit measurements on 3, 5 and 6 April; snow pits of sooted snow spots S5 and S7 on 10 April; snow pits of S5, S7 and reference snow* on 17 April	–
Results presented in this paper	Table 2, section "Elemental carbon in SoS2013 surface snow"	Fig. 4b, section "SoS2013"	Appendixes 3–10, section "Physical snow characteristics"	Fig. 4b

* reference snow location was moved due to contamination of original reference spot during soot deposition.

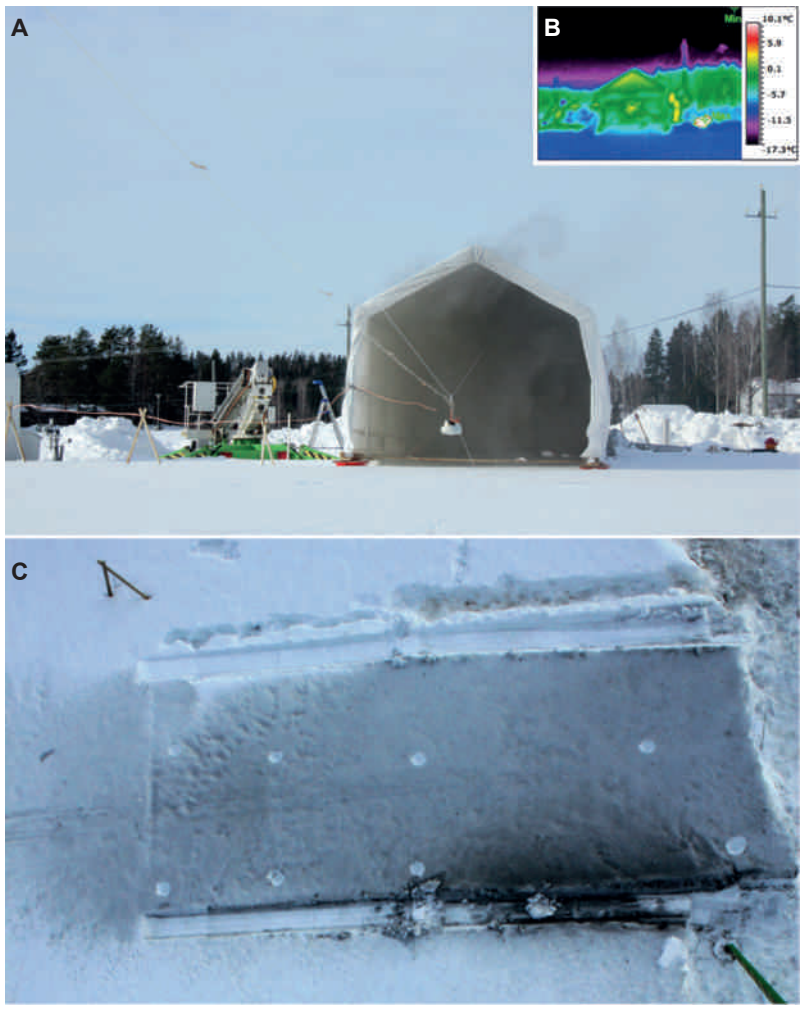

Fig. 1. Experimental set-up in SoS2011. (**A**) Soot production and deposition chamber, (**B**) thermographic infrared image of the temperature ranges during deposition, and (**C**) rectangular soot spot after removing the chamber (overhead view).

compared with the snow samples collected right after the soot deposition. We hypothesize that the snow storm removed part of the top layer, which contained the deposited soot, and therefore no clear effects of soot on snow were observed. Because of the lack of quantitative information on the soot concentration, the measurements from SoS2012 could not be analyzed and interpreted in detail, and are therefore not presented in this paper. The above description is presented here, however, to stress the importance of planning an experiment.

In 2013, several spots were made with varying amounts of soot originating from wood-burning soot (Fig. 2B), one spot by using soot from a peat-burning power plant, one spot by using soot from a residential oil burner, two spots by using glaciogenic silt from Iceland and one spot by using volcanic ash from Iceland (Fig. 2C). After depositing the impurities, pyranometers were set up above the spots (Fig. 2B) as will be described below. One spot was planned to be left as a reference spot with no added soot but it got contaminated during the soot deposition of the other spots in the afternoon of 8 April (named Ref in Table 2), which was the fifth day of measurements. A new reference site, inside the airfield, was therefore created for the post-deposition monitoring. However, no pyranometers were available for this new reference site so there are no continuous albedo data from clean reference snow in SoS2013. The spots with no albedo measurements (Fig. 2C) were created in order to make the physical characterization of

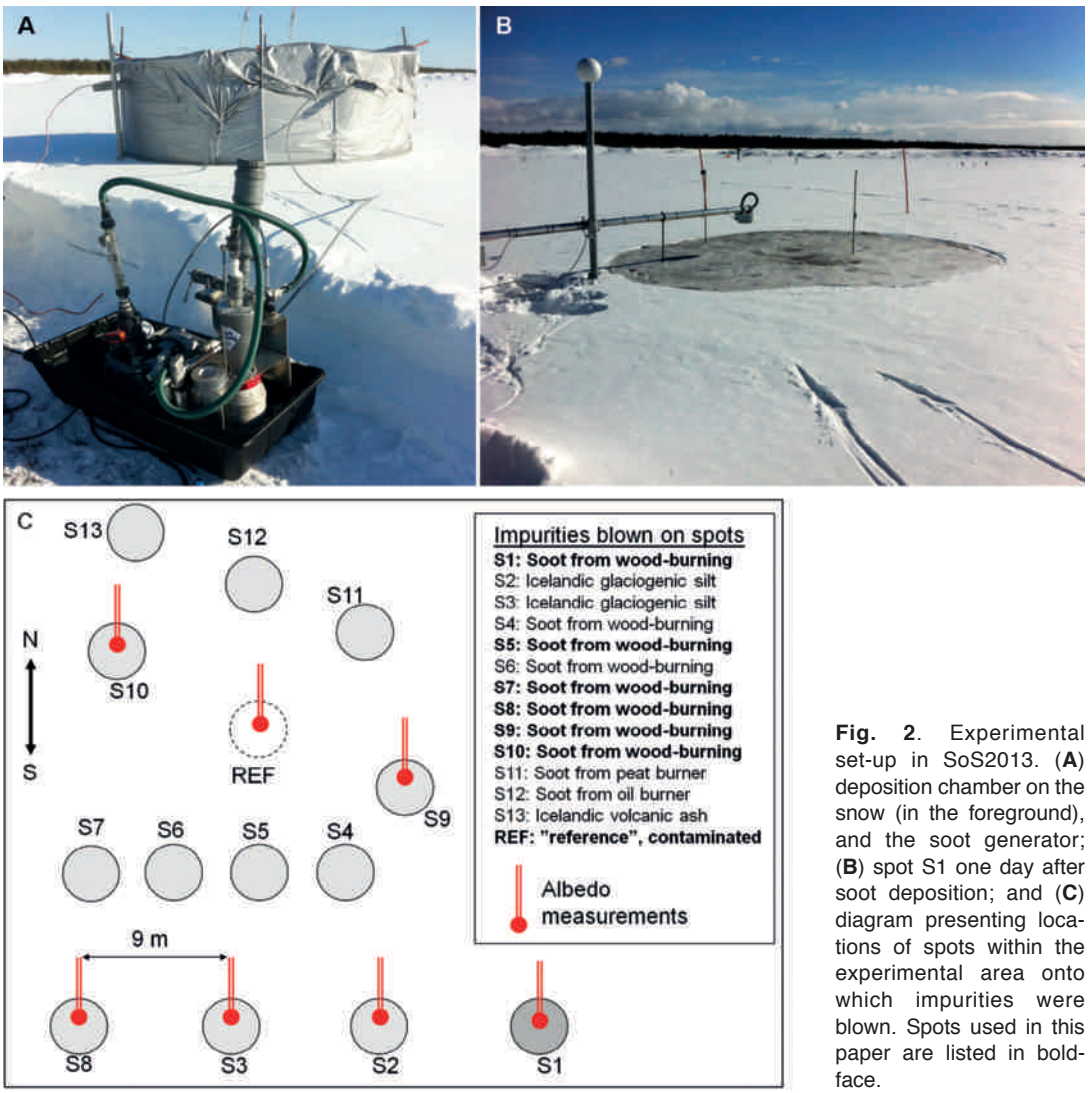

Fig. 2. Experimental set-up in SoS2013. (**A**) deposition chamber on the snow (in the foreground), and the soot generator; (**B**) spot S1 one day after soot deposition; and (**C**) diagram presenting locations of spots within the experimental area onto which impurities were blown. Spots used in this paper are listed in boldface.

Table 2. Surface snow samples and the corresponding EC concentrations, [EC], from SoS2011 and SoS201, including also the spatial variability of [EC] from each measured area or spot, depending on experiment; n/a = no albedo measurements conducted for this spot.

	Number of samples	Average [EC] (ng g^{-1})	[EC] variation (%)	Albedo after soot deposition
SoS2011				
Sooted snow area	10	20900	25	0.52
Reference snow area	6	80	39	0.83
SoS2013, spot number				
1	3	6420	35	0.41
8	4	489	40	0.75
9	4	1030	20	0.70
10	4	232	28	0.77
Ref	2	554	22	0.75
Background sample	1	46		n/a

snow and to enable snow samples to be gathered for analysis of soot content. This requires digging in the snow which would seriously affect albedo measurements. Therefore, it was planned to make duplicate spots with similar amounts of soot and set up the albedo measurement on one of the two. However, due to undetermined losses in the particle blower it turned out that it was not possible to make two spots with similar amounts of soot. The unknown losses made it also impossible to estimate the amount of glaciogenic silt and volcanic ash blown on spots S2, S3, and S13. Even though the original goal of SoS2013 was to also study the effects of the other impurities, only the effects of soot obtained from the wood-burning is discussed in the present paper.

Measurements of albedo, elemental carbon, and physical characteristics of the snow pack

Albedo measurements

Following the deposition of soot at the designated spots, albedo measurements were set up using a set of pyranometers measuring global irradiance (radiant flux in W m^{-2}) with a nominal viewing angle of 2π steradians. One of the pyranometers was installed horizontally looking upwards to measure the downwelling irradiance. Another ones, above each deposition spot, were installed horizontally looking downwards and hence recording the upwelling irradiance. In addition, one pyranometer was installed to measure the upwelling irradiance over pure snow. The albedo at each measuring spot was derived as the ratio of the upwelling to the downwelling irradiance. The pyranometers were set 30 cm above the snow surface and were thereafter lowered as snow melted throughout the experiment to maintain the same height above the snow surface. Determination of the height of the sensor was based on the requirement that the potential specular component of the reflection should emanate from the deposited surface throughout most of the day, i.e., at solar zenith angles < 80°.

The pyranometers employed in SoS2011 and in SoS2013 were CM11 and CMP6 sensors, respectively, manufactured by Kipp & Zonen B.V. The spectral range of the CM11 covers the wavelengths from 310 nm to 2800 nm, while the CMP6 covers the wavelengths from 285 nm to 2800 nm, with the spectral response close to unity throughout the whole wavelength range. Following the classification given by ISO9060:1660 (1990), CM11 and CMP6 sensors comply with the specifications defined for the secondary standards and first class instruments, respectively. In the classification defined by WMO/CIMO (WMO 2012), CM11 belongs to the category of "high quality", and CMP6 to the category of "good quality". The scale of the pyranometers used in the campaigns is traceable to World Radiometric Reference (WRR). Detailed uncertainty budgets were derived for every sensor following the guidelines given by ISO GUM (JCGM 2008), the specifications provided by ISO9060:1660 (1990) standard, and the procedure described by Kratzenberg *et al.* (2006). As a result, the expanded standard (2σ) uncertainty for CM11 sensors was found to be ±2.8% and for CMP6 sensors ±6.0%–6.1%.

The cosine response of the CM11 and CMP6 sensors is close to an ideal cosine at solar elevation angles < 10°. The error in the directional response for 1000 W m^{-2} of direct beam irradiance is less than 10 W m^{-2} for CM11 and less than 20 W m^{-2} for CMP6 at all solar zenith and azimuth angles (Kipp & Zonen 2000, 2014; C. Lee (Kipp & Zonen) pers. comm.).

Due to the large field of view of the pyranometer, reflections from the surrounding non-deposited snow surface have an impact on the measurements of reflected global radiation above the deposited area. The albedo derived using the measurement set-up described herein essentially quantifies the magnitude of this disturbance in the albedo. Measurements over pure non-deposited snow represent the reference case, whereas measurements over deposited areas yield the cases of disturbance caused by deposition.

Elemental carbon measurements in snow

In the experiments, soot (which includes BC) was spread onto the snow surface, but actual BC concentrations were not measured. The definition of BC is operational: it is measured with

optical methods, where it is assumed that the light-absorbing substance is BC. However, in this study instead of BC the concentration of Elemental Carbon (EC) was measured. EC is also defined by the method; it is measured with thermal methods [for definitions *see* e.g. Andreae and Gelenscer (2006), and Bond *et al*. (2013)]. It has been observed in several studies that EC is the most efficient light-absorbing substance in aerosols so EC and BC are often considered to be equivalent even though there is a clear difference in their definitions.

Snow samples for EC analysis were collected in 5 by 5 cm increments from each spot after the soot had been deposited (within 12 hours of deposition). In addition to this sampling in SoS2013, snow samples were collected from two spots (S5 and S7) at a later stage, specifically nine days after soot deposition. The purpose of these measurements was to observe if the soot particles would remain in the surface snow or not. This temporal study was in spots where albedo measurements were not conducted.

Collected snow samples were analyzed for Organic Carbon (OC) and EC content using a Sunset Laboratory Thermal-Optical Carbon Aerosol Analyzer (OC/EC; Birch and Cary 1996) following the filter-based method used in e.g. Forsström *et al*. (2009, 2013) and Svensson *et al*. (2013). Briefly, the frozen snow samples were melted quickly in a microwave oven and filtered through a sterilized microquartz filter, which was then analyzed with OC/EC using the latest recommended analysis protocol EUSAAR_2 (Cavalli *et al*. 2010). The analysis yields the mass of EC on the filter. The concentration in snow is calculated by dividing the EC mass by the mass of snow in the sample, yielding concentrations which are typically presented as ng of EC in g of snow, i.e., ng g^{-1}, also known as parts per billion (ppb).

Uncertainties of the filter method are related to representativeness of the punch taken for the analysis (typically 1.5 cm^2 of the filter which has an area of ~10 cm^2), and the efficiency of the filter to capture all the EC particles from the liquid sample during filtering (also known as undercatch). Based on relative standard deviation of EC concentrations measured for different filter punches from the same filter, representativeness of the filter punch has been reported to be on the order of 20% (Svensson *et al*. 2013, Ruppel *et al*. 2014). This value is based on filters with a visible gradient of impurities. From our experience, however, filters tend to have impurities uniformly distributed on their surfaces (which was the case for the majority of the filters in our experiments), resulting in a much lower difference between punches (less than 5% as in Ruppel *et al*. 2014).

Undercatch is another uncertainty issue that has been shown to take place during filtering (Ogren *et al*. 1983, Lavanchy *et al*. 1999, Doherty *et al*. 2010, Forsström *et al*. 2013, Lim *et al*. 2014, Torres *et al*. 2014). The efficiency has been shown to be very inconsistent, ranging from 10% to 95%, among different studies and methods to evaluate the efficiency of filters. Filters have been stacked on top of each other or put in series (separated) to increase the efficiency of collecting EC (or BC with optical measurement methods) particles, both of which have recently been shown to be misleading in the actual efficiency of the filters, thus indicating a higher efficiency than there actually is (Torres *et al*. 2014). Additionally, liquid samples have been measured with a different instrument (single particle soot photometer, SP2) before and after filtration to observe the amount of particles percolating through the filter (Lim *et al*. 2014, Torres *et al*. 2014). It was shown that up to 90% of the BC particles could possibly penetrate through the filter (Torres *et al*. 2014), while, in contrast, Lim *et al*. (2014) found that as little as 10% of the BC particles could be passing through the filter. This discrepancy seems to depend on the origin of the liquid sample, and consequently the BC particles in it, as well as agglomeration processes occurring between BC particles and other light-absorbing impurities such as dust in the liquid. The majority of BC particles that are percolating through the filter during filtration seem to be smaller in size (Lim *et al*. 2014). In our experiments, the size distribution of the EC particles was shifted towards the larger sizes (as many larger particles were observed in the electron microscopy images). Therefore, we claim that we had a relatively high efficiency of our filters during filtering. Nonetheless, the EC concentrations from the experiments are probably an underestimation of the true EC concentration

in the snow samples. At this time, we are unfortunately not able to quantify the underestimation of EC, however, we consider it to be < 22%, based on Forsström *et al*. (2013).

Electron microscopic analyses

In addition to the OC/EC analysis, one snow sample containing soot particles from SoS2013 was analyzed using electron microscopy at the Chemistry Department of the University of Helsinki. The sample was taken immediately after depositing the snow and transported frozen to Helsinki. There it was melted over a smooth silicon plate and dried by letting the water evaporate inside an over-pressurized, clean hood to minimize the possibility of contamination. A small amount, of ethanol (< 10 ml) was added to the snow before it was melted in order to minimize agglomeration of particles during the melting and drying. The particles were studied with a Hitachi Hi-tech S-4800 field-emission electron microscope fitted with an Oxford Instruments Inca 350 energy-dispersive X-ray microanalysis (EDS) system. Soot particles were identified as such by EDS measurements with both 5 kV and 20 kV acceleration voltages. The 5 kV measurements were used for detecting carbon and oxygen in the soot particles, and the 20 kV measurements were used to check for metals present in mineral dust, such as Na, Al, Ca, Fe. While some mixed soot/mineral particles were found, particles without mineral content were mainly used for assessing particle sizes. Soot particle sizes were spread over three orders of magnitude, from 0.1 to 10 μm in size (Fig. 3). Particles larger than 5 μm were rare and particles smaller than 1.0 μm were the most numerous. The 0.1 to 1.0 μm particles were present both as individual particles and as larger microscale agglomerates.

Snow physical characteristics measurements

In SoS2011, two snow pits were dug (one in the clean reference site and the other in the snow with the soot) on 1 April, which was approximately one month after soot deposition. In the pits, the snow stratigraphy was measured, including thickness, density, hardness (6 step hand test), grain size, and the shape (following the International Classification for Seasonal Snow on the Ground, Fierz *et al*. 2009). The grain sizes and types were determined using an 8× magnifying glass and a millimeter-scale grid. The reported snow grain size is the greatest extension of a grain.

In SoS2013, the snow characteristics of the snowpack were recorded at a few different sites before the soot deposition. During melting, another set of observations were made at two spots (S5 and S7) and a reference area to record effects of the BC on the snow properties. The snow pits were dug in a similar manner as in SoS2011 with slight differences in the methodology of grain size determination. The snow layers were first defined based on visual and manual detection of density, hardness, and grain size differences. For each separate layer, the hardness index, wetness index, and snow grain type were defined following Fierz *et al*. (2009). Each snow pit had its temperature profile (every 10 cm) and a density profile (every 5 cm) recorded. For snow grain-size determination, a small sample of snow for each layer was macro-photographed against a 1 mm grid. From the photographs, the average, minimum, and maximum diameter of a 'typical' snow grain was then visually estimated to the closest 0.25 mm.

Results and discussion

Albedo

The time resolution of the raw albedo data was one minute, but here the temporal evolution of the albedo from the contaminated and clean snow is presented as 1-h averages at solar noon ± 30 minutes (Fig. 4). The temperature and the daily precipitation time series were also plotted for both experiments to help in the interpretation of albedo variations. Unfortunately, temperature and precipitation were not measured in the immediate vicinity of the experimental fields: the 2011 weather data originate from the FMI measurements at the Helsinki-Vantaa airport about 17 km east-southeast of the experiment, and the 2013 data from the FMI Sodankylä observatory about 3.5 km south of the site.

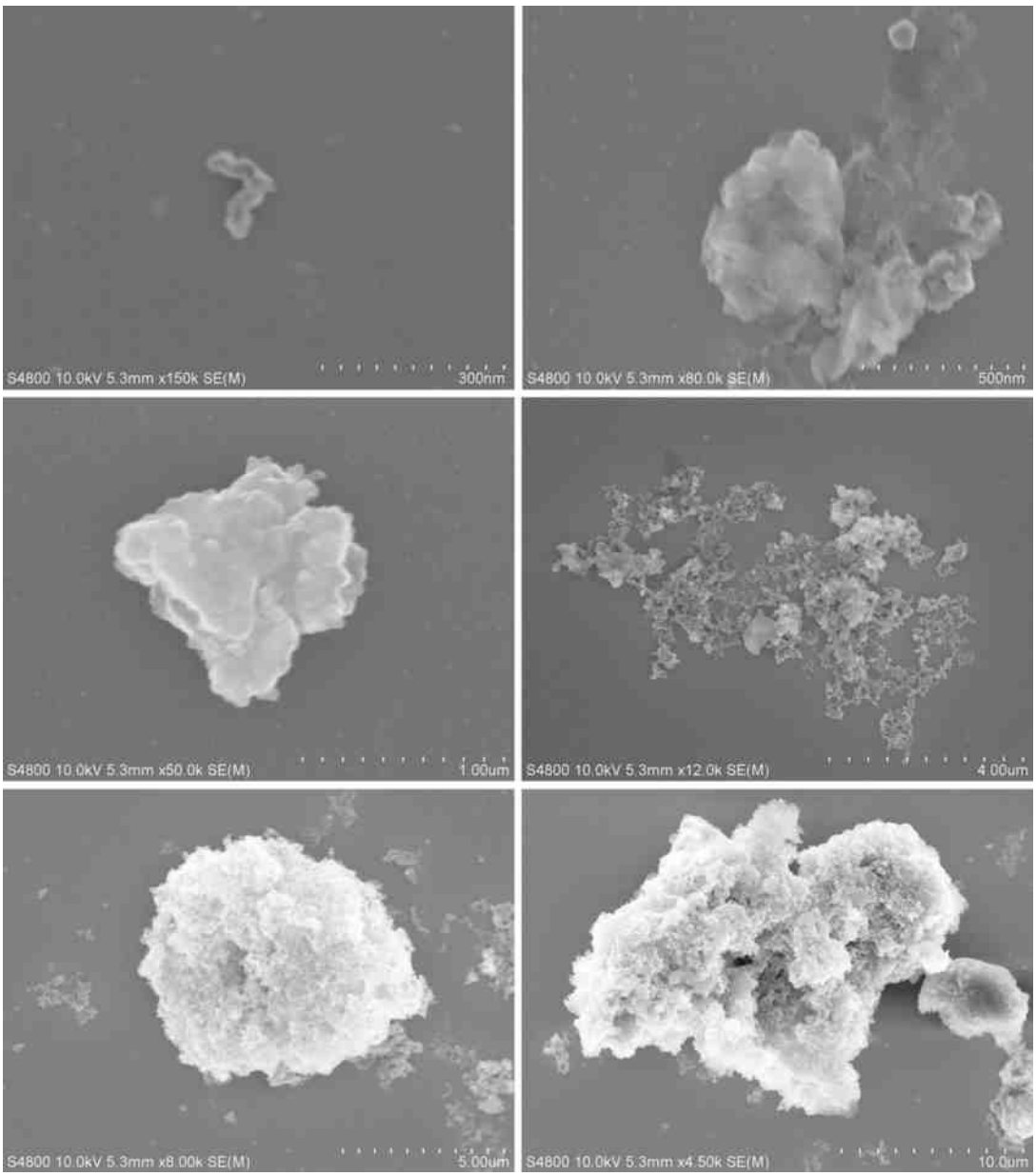

Fig. 3. SEM images of soot particles of various sizes originating from chimney sweeping of wood-burning residential homes, deposited onto spot 1 in SoS2013.

SoS2011

After the soot deposition, the snow-surface albedo dropped to 0.52, while the albedo of the reference snow was 0.83 (Fig. 4a). At this time, the average corresponding EC concentrations of the soot-doped-snow and clean-snow surfaces were 20 900 ng g^{-1} and 80 ng g^{-1}, respectively (Table 2). The albedo of the soot-covered snow decreased the next day to 0.39, after which it increased for two days, and thereafter reached a minimum value of 0.35 on 10 March. During the same period, the reference-snow albedo increased to 0.86 on the second day of measurements, and thereafter had some small fluctuations until it reached 0.80 on 10 March. A pos-

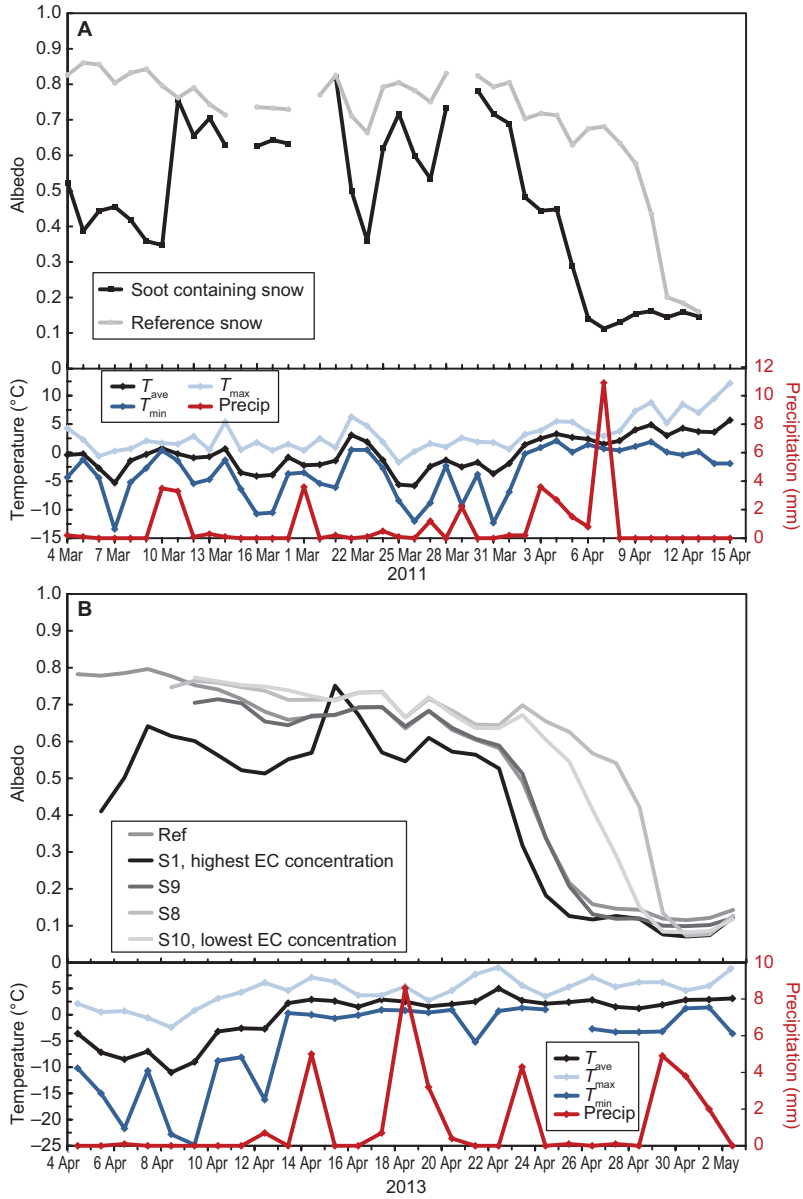

Fig. 4. Albedo time series and meteorological conditions during the experiments: (**A**) SoS2011 and (**B**) SoS2013.

sible explanation for the rapid decrease of the soot-containing-snow albedo is that the daytime temperatures were often close to or above zero, which would imply heating of snow and grain size growth. With larger snow grains the albedo-reducing effect of soot is further increased (Warren and Wiscombe 1980, Hadley and Kirchstetter 2012).

Snowfall on 10 and 11 March resulted in an increase of the albedo of the sooted snow to 0.76, while that of the reference decreased to 0.76 during the same time. Our hypothesis is that the newly-fallen snow had an albedo of 0.76, which was observed in both of the snow patches. Following this event, the albedo of the sooted snow decreased somewhat and remained in the range of 0.7–0.6 for the following week, while the albedo of the reference snow was about 10% higher at that time. Another major snowfall event on 19 March covered the pyranometers, resulting in the data gap on 19–20 March. During this event, the snow accumulated

onto the upward-looking sensor preventing the instrument from proper collection of photons, resulting in the irradiance values close to zero, and consequently albedo values exceeding unity. After cleaning the pyranometers on 21 March the albedo increased to 0.82 and 0.83 for the sooted and the reference snow, respectively. During the subsequent two days, a rapid decrease in the albedo of the sooted snow occurred, while that of the reference snow did not decease to the same degree. A possible explanation for the decrease of the sooted snow albedo is that the soot below the fresh snow absorbed solar radiation which increased melting of the new snow. This also led to a higher temperature and again morphological changes in the fresh snow above the soot layer. The rapid decrease in albedo during this period was enhanced by the meteorological conditions, as the temperature reached above 0 °C (for both average and minimum), which promotes snow grain growth and an ensuing decrease in albedo.

Similar events, with new snow, occurred later with the albedo fluctuating until 2 April, when snowmelt started and the albedo steadily decreasing until the snowpack was completely gone on 6 April. This was not the case for the reference snow as the albedo remained in the range of 0.81–0.68 between 1 and 7 April. The rapid decrease started after this date and on 11 April the albedo was down to 0.2, with the entire snowpack melted at that time.

SoS2013

After soot deposition, the albedo was the lowest at the spots with the highest amount of soot and vice versa, the albedo was the highest at the spots with the lowest amount of soot (*see* Table 2 for EC concentrations of the different spots). There were differences and similarities in the albedo time series of SoS2013 and SoS2011. Probably the most obvious difference was at the beginning of the experiment. The albedo time series (Fig. 4B) shows a sharp increase of 0.23 in the albedo of the most contaminated spot during the first two measurements days of SoS2013, just opposite to the decreasing albedo of the dark spot of SoS2011. This increase in SoS2013 could be explained by the fact that after deposition, the soot particles sunk into the snow surface, within minutes of deposition, as visually observed and further described in Peltoniemi *et al*. (2015). The soot particles sunk during the day at elevated solar radiation, and thereafter stopped sinking during the nights when the temperature was well below zero (indicated by the temperature minimum in Fig. 4b). There was a minor snowfall on 6 April which may have contributed to the increase in albedo as well. The albedo started to decrease again on the third day of measurements for the most contaminated spot. On 14 April, a snow shower put few centimeters of fresh snow on the snowpack. A distinct increase in the albedo was observed between 14 and 15 April for the most contaminated spot. This increase was not as pronounced for the other spots. Similar to the snowfall events in SoS2011, the melting of the fresh snow and decrease in albedo occurred fastest on the spot where the soot concentration was highest. It was also around this time (14 April 2013) that the melting accelerated as the average temperature remained above 0 °C for the remaining part of the experiment. The snow depth was approximately 50 cm on 15 April, while on 17 April it had decreased to roughly 35 cm. Another event with an increase in the albedo, visible in all spots, occurred on 18 and 19 April. During this time the pyranometer sensors were all lowered by 20 cm, which could potentially explain the albedo increase.

On 22 April, the albedo began to decrease rapidly starting with the spot with the highest BC concentration changing its albedo from 0.55 to 0.15 during 72 hours. The spots with lower BC concentrations followed this rapid decrease in albedo a few days later. The temporal variation of the albedo at Spot S9 (second highest EC concentration) and the contaminated reference spot (named Ref in Fig. 4B) were nearly identical during this fast albedo reduction. The albedo decreased earlier at the spot with the lowest EC concentration (S10) than at the spot with the second lowest EC concentration (S8). However, since at this time snow samples were not collected for determination of the EC concentrations for these spots, those concentrations are unknown. Further, it is unclear to what extent BC affected snowmelt (especially with lower EC concentrations) when the snowpack height was

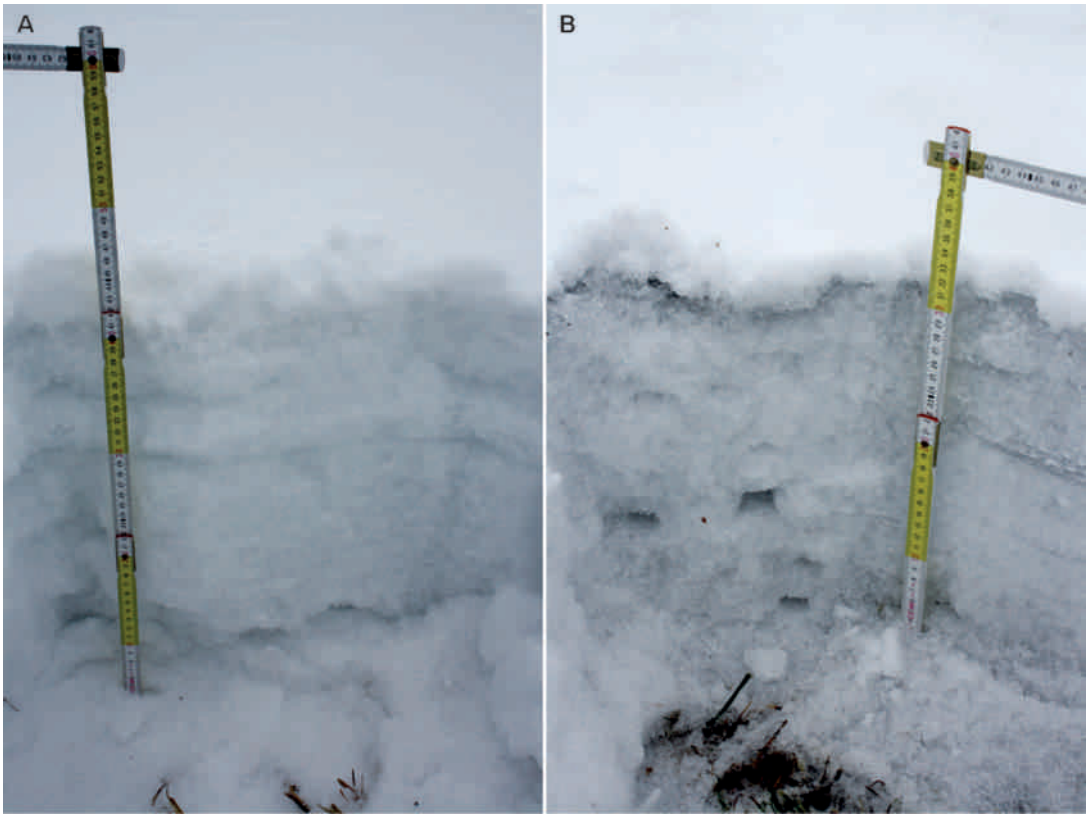

Fig. 5. Snow pits from SoS2011. (**A**) Reference snow about one month after deposition of the soot onto the snow in SoS2011, and (**B**) Soot-contaminated snow at the same time.

smaller than ~30 cm, when one would expect the albedo of the underlying ground to have a significant effect on snow melt.

Physical snow characteristics

In SoS2011, the melting rates of the snow at the reference site and at the soot-contaminated spot were 3 cm and 7 cm per day, respectively. From the snow pits dug and studied one month after soot deposition in SoS2011, it was evident that the snow containing the soot had changed more than the reference snow (Appendixes 1 and 2, Fig. 5). Although, no snow-pit measurements were performed before soot deposition it is very likely that those changes were due to the deposited soot since the snow pits were only 15 m apart on a homogenous farming field and the EC concentrations were high. As no other snow pits were dug, it cannot, however, be considered proven. The soot-doped snow had transformed to a more homogenous snowpack containing rounded polycrystal snow grains, whereas the grain shapes of the reference snow were more heterogeneous. Similarly, the hardness test revealed a more uniform pattern in the sooted snow, while the reference site was more diverse. The snow depth for the dirty snowpack was at that time 35 cm, while the clean snow had a depth of 50 cm. Both of the pits had a layer of freshly fallen snow (4-cm deep at the reference site and 2-cm deep at the sooted snow), containing 0.5-mm snow grains. The grain size of the remaining snow was 2 mm, except for the bottom 5 cm at the reference site, where it was 1 mm. The snow density for the two snow pits was practically the same. It varied between 340 and 400 kg m^{-3} in the top part of the snowpack and was 460 kg m^{-3} at the bottom. Since the snowpack had brittle layers and also some very loose layers, it was difficult to conduct the

density measurements and therefore only few density data were obtained.

Before the soot deposition in SoS2013, the density in the surface layer varied between 0.208 and 0.290 g cm^{-3}, with an average of 0.247 g cm^{-3} for the three pits measured before applying the soot to the snow (Appendixes 3–7). Irregular precipitation particles were visible in the top centimeters of those pits, after which rounded faceted crystals were present before the depth hoar grains in the bottom of the snowpack. The average visual grain sizes in the top layer was 0.25 mm and 0.5 mm, followed by 0.75 mm and 1 mm in the subsequent layer (grain size measurements were conducted for two out of the three pits sampled before soot deposition). By 10 April 2013, snow-pit measurements in two of the sooted spots (S5 and S7) revealed that the precipitation particles in the surface layers had melted and a hard melt-freeze layer had developed near the snow surface (Appendixes 8–11). The average surface grain sizes at these spots were estimated to be 0.5 mm and 1 mm, respectively. In addition, larger aggregates produced by snow grains melting and refreezing together were found near the surface. Snow-pit measurements made two days earlier in the nearby mire and forested areas, revealed the same kind of snow stratification, which would indicate that the melt-freeze layers were not only produced by the presence of light absorbing impurities but were caused by the changes in the weather conditions as well. It is, however, hypothesized that the impurities may enhance the development of surface crusts by enhancing the snow melt during the sunny hours, while the air temperature still drops below zero at nighttime. The snow characteristics of spots S5 and S7 plus a clean reference snow were measured again on 17 April 2013. At that time, snowmelt had already started with the temperature of the whole snowpack being 0 °C, and snow grain types of rounded melt forms were recorded (Appendixes 12–17). The average surface grain size in all three spots was estimated to be 1 mm.

During SoS2013, we observed that the soot containing snow lowered the density of melting snow (Meinander *et al*. 2014). We also observed that light-absorbing impurities deposited on the snow enhance the immediate metamorphosis under strong sunlight (Peltoniemi *et al*. 2015). After soot deposition, the contaminated snow surface was darker than the pure snow in all viewing directions, but as stated above, we observed the soot particles sinking into the snow, thus increasing its surface roughness.

Elemental carbon in SoS2013 surface snow

For the two spots (S5 and S7) which were used for the temporal study of the soot particles, we calculated the EC mass concentrations in the surface layers, by multiplying the EC concentration in the surface layer with the surface density of the snow, and also by subtracting the background EC mass concentration in the reference snow surface layer (Appendix 7). Since the density of the surface layer was not measured in S7, the average density from all snow surface layer (0–5 cm) measurements before soot deposition was used in these calculations.

The EC mass concentrations on 10 April could thereafter be compared with the EC mass concentrations from surface samples collected on 17 April, and thus provide a fraction of the EC particles which had remained in the surface layer during this time while melting had occurred.

On 10 April, the EC mass concentration was 374 ng cm^{-3} for S5 (Appendix 9) and 323 ng cm^{-3} (Appendix 11) for S7. After the seven day period, the EC mass concentration was 233 ng cm^{-3} for S5 (Appendix 15), while in the surface layer of S7 then EC mass concentration was 154 ng cm^{-3} (Appendix 17). In other words, 48% of the EC particles had remained in the surface layer during this period in S7, while 62% of the EC particles remained in S5. Using a lower background EC mass concentration, from a snow sample collected a few kilometers away from the FMI observatory and which had not been at risk of contamination, we calculated that 56% of the EC particles remained at the surface in S7, while the number was 70% for S5, hence providing upper estimates for the amount of particles remaining in the surface snow during melt.

Based on our values, about half of the initial soot which had been deposited to the snow sur-

face had been removed. In Conway *et al*. (1996), where hydrophobic and hydrophilic soot was also investigated to observe movement of the soot particles, about 50% of the initial hydrophobic soot had been flushed through the snowpack after 10 days, while the hydrophilic soot had 1% of the initial soot remained in the upper 50 cm of the snowpack. In comparison, ambient measurements have shown that confined to the top centimeters of the snowpack, the BC concentrations in the snow during the melt have been found to increase by a factor of 2–7 (Doherty *et al*. 2013, Sterle *et al*. 2013). Doherty *et al*. (2013) found an even higher amplification factor of ~10–15, when the melting-snow BC concentrations were compared with the concentrations measured earlier in the year at a site near Dye-2, on the Greenland ice sheet.

Parameterization and comparison with previous works

The albedo measured during the first three days of the SoS experiments was plotted against the EC concentration, [EC] (Fig. 6). Fitting was done using the following function:

$$\text{albedo} = b \times [\text{EC}]^c + d, \qquad (1)$$

where b, c and d are the fitting parameters. Different fittings were made by excluding and including the most contaminated spot from SoS2011, for individual days 1, 2 and 3, as well as for the all three days together (Table 3). In all fittings the highest albedo was that of the reference spot in SoS2011, 0.83 ± 0.02 (based on the 1-week average). A similar function was also used in a recent BC snow-modeling effort by Hienola *et al*. (2015).

Data from Hadley and Kirchstetter (2012) and Pedersen *et al*. (2015) are also presented in Fig. 6 for comparison. The work of Pedersen *et al*. (2015) was based on measurements of EC concentrations and the corresponding spectral albedo of the snow. They parameterized their spectral data essentially with the same function as ours (Eq. 1) but presented the resulting curve for the broadband albedo only in a figure (Pedersen *et al*. 2015: fig. 8). We digitized their fig. 8, fitted the function (Eq. 1), and obtained b = 0.001049 and c = 0.6334 for cloudy conditions, and b = 0.0009190 and c = 0.6332 for clear-sky conditions that describe the dependence on EC concentration. The corresponding lines were then forced to go through our reference albedo *versus* EC point to get the factor d in Eq. 1 (Fig. 6). It is evident that our experimental data agree quite well with those of Pedersen *et al*. (2015).

The behavior of albedo with EC concentration in the SoS experiments also seems to generally follow that observed in the laboratory study by Hadley and Kirchstetter (2012). It especially applies for the two lower snow grain sizes used in their experiments (110 and 130 μm), while their grain size of 220 μm showed a greater albedo reduction with similar EC concentrations (Fig. 6). Thus, our experiments show how the effects of BC on natural snow in outdoor conditions are not as pronounced as those in the laboratory conditions used in Hadley and Kirchstetter (2012). Since their laboratory study applies to a solar zenith angle of 0°, when the albedo reduction due to BC is the strongest, it is in agreement with our outdoor light conditions, where the solar zenith angle is different.

Table 3. Parameters *b*, *c* and *d* obtained by fitting Eq. 1 to the observations. ExclDS11 = fitting excluding the dark spot in 2011, and InclDS11 = fitting including the dark spot in 2011.

	Day 1		Day 2		Day 3		Days 1–3	
	ExclDS	InclDS11	ExclDS11	InclDS11	ExclDS11	InclDS11	ExclDS11	InclDS11
b	–0.140	–2.557	–0.127	–0.257	–0.425	–0.085	–0.150	–0.358
c	0.617	0.028	0.545	0.275	0.100	0.489	0.455	0.185
d	0.851	3.238	0.851	0.965	1.152	0.827	0.868	1.062

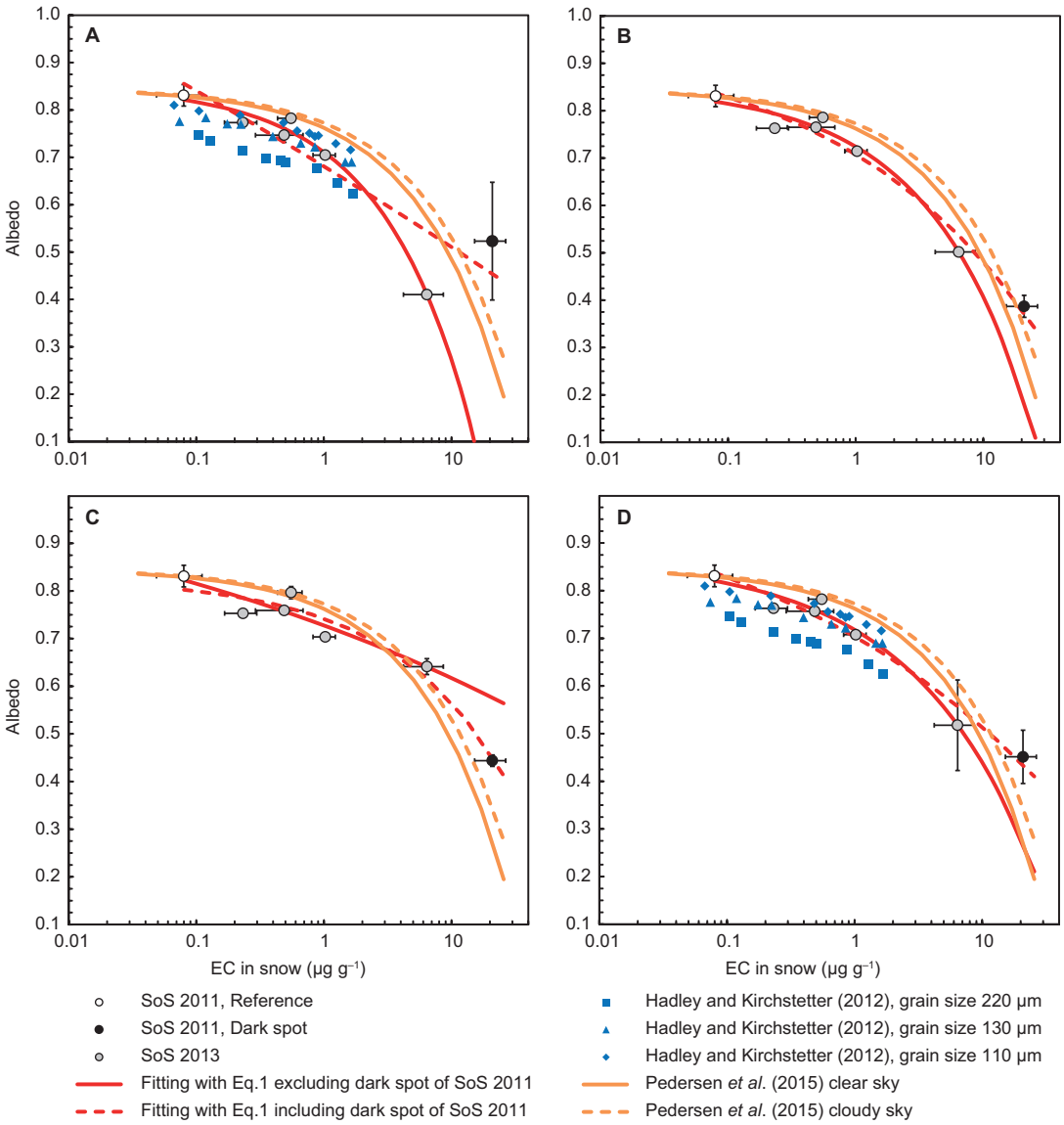

Fig. 6. Broadband albedos at noon on days 1–3 as a function of the EC concentration in the surface layer: (**A**) day 1, (**B**) day 2, (B) day 3, and (**D**) days 1–3. In all plots, the SoS2011 reference albedo is the average over solar noon albedos during the first week of the experiment. In **A–C,** the gray and black circles are 60-minute albedo averages at solar noon, the vertical and horizontal bars are standard deviations for albedo and EC, respectively. In **D,** the circles are the albedo averages at solar noon of the days 1–3, and the vertical and horizontal bars are standard deviations for albedo and EC, respectively.

Conclusions and recommendations for the future

In our soot on snow experiments it was found that BC has an effect on the broadband albedo of natural snow. This has been verified in controlled, laboratory studies and with artificial snowpacks, but to our knowledge no such results have been published from field experiments using natural snow and dry deposition of soot. With higher amounts of soot we observed a greater reduction in snow albedo than with lower soot concentrations. It was further observed that the BC effect on snow may be masked by

deposition of new snow, burying the original soot layer in the snowpack. Melting of the newly-added snow progressed faster for the snow patch containing the buried soot layer, however, than for the reference snow where no impurities were added.

With the approach used in our experiments certain challenges were present. For example, at low soot concentrations it would be difficult to observe the BC effect clearly since snow albedo depends on many other parameters, particularly snow grain size. In parts-per-billion concentrations of soot (on the order of 10's) in the snow, which has been reported in the Arctic snowpack (e.g. Doherty *et al*. 2010), the albedo reduction caused by the BC is so small that any measured albedo reduction could be caused by the uncertainties introduced when carrying out an experiment of this nature. Performing the experiments outdoors brought additional natural challenges such as non-ideal meteorological conditions as well as different solar circumstances, which cannot be reproduced in laboratory facilities. Nevertheless, our goal was to conduct these experiments since it had not been done before. BC in snow still requires experimental studies in order to better constrain the BC forcing on snow and to improve the process understanding associated with BC in the snow.

The soot particles did not all remain on the snow surface with time. About half of the initial soot amount was in the surface layer after seven days of melting. These numbers can be considered qualitative since several uncertainties exist. Additional experiments are needed to deliver sound quantitative numbers on this topic.

The experience gained during the three SoS experiments leads to the following recommendations for future studies:

1. To avoid surface effects on the melting rate, experimental spots should be located where the underlying surface albedo is spatially homogeneous and preferably high.
2. As it is difficult to deposit soot onto the snow in a controlled way with the two methods used here, a development of different blowing system should be considered.
3. The measurements should be commenced immediately after soot deposition. It was observed that within minutes the soot start to interact with the snow crystals (especially during sunny days), as the particles sunk into the snow immediately following deposition.
4. More detailed observations of the physical snow properties are needed to study the temporal dynamics of BC in the snowpack, and to more accurately provide quantitative numbers on the process of BC sticking at the snow surface.
5. Broadband albedo measurements should be compared with the spectral albedo measurements of soot-contaminated snow to better constrain the BC effect on snow albedo.

Acknowledgements: We would like to thank Antti Aarva for helping us with numerous issues throughout these experiments. The work of the technical staff at FMI, Sodankylä, during SoS2013 is very much appreciated. The Chimney sweeping company (Consti Talotekniikka Oy) is acknowledged for supplying us with the soot. The authors wish to acknowledge Mr. Markku Sinkkonen at Vaisala Oyj and Mr. Clive Lee at Kipp & Zonen for providing the information needed for the compilation of the uncertainty budgets for the pyranometers. Mr. Timo Vainio is acknowledged for the use of his farming field in SoS2011 and Mrs. Anita Virkkula for preparing the experimental chamber. We would also like to thanks Odelle Hadley and Thomas Kirchstetter for sharing their data. This work has been supported by the Academy of Finland through the projects: Arctic Absorbing Aerosols and Albedo of Snow (project no. 3162), and the Electromagnetic Wave Scattering in a Complex Random Medium (project no. 260027). This work has also been supported by the EU LIFE+ project MACEB (project no. LIFE09 ENV/FI/000572the European Commission ERC Advanced Grant No. 320773 (SAEMPL); the Maj and Tor Nessling Foundation (projects 2012456 and 2013093); the KONE foundation; and the Nordic research and innovation initiative Cryosphere-Atmosphere Interactions in a Changing Arctic Climate (CRAICC). Research at the Ural Federal University is supported by the Act 211 of the Government of the Russian Federation, Agreement No. 02.A03.21.0006.

References

Andreae M.O. & Gelencsér A. 2006. Black carbon or brown carbon? The nature of light-absorbing carbonaceous aerosols. *Atmos. Chem. Phys.* 6: 3131–3148.

Birch M.E. & Cary R.A. 1996. Elemental carbon-based method for monitoring occupational exposures to particulate diesel exhaust. *Aerosol. Sci. Tech.* 25: 221–241.

Bond T.C., Doherty S.J., Fahey D.W., Forster P.M., Berntsen T., DeAngelo B.J., Flanner M.G, Ghan S., Kärcher B., Koch D., Kinne S., Kondo Y., Quinn P.K., Sarofim M.F., Schultz M.G., Schulz M., Venkataraman C., Zhang H.,

Zhang S., Bellouin N., Guttikunda S.K., Hopke P.K., Jacobson M.Z., Kaiser J.W., Klimont Z., Lohmann U., Schwarz J.P., Shindell D., Storelvmo T., Warren S.G. & Zender C.S. 2013. Bounding the role of black carbon in the climate system: a scientific assessment. *J. Geophys. Res.* 188: 5380–5552.

Brandt R.E., Warren S.G. & Clarke A.D. 2011. A controlled snowmaking experiment testing the relation between black-carbon content and reduction of snow albedo. *J. Geophys. Res.* 116, D08109, doi:10.1029/2010JD01533.

Cavalli F., Viana M., Yttri K.E., Genberg J. & Putaud J.-P. 2010. Toward a standardised thermal-optical protocol for measuring atmospheric organic and elemental carbon: the EUSAAR protocol. *Atmos. Meas. Tech.* 3: 79–89.

Clarke A.D. & Noone K.J. 1985. Soot in the Arctic snowpack: a cause for perturbations in radiative transfer. *Atmos. Environ.* 19: 2045–2053.

Conway H., Gades A. & Raymond C.F. 1996. Albedo of dirty snow during conditions of melt. *Water Resour. Res.* 32: 1713–1718.

Doherty S.J., Warren S.G., Grenfell T.C., Clarke A.D. & Brandt R.E. 2010. Light-absorbing impurities in Arctic snow. *Atmos. Chem. Phys.* 10: 11647–11680.

Doherty S.J., Grenfell T.C., Forsstrom S., Hegg D.L., Brandt R.E. & Warren S.G. 2013. Observed vertical redistribution of black carbon and other insoluble light-absorbing particles in melting snow. *J. Geophys. Res.* 118: 1–17.

Fierz C., Armstrong R.L., Durand Y., Etchevers P., Greene E., McClung D.M., Nishimura K., Satyawali P.K. & Sokratov S.A. 2009. *The international classification for seasonal snow on the ground*. IHP-VII Technical Documents in Hydrology no. 83, IACS Contribution no. 1, UNESCO-IHP, Paris.

Fily M., Bourdelles B., Dedieu J.P. & Sergent C. 1997. Comparison of in situ and Landsat Thematic Mapper derived snow grain characteristics in the Alps. *Remote Sens. Environ.* 59: 452–460.

Flanner M.G., Zender C.S., Randerson J.T. & Rasch P.J. 2007. Present-day climate forcing and response from black carbon in snow. *J. Geophys. Res.* 112, D11202, doi:10.1029/2006JD008003.

Forsström S., Ström J., Pedersen C.A., Isaksson E & Gerland S. 2009. Elemental carbon distribution in Svalbard snow. *J. Geophys. Res.* 114, D19112, doi:10.1029/2008JD011480.

Forsström S., Isaksson E., Skeie R.B., Ström J., Pedersen C.A., Hudson S.R., Berntsen T.K., Lihavainen H., Godtliebsen F. & Gerland S. 2013. Elemental carbon measurements in European Arctic snow packs. *J. Geophys. Res.* 118: 13614–13627.

Hadley O.L. & Kirchstetter T.W. 2012. Black-carbon reduction of snow albedo. *Nat. Clim. Change* 2: 437–440.

Hienola A.I., O'Donnell D., Pietkäinen J-K., Svensson J., Lihavainen H., Virkkula A., Korhonen H. & Laaksonen A. 2015. The radiative impact of Nordic anthropogenic black carbon. *Tellus* 68, 27428, doi:/10.3402/tellusb.v68.27428.

ISO9060:1990 1990. *Solar energy — specification and classification of instruments for measuring hemispherical solar and direct solar radiation*. International Organization for Standardization.

JCGM 2008. *Guide to the expression of uncertainty in measurement (ISO/IEC Guide 98-3:2008), ISO GUM 1995 with minor corrections*, 1st ed. Available at http://www.iso.org/sites/JCGM/GUM/JCGM100/C045315e-html/C045315e.html?csnumber=50461.

Kaspari S., Painter T.H., Gysel M., Skiles S.M. & Schwikowski M. 2014. Seasonal and elevational variations of black carbon and dust in snow and ice in the Solu-Khumbu, Nepal and estimated radiative forcings. *Atmos. Chem. Phys.* 14: 8089–8103.

Kipp & Zonen 2000. *Instruction manual CM11 & CM14 Series Pyranometer/Albedometer*, ver. 1104. Kipp & Zonen, Delft, Holland.

Kipp & Zonen 2014. *Instruction manual CMP & CMA Series Pyranometer/Albedometer*, ver. 1401. Kipp & Zonen, Delft, Holland.

Kratzenberg M., Beyer H., Colle S. & Albertazzi A. 2006. Uncertainty calculations in pyranometer measurements and application. In: *ASME 2006 International Solar Energy Conference (ISEC2006), July 8–13, Denver, Colorado, U.S.A.*, American Society of Mechanical Engineers, paper ISEC2006-99168, pp. 689–698, doi:10.1115/ISEC2006-99168.

Lavanchy V.M.H., Gäggler H.W., Schotterer U., Schwikowski M. & Baltensperger U. 1999. Historical record of carbonaceous particle concentrations from a European high-alpine glacier (Colle Gnifetti, Switzerland). *J. Geophys. Res.* 104: 21227–21236.

Lim S., Faïn X., Zanatta M., Cozic J., Jaffrezo J.-L., Ginot P. & Laj P. 2014. Refractory black carbon mass concentrations in snow and ice: method evaluation and inter-comparison with elemental carbon measurement. *Atmos. Meas. Tech.* 7: 3307–3324.

Meinander O., Kontu A., Virkkula A., Arola A., Backman L., Dagsson-Waldhauserová P., Järvinen O., Manninen T., Svensson J., de Leeuw G. & Leppäranta M. 2014. Brief communication: Light-absorbing impurities can reduce the density of melting snow. *The Cryosphere* 8: 991–995.

Meinander O., Kazadzis S., Arola A., Riihelä A., Räisänen P., Kivi R., Kontu A., Kouznetsov R., Sofiev M., Svensson J., Suokanerva H., Aaltonen V., Manninen T., Roujean J.-L. & Hautecoeur O. 2013. Spectral albedo of seasonal snow during intensive melt period at Sodankylä, beyond the Arctic Circle. *Atmos. Chem. Phys.* 13: 3793–3810.

Ogren J.A., Charlson R.J. & Grobllckl P.J. 1983. Determination of elemental carbon in rainwater. *Anal. Chem.* 55: 1569–1572.

Pedersen C.A., Gallet J.-C., Ström J., Gerland S., Hudson S.R., Forsström S., Isaksson E. & Berntsen T.K. 2015. In situ observations of black carbon in snow and the corresponding spectral surface albedo reduction. *J. Geophys. Res.* 120: 1476–1489.

Peltoniemi J.I., Gritsevich M., Hakala T., Dagsson-Waldhauserová P., Arnalds Ó., Anttila K., Hannula H.-R., Kivekäs N., Lihavainen H., Meinander O., Svensson J., Virkkula A. & de Leeuw G. 2015. Soot on Snow experiment: bidirectional reflectance factor measurements of contaminated snow. *The Cryosphere* 9: 2323–2337.

Qu B., Ming J., Kang S.-C., Zhang G.-S., Li Y.-W., Li C.-D.,

Zhao S.-Y., Ji Z.-M. & Cao J.-J. 2014. The decreasing albedo of the Zhadang glacier on western Nyainqentanglha and the role of light-absorbing impurities. *Atmos. Chem. Phys.* 14: 11117–11128.

Rypdal K., Rive N., Berntsen T.K., Klimont Z., Mideksa T.K., Myhre G. & Skeie R.B. 2009. Costs and global impacts of black carbon abatement strategies. *Tellus* 61B: 625–641.

Ruppel M.M., Isaksson E., Ström J., Beaudon E., Svensson J., Pedersen C.A. & Korhola A. 2014. Increase in elemental carbon values between 1970 and 2004 observed in a 300-year ice core from Holtedahlfonna (Svalbard). *Atmos. Chem. Phys.* 14: 11447–11469.

Skeie R.B., Berntsen T.K., Myhre G., Pedersen C.A., Ström J., Gerland S. & Ogren J.A. 2011. Black carbon in the atmosphere and snow, from pre-industrial times until present. *Atmos. Chem. Phys.* 11: 6809–6836.

Sterle K.M., McConnell J.R., Dozier J., Edwards R. & Flanner M.G. 2013. Retention and radiative forcing of black carbon in eastern Sierra Nevada snow. *The Croysphere* 7: 365–374.

Svensson J. Ström J., Hansson M., Lihavainen H. & Kerminen V.-M. 2013. Observed metre scale horizontal variability of elemental carbon in surface snow. *Environ. Res. Lett.* 8, 034012, doi:10.1088/1748-9326/8/3/034012.

Torres A., Bond T.C., Lehmann C.M.B., Subramanian R. & Hadley O.L. 2014. Measuring organic carbon and black carbon in rainwater: evaluation of methods. *Aerosol Sci. Technol.* 48: 239–250.

Warren S.G. & Wiscombe W.J. 1980. A model for the spectral albedo of snow. II: Snow containing atmospheric aerosols. *J. Atmos. Sci.* 37: 2734–2745.

WMO 2012: *Guide to meteorological instruments and methods of observation*, edition 2008 updated in 2010. WMO no. 8, Secretariat of the World Meteorological Organization, Geneva, Switzerland.

Xu B., Cao J., Joswiak D.R., Liu X., Zhao H. & He J. 2012. Post-depositional enrichment of black soot in snowpack and accelerated melting of Tibetan glaciers. *Environ. Res. Lett.* 7, 014022, doi:10.1088/1748-9326/7/1/014022.

Appendix 1. Reference snow stratigraphy about one month after soot deposition in SoS2011. Snow depth from the snow surface and the remaining parameters following Fierz *et al.* (2009).

Depth (cm)	Grain shape	Morphological classification subclass shape	Hardness	Size (mm)
0–4	RGlr	rounded	2	0.5–0.7
4–9	FCsf	faceted and some cup shaped	3	2
9–15	MFpc	rounded polycrystals	4	2
15–16		refrozen layer, rounded crystals	5	
16–45	FCxr	rounded by melting, some facted still left	3	2
45–50	MFpc	rounded polycrystals	4	1

Appendix 2. Soot contaminated snow stratigraphy about one month after soot deposition in SoS2011. Snow depth from the snow surface and the remaining parameters following Fierz *et al.* (2009).

Depth (cm)	Grain shape	Morphological classification subclass shape	Hardness	Size (mm)
0–2	RGlr	rounded	2	0.5
2–5	MFpc	rounded polycrystals	3	2
5–35	MFpc	rounded polycrystals	4	2

Appendix 3. Reference snow pit measured on 3 April 2013, in SoS2013.

Depth (cm)	Grain shape	Size	Hardness	Wetness	Grain size (mm)		
					Min	Max	Mean
0–3	Ppir	fine	1	2	0	1	0.25
3–16	RGxf	coarse	1	1	0.5	1.5	0.75
16–20	RGxf	coarse	1	1	0.25	1.75	1
20–31	Fcso	coarse/very coarse	1	1	0.5	2.5	1
31–39	FCso	coarse	2	1	0.5	2.25	1.25
39–52	DHcp + DHch	very coarse	1	1	0.5	4	1.5
52–66	DHcp	very coarse	4	1	0.75	4.25	2.25

Appendix 4. Reference snow pit measured on 3 April 2013, in SoS2013; n/a = not available.

Temperature		Density	
Depth (cm)	°C	Depth (cm)	g cm^{-3}
air	1.1	0–5	0.244
6	–6.6	5–10	0.272
16	–6.3	10–15	0.256
26	–5	15–20	0.248
36	–4.4	20–25	0.256
46	–3.8	25–30	0.300
56	–3.5	30–35	0.300
66	–3.2	35–40	0.244
		40–45	0.292
		45–50	0.324
		50–55	0.232
		55–60	n/a

Appendix 5. Reference snow pit measured on 5 April 2013, in SoS2013.

Depth (cm)	Grain shape	Density		Comments
		Depth (cm)	g cm^{-3}	
0–0.5	PPir	0–5	0.290	small crystalline, not dendritic
0.5–1.5	RGxf	5–10	0.360	more icy, more granular
1.5–4	FCsf	10–15	0.280	even more icy, grains larger
4–12.5	FCsf	15–20	0.240	similar as above
12.5–15	FCco	20–25	0.240	ice lens below harder
15–19	MFcf	25–30	0.300	rough icy grains
19–29	FCso	30–35	0.300	larger icy grains
29–32	FCso	35–40	0.250	below harder
32–42	FCso + DHcp	40–45	0.280	larger icy grains
42–47	DHcp + DHch	45–50	0.280	larger faceted icy grains
47–59	DHcp + DHch	50–55	0.250	larger icy grains, planar
59–64	DHcp + DHch	55–60	0.240	icy deep hoar
		59–64	0.220	

Appendix 6. Reference snow pit measured on 6 April 2013, in SoS2013.

Depth (cm)	Grain shape	Size	Hardness	Wetness	Grain size (mm)		
					Min	Max	Mean
0–1	Ppir	medium	1	1	0.25	0.75	0.50
1–9	RGxf	coarse	1	1	0.25	1.50	1.00
9–10	FCxr	coarse	1	1	0.50	2.50	1.00
10–16	FCxr	coarse	1	1	0.25	1.75	1.00
16–22	FCso	coarse	2	1	0.75	3.25	1.50
22–32	FCso	coarse	1	1	0.75	3.00	2.00
32–40	FCso	coarse	3	1	0.50	2.50	1.25
40–53	DHcp + DHch	very coarse	1	1	1.00	4.00	2.50
53–65	DHcp	very coarse	5	1	1.00	5.00	2.75

Appendix 7. Reference snow pit measured on 6 April 2013, in SoS2013; n/a = not available.

Temperature		Density		EC		
Depth (cm)	°C	Depth (cm)	g cm^{-3}	Depth (cm)	ng g^{-1}	ng cm^{-3}
air	–7.0	0–5	0.208	0–5	45.8	10.4
0	–10.0	5–10	0.224			
5	–11.8	10–15	0.248			
15	–8.9	15–20	0.320			
25	–5.8	20–25	0.252			
35	–4.7	25–30	0.244			
45	–3.7	30–35	0.296			
55	–3.2	35–40	0.280			
65	–2.8	40–45	0.260			
		45–50	0.272			
		50–55	0.280			
		55–60	0.320			
		60–65	n/a			

Appendix 8. Snow stratigraphy of S5, sampled on 10 April 2013, in SoS2013.

Depth (cm)	Grain shape	Size	Hardness	Wetness	Grain size (mm)		
					Min	Max	Mean
0–1	MFcr	very fine-very coarse	4	2	0.25	1.50	0.50
1–3	FCsf	coarse	1	1	0.75	2.00	1.25
3–13	FCxr	coarse	1	1	0.75	2.00	1.25
13–16	MFcr	medium	3	1	0.50	2.00	0.75
16–21	RG	coarse	3	1	0.75	1.50	1.00
21–28	FC/DH	very coarse	1	1	0.75	3.00	1.50
28–30	MFpc/MFcr	coarse	4	1	0.75	3.00	1.00
30–36	RGlr	coarse	4	1	0.25	1.50	1.00
36–44	FC/DH	coarse/very coarse	1	1	0.75	3.50	1.50
44–48	DH	very coarse	1	1	1.00	4.00	2.00
48–52	DH/MF	very coarse	6	1	0.75	3.50	2.50
52–56	DH	very coarse	1	1	0.50	4.00	3.00

Appendix 9. Snow stratigraphy of S5, sampled on 10 April 2013, in SoS2013; n/a = not available.

Temperature		Density		EC		
Depth (cm)	°C	Depth (cm)	g cm^{-3}	Depth (cm)	ng g^{-1}	ng cm^{-3}
air	0.7	0–5	0.168	0–5	1690	374
0	0.1	5–10	0.224			
6	–1.1	10–15	0.308			
16	–5.6	15–20	0.256			
26	–5.7	20–25	0.224			
36	–5.3	25–30	0.320			
46	–4.4	30–35	0.276			
56	–3.7	35–40	0.248			
		40–45	0.264			
		45–50	n/a			
		50–56	n/a			

Appendix 10. Snow stratigraphy of S7, sampled on 10 April 2013, in SoS2013.

Depth (cm)	Grain shape	Size	Hardness	Wetness	Grain size (mm)		
					Min	Max	Mean
0–1	MFcr	coarse	5	1	0.75	1.50	1.00
1–2.5	FCxr	coarse	1	1	0.50	1.75	1.25
2.5–3	MFcr	coarse	3	1	1.00	1.50	1.25
3–12.5	Fcxr	coarse	1	1	0.50	1.50	0.75
12.5–13	MFcr	medium	5	1	0.25	1.50	0.75
13–16.5	FCxr	medium	1	1	0.50	1.50	0.75
16.5–25.5	DHxr	coarse/very coarse	1	1	0.75	3.00	2.00
25.5–36.5	DHxr	medium/coarse	3	1	0.50	2.50	1.25
36.5–46.5	DHcp	very coarse	2	1	1.25	4.00	2.00

Appendix 11. Snow stratigraphy of S7, sampled on 10 April 2013, in SoS2013; n/a = not available.

Temperature		Density		EC		
Depth (cm)	°C	Depth (cm)	g cm^{-3}	Depth (cm)	ng g^{-1}	ng cm^{-3}
air	–0.6	0–5	n/a	0–5	1470	323
0	–3.7	5–10	0.252			
6.5	–4.4	10–15	0.252			
16.5	–6.2	15–20	0.224			
26.5	–6.0	20–25	0.224			
36.5	–5.1	25–30	0.292			
46.5	–4.2	30–35	0.296			
		35–40	0.22			
		40–45	0.26			

Appendix 12. Reference snow pit observed on 17 April 2013, in SoS2013.

Depth (cm)	Grain shape	Size	Hardness	Wetness	Grain size (mm)		
					Min	Max	Mean
0–2	MFcl	coarse	1	3	0.50	1.25	1.00
2–32	MFcl	coarse	1	3	0.75	2.00	1.25
32–34	MFcr	very coarse	6	1	0.50	2.50	1.50
34–38	MFcl	very coarse	1	3	0.50	2.50	1.25

Appendix 13. Reference snow pit (continued) observed on 17 April 2013, in SoS2013; n/a = not available.

Temperature		Density		EC		
Depth (cm)	°C	Depth (cm)	g cm^{-3}	Depth (cm)	ng g^{-1}	ng cm^{-3}
air	2.9	0–5	0.420	0–5	134	52.2
0	0.1	5–10	0.382	5–10	55.3	21.1
8	0.0	10–15	0.392	10–15	87.9	34.4
18	0.0	15–20	0.372	15–20	n/a	n/a
28	0.0	20–25	0.396	20–25	n/a	n/a
38	0.0	25–30	0.400			
		30–38	0.496			

Appendix 14. Snow stratigraphy of S5 on 17 April 2013, in SoS2013; n/a = not available.

Depth (cm)	Grain shape	Size	Hardness	Wetness	Grain size (mm)		
					Min	Max	Mean
0–1	MFcl	coarse	1	3	0.75	1.50	1.00
1–16	MFcl	coarse	1	3	0.50	1.50	1.25
16–25	MFcl	very coarse	1	3	1.00	4.00	2.50
25–29	MFcl	very coarse	1	3	1.00	3.00	2.00
29–30	IFil	n/a	6	1			n/a
30–33	Mfsl	n/a	1	n/a	0.75	2.00	1.00

Appendix 15. Snow stratigraphy of S5 (continued) on 17 April 2013, in SoS2013; n/a = not available.

Temperature		Density		EC		
Depth (cm)	°C	Depth (cm)	g cm^{-3}	Depth (cm)	ng g^{-1}	ng cm^{-3}
air	3.2	0–5	0.384	0–5	730	233
0	0.1	5–10	0.388	5–10	118	24.3
3	0.0	10–15	0.396	10–15	88.4	0.559
13	0.0	15–20	0.404	15–20	64.5	n/a
23	0.0	20–25	0.392	20–25	55.9	n/a
33	0.0	25–33	0.608			

Appendix 16. Snow stratigraphy of S7 on 17 April 2013, in SoS2013; n/a = not available.

Depth (cm)	Grain shape	Size	Hardness	Wetness	Grain size (mm)		
					Min	Max	Mean
0–2	MFcl	coarse	1	3	0.50	1.50	1.00
2–17	MFcl	coarse	1	3	0.50	1.50	1.25
17–26	MFcl	very coarse	1	3	0.50	3.00	2.00
26–32	MFpc/cl	very coarse	4	2	1.00	3.00	2.00
32–33	IF	n/a	6	1	n/a	n/a	n/a
33–35	MFsl	n/a	1	5	n/a	n/a	n/a

Appendix 17. Snow stratigraphy of S7 (continued) on 17 April 2013, in SoS2013; n/a = not available.

Temperature		Density		EC		
Depth (cm)	°C	Depth (cm)	g cm^{-3}	Depth (cm)	ng g^{-1}	ng cm^{-3}
air	3.2	0–5	0.368	0–5	529	154
0	0.0	5–10	0.384	5–10	6.98	–18.4
5.0	0.0	10–15	0.404	10–15	5.27	–32.3
15.0	0.0	15–20	0.36	15–20	n/a	n/a
25.0	0.0	20–25	0.416	20–25	n/a	n/a
35.0	–0.1	25–30	0.708	25–30	n/a	n/a
		30–35	n/a			

PAPER III

Brief communication: Light-absorbing impurities can reduce the density of melting snow

The Cryosphere, 8, 991–995, 2014
www.the-cryosphere.net/8/991/2014/
doi:10.5194/tc-8-991-2014

The Cryosphere
Open Access

Brief communication: Light-absorbing impurities can reduce the density of melting snow

O. Meinander[1], A. Kontu[2], A. Virkkula[1], A. Arola[3], L. Backman[1], P. Dagsson-Waldhauserová[4,5], O. Järvinen[6], T. Manninen[1], J. Svensson[1], G. de Leeuw[1,6], and M. Leppäranta[6]

[1]Finnish Meteorological Institute, Helsinki, Finland
[2]Arctic Research Center, Finnish Meteorological Institute, Sodankylä, Finland
[3]Kuopio Unit, Finnish Meteorological Institute, Kuopio, Finland
[4]University of Iceland, Department of Physics, Reykjavik, Iceland
[5]Agricultural University of Iceland, Faculty of Environment, Hvanneyri, Iceland
[6]Department of Physics, University of Helsinki, Helsinki, Finland

Correspondence to: O. Meinander (outi.meinander@fmi.fi)

Received: 20 November 2013 – Published in The Cryosphere Discuss.: 10 January 2014
Revised: 10 April 2014 – Accepted: 14 April 2014 – Published: 26 May 2014

Abstract. Climatic effects of black carbon (BC) deposition on snow have been proposed to result from reduced snow albedo and increased melt due to light-absorbing particles. In this study, we hypothesize that BC may decrease the liquid-water retention capacity of melting snow, and present our first data, where both the snow density and elemental carbon content were measured. In our experiments, artificially added light-absorbing impurities decreased the density of seasonally melting natural snow. No relationship was found in case of natural non-melting snow. We also suggest three possible processes that might lead to lower snow density.

1 Introduction

For seasonal snow, snow melting is an important part of the natural annual hydrological cycle. It is forced by atmospheric sensible heat flux and solar radiation, where the albedo is a critical factor due to its large variability. Snow albedo depends primarily on the grain size, wetness, impurities in the near-surface snow layer, and directional distribution of the down-welling irradiance. Deposition of anthropogenic emissions to snow cover potentially causes albedo changes. In terms of its climate forcing, black carbon (also known as light-absorbing aerosol) has been hypothesized to be the second most important human emission, and only carbon dioxide is estimated to have a greater forcing (Bond et al., 2013). The climatic effects of black carbon (BC) in snow are due to reduced snow albedo caused by absorption of solar radiation, and induced melt of darker snow, which again lowers the albedo via the albedo feedback mechanism (e.g. Warren and Wiscombe, 1980; Doherty et al., 2010).

Snow melt starts when snow temperature reaches the melting point. Then, if the heating continues, the volume of liquid water increases until the holding capacity or the saturation point of liquid water is reached. This capacity is 3–5 % on a mass basis and depends on snow grain structure and packing (DeWalle and Rango, 2008). When the flow of melt water begins, the impurities may either be washed down through the snow with the flow, or remain in the snow. It has been shown that BC is less likely to be washed down through the snow with melt water (Conway et al., 1996; Doherty et al., 2013).

Hence, if we consider natural snow with anthropogenic BC, we can assume this impurity to remain in the melting snowpack, not to be washed down, and to potentially cause changes in the snow properties and structure, as compared to clean snow. Therefore, we hypothesize that BC in snow might affect the liquid-water retention capacity of melting snow. To test this hypothesis, we use our data of cold and melting snow, where both the snow density and BC content were measured.

2 Materials

All our snow density and BC data have been obtained for natural seasonally melting snow in Sodankylä (67°25′ N, 26°35′ E), Finland, north of the Arctic Circle. By natural snow we refer to a snow pack that has formed from snowfall (i.e. has not been produced by a snow cannon, and has not been affected by human activity, e.g. snow clearing). The data contain cases of cold and melting snow, both with and without experimentally added impurities (Table 1).

The cold snow samples were snow on a lake (17 March 2009), various sites around the Sodankylä area (13 and 19 March 2009 and 23–24 March 2010), and a fenced experimental field (6 and 10 April 2013). The melting snow data were from the experimental field only (17–18 April 2013 before and after rain).

The data originate from three campaigns: the Soot on Snow experiment in 2013 (SoS-2013); the Snow Reflectance Transition Experiment (SNORTEX 2008–2010, see Meinander et al., 2013 for more details); and the SnowRadiance-campaign (SR-2009). The SoS-2013 campaign was carried out at the Sodankylä airport to study the effects of deposition of impurities on surface reflectance, albedo and melt of seasonal snow. The experimental area was a large, flat, fenced open space, and the gravel ground was not covered with concrete or asphalt (Fig. 1). Different amounts of impurities were deposited to snow on different spots, each with diameter of 4 m, and thereafter the spots were monitored until the snow had melted. The sites were left to develop naturally, introducing as little disturbance as possible. Here we used data from three experimental spots with chimney soot, one spot with Icelandic volcanic sand from Ólafur Arnalds (Agricultural University of Iceland) and Haraldur Olafsson (University of Iceland), and one reference spot.

The SnowRadiance (SR) was an ESA-funded project aiming at determining snow properties from optical satellite measurements. The BC samples were collected from the snow over ice on Lake Orajärvi. The lake is frequently used in the winter, e.g. for snowmobiling.

During the SoS-2013, the SNORTEX-2009, and the SR-2009 campaigns, surface snow samples were collected for analysis of their elemental carbon (EC) and organic carbon (OC) concentrations using the filter-based thermal-optical method, described and used in, for example, Forsström et al. (2009). The EC is used as a proxy of BC, due to the measurement technique used. In the SNORTEX-2010 campaign, the sampling, filtering, and laboratory spectrometer analysis followed the procedures presented in Doherty et al. (2010). Several samples were collected from each location.

The snow densities (weight per volume) were measured manually, for either the whole snowpack vertical column (snow tube for SR and SNORTEX data), or for separate horizontal snow layers (density cutter for SoS data to measure the density of the visually dirty surface snow). One density measurement for each location was made. To estimate the standard deviation of the density measurement, an earlier data set of FMI was applied. Sampling of wet snow for density measurements may be difficult since liquid water easily escapes from the sampling box. Here the SoS data for melting snow was obtained for two subsequent days (Table 1), before and after rainfall. The snow was then wet, but not dripping wet, and no water escape from sampling was detected.

Figure 1. The SoS-2013 experiment. **(a)** Top: the flat and open experimental field with the seasonal snow pack; **(b)** bottom left: the ground under the snow, i.e. a natural gravel surface, not covered by concrete or asphalt, offered an uniform surface for the snow cover; **(c)** bottom right: previously added impurities were visible on the surface of the melting snow, here volcanic sand.

In the SoS-2013 data, snow hardness, grain sizes, and grain shapes were estimated and classified according to the International Classification for Seasonal Snow on the Ground (Fierz et al., 2009).

3 Results

In our data for non-melting natural snow from the SR-2009, SNORTEX-2009, SNORTEX-2010 and SoS-2013 campaigns, the BC concentrations varied between 8 and 126 ppb, and snow densities were 200–264 kg m^{-3}. The density did not depend on the BC content (Fig. 2a, the dots inside the circle).

Table 1. The origin of our Sodankylä snow density data coupled with BC analysis results. The campaigns are explained in the text.

Year	Date	Data origin	Location	Snow	Artificial impurities	BC analysis
2009	17 Mar	SR campaign	Snow on lake Orajärvi	Cold snow	No	Thermal-optical
2009	13, 19 Mar	SNORTEX	Sodankylä area	Cold snow	No	Thermal-optical
2010	23, 24 Mar	SNORTEX	Sodankylä area	Cold snow	No	Spectrometer (Doherty et al., 2010)
2013	6, 10 Apr	SoS-2013	Sodankylä airport	Cold snow	Yes	Thermal-optical
2013	17 Apr	SoS-2013	Sodankylä airport	Melting, before rain	Yes	Thermal-optical
2013	18 Apr	SoS-2013	Sodankylä airport	Melting, after rain	Yes	Thermal-optical

However, in our SoS-experiment data of 6 April 2013, the snow with the BC maximum of 1465 ppb (Fig. 2a, one data point for wood burning soot), had the lowest density of all our data, 168 kg m^{-3}. MFcr-grains (melt–freeze crust, as a result of melting and freezing) were 0.25–1.5 mm in diameter, the surface hardness value was 4 (hard snow) and the snow depth was 56 cm. For comparison, with the reference non-sooted natural snow at that time (10 April 2013) on the same experimental field: the Ppir-grains (Precipitation particles) were irregular crystals, of 0.25–0.75 mm in diameter. The BC concentration was 126 ppb, the density was 210 kg m^{-3}, the hardness value was 1 (very soft snow), and the snow depth was 65 cm.

Our experimental data show that for the seasonally melting natural Arctic snow, with and without artificially added soot or volcanic ash, there was a correlation between the density and the BC content of snow (Fig. 2b). This was the case both prior to a rain period, and the next day after the rain. The densities and the corresponding BC contents were measured separately for the top 5 cm of the snow, not for the whole snow pack, and the impurities of volcanic sand, soot from oil burner and wood burning soot were visually observed to remain on the snow surface, too (Fig. 1). All the grains of the surface layer were melt–freeze crust (MFcr).

The BC concentrations in individual snow samples varied from 9 to 730 ppb. From these, the averages for each experimental spot were calculated (92–310 ppb), and plotted in Fig. 2b. The standard deviation (σ) for the clean reference snow samples (no added impurities) was 34 ppb ($n = 7$), and most often σ was larger for spots with added impurities, dependent on the number of samples (from 1 to 5) and the spot properties; e.g. for one spot with added soot, it was $\sigma = 28$ ppb ($n = 5$). The Eq. (1) shows the relation between the snow density ρ_s [kg m^{-3}], and the BC content C_{BC} [ppb] for the melting snow derived from the SoS-2013 data ($R^2 = 0.66$):

$$\rho_s = -0.27 C_{BC} + 440.6, \quad (1)$$

where $C_{BC} = [92{,}310]$ ppb. The 95 % confidence interval of the slope of the Eq. (1) is from -0.46 to -0.08, that is, we are 95 % confident that the true slope of this equation is in the range defined by -0.27 ± 0.19.

For the snow density, we had one measurement for each location. Therefore, using a previous FMI Sodankylä snow density data set (unpublished data), the average standard deviation was determined, providing a value of 17 kg m^{-3} ($n = 79$ pairwise measurements, $n_{tot} = 158$, $\rho_s = [104{,}408]$ kg m^{-3}) for the Sodankylä data.

4 Discussion and conclusions

All our data of cold snow and melting snow represent the natural seasonal snow cover in Sodankylä, north of the Arctic Circle. For the cold snow, the density was 200–264 kg m^{-3} with BC 8–126 ppb. Our experimental results for an excessive (1465 ppb) amount of added BC (wood-burning soot) show a reduction of the cold snow density. This result is based on comparison of one sooted vs. one reference spot only; more data are needed to confirm this result. Earlier, Meinander et al. (2013) reported on a larger data set (their Table 3), where the snow BC content, in Sodankylä snow cover in 2009–2011, varied in one sampling location between 9 and 106 ppb in the natural snow cover. Thus, our cold snow data presented here represents well the natural BC variability in Sodankylä.

Artificially added impurities in our experiments on natural snow decreased the snow density of melting snow (Fig. 2, Eq. 1). Moreover, the densities were measured both prior to and after rainfall (4.9 mm water in 3 h), which occurred between two subsequent measurement days. In both cases, the larger the BC content, the smaller the density. Thus the rain did not change this order, which further supported our hypothesis that the impurities may affect the water retention capacity. Furthermore, according to our recent laboratory experiment (unpublished data), we found that snow with artificially added soot released melt water sooner than snow without added soot. For this experiment, we added a known amount of soot to a snow sample, mixed the soot and snow, and let the snow melt indoors, while measuring the melt water on a drip pan as a function of time. The results showed

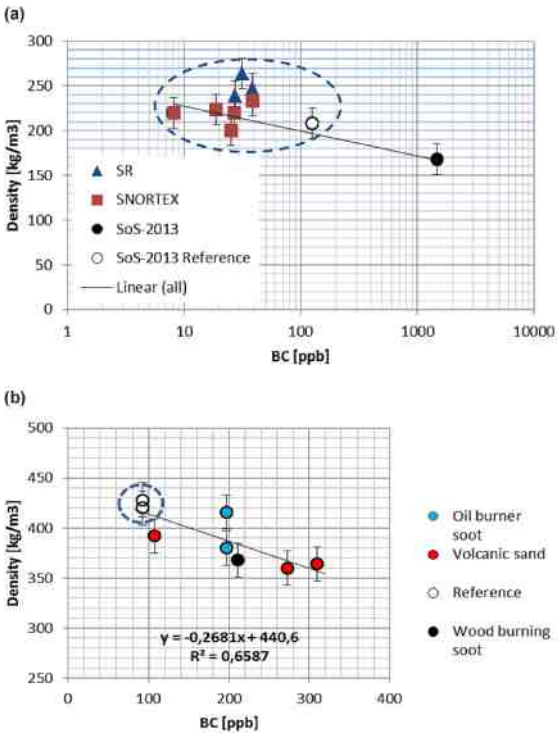

Figure 2. The black carbon (BC) content [ppb] vs. density [kg m^{-3}] for the natural seasonal snow cover in Sodankylä, north of the Arctic Circle with and without artificially added impurities. The line is the least squares linear fit through all the points. **(a)** Cold snowpack: for natural snow without added impurities, BC concentrations were 8–126 ppb, and snow densities were 200–264 kg m^{-3} and for the reference SoS-2013 spot BC was 126 ppb and the snow density was 210 kg m^{-3} (within the circle); when wood-burning soot was artificially deposited to this SoS-spot, BC in snow was measured to be 1465 ppb, and snow density decreased to 168 kg m^{-3} (outside the circle). **(b)** Melting snow: SoS-2013 data for reference spots (within the circle), and spots with artificially added impurities of volcanic sand, soot from oil burner and wood burning soot (outside the circle). The densities and corresponding carbon contents were measured separately for the specified surface layers, not for the entire snow pack.

that while the control snow started to release melt water after 40 min, the snow with added soot released melt water already after 12 min. When cold water was added on snow, the control snow released water after 29 min, while the same amount of water in sooted snow caused water to release already after 7 min. All the snow samples were of the same size (same weight and volume) representing the same natural snow, and mechanically treated the same way whether soot was added or not, for example, the control snow was also mixed although no soot was added. Hence, these new experimental data were found to support our hypothesis that BC may decrease the liquid-water retention capacity of melting snow.

As a summary, according to our experience and observations, we suggest three possible processes that might lead to the lower snow density:

1. *A semi-direct effect of absorbing impurities*. Absorbing impurities would cause melt and/or evaporation from the liquid phase and sublimation from the solid phase of the surrounding snow, resulting in air pockets around the impurities, and thus lower snow density. We have empirical observations, where impurities (both organic and inorganic) in the snow have been surrounded by air pockets.

2. *BC effect on the adhesion between liquid water and snow grains*. If BC reduces adhesion, the liquid-water holding capacity decreases. For linear warming the influence on the density of wet snow is then max 5 % (at this level water flow starts in natural snow). However, with daily cycles, warm days and cold nights, the weaker adhesion may push liquid water down more day-by-day and then the influence to the density would be larger. This way also melt–freeze metamorphosis would produce less dense snow.

3. *BC effect on the snow grain size.* Absorbing impurities would increase the melting and metamorphosis processes, resulting in larger snow grains, which would lower the water retention capacity. Earlier, Yamaguchi et al. (2010) have suggested that the water retention curve of snow could be described as a function of grain size using soil physics models. Here our data showed some slight indication for the possibility of soot in snow to result in larger snow grain sizes via increased melt and metamorphosis, and our data did not show clear evidence against this possibility.

Volcanic sand is assumed not to contain BC (Dadic et al., 2013, Fig. 12a). This assumption is further supported by our own EC analysis of volcanic sand samples with the thermal – optical method showing hardly any EC. Instead, the BC in our volcanic sand spot can be assumed to originate either from long-range transport, or from our other experimental spots with added soot; carbonaceous material in volcanic aerosols has also been proposed to be due to tropospheric air that is entrained into the volcanic jet and plume (Andersson et al., 2013). Our observations and measurements indicate that for a visually darker snow surface, the analyzed BC content is larger and the measured snow density is smaller, regardless of whether soot or volcanic sand had been added to the spot.

The significance of our results on reduction of snow density, and possibly also decreasing water holding capacity due to the black carbon, may be due to the fact that (i) snow density is an important snow parameter that has been found to

correlate with several factors affecting the snow melt, such as snow age and liquid-water holding capacity (Kuusisto, 1984); (ii) snow density multiplied by snow depth equals the important climate model parameter of snow water equivalent (SWE); and (iii) our results may have potential in reducing the uncertainties (IPCC, 2013) related to the effect of black carbon on snow melt and climate change.

In nature, the low density of new dry snow increases due to gravitational settling, wind packing, sintering, and melt–freeze events. These processes depend on the grain size, shape and organization, and snow temperature. The density of snow is also affected by water vapour diffusion in the snow pack, as well as by the temperature and the vegetation under the snow. In our experimental data, we can assume similar environmental conditions with only the impurity contents in snow being the varying factor; our results are for natural snow on natural ground, and we did not have data for drainage of melt water in the snowpack. Here we reported our first results, and more data are needed to further study the effect of light-absorbing impurities on density and water retention capacity of melting snow.

Acknowledgements. The authors thank all the participants of the campaigns of SoS-2013, SNORTEX-2010, SNORTEX-2009 and SR-2009, especially Antti Aarva. Filters from the 2010 snow samples were analyzed for BC by S. Doherty. We gratefully acknowledge support from the Academy of Finland (A4-project), and the Nordic Center of Excellence (NCoE), Nordic Top Research Initiative "Cryosphere-atmosphere interactions in a changing Arctic climate" (CRAICC), and the EU Life+ project Mitigation of Arctic warming by controlling European black carbon emissions, MACEB (project no. LIFE09 ENV/FI/000572).

Edited by: M. Boy

References

Andersson, S. M., Martinsson, B. G., Friberg, J., Brenninkmeijer, C. A. M., Rauthe-Schöch, A., Hermann, M., van Velthoven, P. F. J., and Zahn, A.: Composition and evolution of volcanic aerosol from eruptions of Kasatochi, Sarychev and Eyjafjallajökull in 2008–2010 based on CARIBIC observations, Atmos. Chem. Phys., 13, 1781–1796, doi:10.5194/acp-13-1781-2013, 2013.

Bond, T. C., Doherty, S. J., Fahey, D. W., Forster, P. M., Berntsen, T., DeAngelo, B. J., Flanner, M. G., Ghan, S., Kärcher, B., Koch, D., Kinne, S., Kondo, Y., Quinn, P. K., Sarofim, M. C., Schultz, M. G., Schulz, M., Venkataraman, C., Zhang, H., Zhang, S., Bellouin, N., Guttikunda, S. K., Hopke, P. K., Jacobson, M. Z., Kaiser, J. W., Klimont, Z., Lohmann, U., Schwarz, J. P., Shindell, D., Storelvmo, T., Warren, S. G. and Zender, C. S.: Bounding the role of black carbon in the climate system: A scientific assessment, J. Geophys. Res.-Atmos., 118, 5380–5552, doi:10.1002/jgrd.50171, 2013.

Conway, H., Gades, A., and Raymond, C. F.: Albedo of dirty snow during conditions of melt, Water Resour. Res., 32, 1713–1718, 1996.

Dadic, R., Mullen, P. C., Schneebeli, M., Brandt, R. E., and Warren, S. G.: Effects of bubbles, cracks, and volcanic tephra on the spectral albedo of bare ice near the Transantarctic Mountains: Implications for sea glaciers on Snowball Earth, J. Geophys. Res.-Earth, 118, 1658–1676, doi:10.1002/jgrf.20098, 2013.

DeWalle, D. R. and Rango, A.: Principles of snow hydrology, Cambridge University Press, Cambridge, UK, 2008.

Doherty, S. J., Warren, S. G., Grenfell, T. C., Clarke, A. D., and Brandt, R. E.: Light-absorbing impurities in Arctic snow, Atmos. Chem. Phys., 10, 11647–11680, doi:10.5194/acp-10-11647-2010, 2010.

Doherty, S. J., Grenfell, T. C., Forsström,S., Hegg, D. L., Brandt, R. E., and Warren, S. G.: Observed vertical redistribution of black carbon and other insoluble light-absorbing particles in melting snow, J. Geophys. Res.-Atmos., 118, 5553–5569, 2013.

Fierz, C., Armstrong, R. L., Durand, Y., Etchevers, P., Greene, E., McClung, D. M., Nishimura, K., Satyawali, P. K. and Sokratov, S. A.: The International Classification for Seasonal Snow on the Ground, IHP-VII Technical Documents in Hydrology No. 83, IACS Contribution No. 1, UNESCO-IHP, Paris, 2009.

Forsström, S., Ström, J., Pedersen C. A., Isaksson, E., and Gerland, S.: Elemental carbon distribution in Svalbard snow, J. Geophys. Res., 114, D19112, doi:10.1029/2008JD011480, 2009.

IPCC, "Climate Change 2013: The Physical Science Basis. Working Group I Contribution to the IPCC 5th Assessment Report – Changes to the Underlying Scientific/Technical Assessment" (IPCC-XXVI/Doc.4), http://www.ipcc.ch/report/ar5/wg1/ (last access: 22 May 2014), 2013.

Kuusisto, E.: Snow accumulation and snowmelt in Finland. Publications of the Water Research Institute, National Board of Waters, Finland, No. 55, 149 pp., 1984.

Meinander, O., Kazadzis, S., Arola, A., Riihelä, A., Räisänen, P., Kivi, R., Kontu, A., Kouznetsov, R., Sofiev, M., Svensson, J., Suokanerva, H., Aaltonen, V., Manninen, T., Roujean, J.-L., and Hautecoeur, O.: Spectral albedo of seasonal snow during intensive melt period at Sodankylä, beyond the Arctic Circle, Atmos. Chem. Phys., 13, 3793–3810, doi:10.5194/acp-13-3793-2013, 2013.

Warren, S. G. and Wiscombe, W. J.: A model for the spectral albedo of snow. II: Snow containing atmospheric aerosols, J. Atmos. Sci., 37, 2734–2745, 1980.

Yamaguchi, S. Katsushima, T., Sato, A., and Kumakura, T.: Water retention curve of snow with different grain sizes, Cold Reg. Sci. Technol., 64, 87–93, doi:10.1016/j.coldregions.2010.05.008, 2010.

PAPER IV

Contribution of dust and elemental carbon to the reduction of snow albedo in the Indian Himalaya and the Finnish Arctic

Atmos. Meas. Tech. Discuss., https://doi.org/10.5194/amt-2017-186
Manuscript under review for journal Atmos. Meas. Tech.
Discussion started: 12 July 2017

Atmospheric Measurement Techniques Discussions

Contribution of dust and elemental carbon to the reduction of snow albedo in the Indian Himalaya and the Finnish Arctic

Jonas Svensson[1], Johan Ström[2], Niku Kivekäs[1], Nathaniel B. Dkhar[3,4], Shresth Tayal[3,4], Ved P. Sharma[3,4], Arttu Jutila[5], John Backman[1], Aki Virkkula[1], Meri Ruppel[6], Antti Hyvärinen[7], Anna Kontu[8], Henna-Reetta Hannula[8], Matti Leppäranta[5], Rakesh K. Hooda[1,3], Atte Korhola[6], Eija Asmi[1], Heikki Lihavainen[1]

[1]Atmospheric Composition Research, Finnish Meteorological Institute, Helsinki, Finland
[2]Department of Environmental Science and Analytical Chemistry, Stockholm University, Stockholm, Sweden
[3]The Energy and Resource Institute, New Delhi, India
[4]The Energy and Resource Institute University, New Delhi, India
[5]Department of Physics, University of Helsinki, Helsinki, Finland
[6]Department of Environmental Sciences, University of Helsinki, Helsinki, Finland
[7]Expert Services, Finnish Meteorological Institute, Helsinki, Finland
[8]Arctic Research Center, Finnish Meteorological Institute, Sodankylä, Finland

Correspondence to J. Svensson (jonas.svensson@fmi.fi)

Atmos. Meas. Tech. Discuss., https://doi.org/10.5194/amt-2017-186
Manuscript under review for journal Atmos. Meas. Tech.
Discussion started: 12 July 2017

Atmospheric Measurement Techniques Discussions

Abstract

Light-absorbing impurities (LAI) have the potential to substantially affect snow albedo, with subsequent changes on snow melt and impact on climate. To more accurately quantify the snow albedo, the contribution from different LAI needs to be assessed. Here we estimate the main LAI components, elemental carbon (EC) (as a proxy for black carbon) and mineral dust in snow from Indian Himalaya and compared it to snow samples from Arctic Finland. The impurities are collected onto quartz filters and are analyzed thermal-optically for EC, as well as with an additional optical measurement to estimate the light-absorption of dust separately on the filters. Laboratory tests were conducted using substrates containing soot and mineral particles specially prepared to test the experimental setup. Analyzed ambient snow samples show EC concentrations that are in the same range as presented by previous research, for each respective region. In terms of the mass absorption cross section (MAC) our ambient EC had surprisingly about half of the MAC value compared to our laboratory standard EC (chimney soot), suggesting a less light absorptive EC in the snow, which has consequences for the snow albedo reduction caused by EC. In the Himalayan samples, larger contributions by dust (in the range of 50 % or greater for the light absorption caused by the LAI) highlighted the importance of dust acting as a light absorber in the snow. Moreover, EC concentrations in the Indian samples, acquired from a 120 cm deep snow pit (covering possibly the last five years of snow fall), suggest an increase in both EC and dust, while at the same time there is a tendency for a reduction in the MAC value with snow depth. This work emphasizes the complexity in determining the snow albedo, showing that LAI concentrations alone might not be sufficient, but additional transient effects on the light-absorbing properties of the EC need to be considered and studied in the snow. Equally imperative is to confirm the spatial and temporal representativeness of these data by comparing data from several and longer pits explored at the same time.

Atmos. Meas. Tech. Discuss., https://doi.org/10.5194/amt-2017-186
Manuscript under review for journal Atmos. Meas. Tech.
Discussion started: 12 July 2017

Atmospheric Measurement Techniques Discussions

1. Introduction

The deposition of light-absorbing impurities (LAI) in snow influences the radiation budget and can cause enhanced melting (Warren and Wiscombe, 1980). This process affects regions with seasonal snow cover, leading to an earlier snow retreat, which has major implications for thawing and biogeochemical processes acting in the ground (AMAP 2011). In mountainous areas with glaciers, the impurities perturb glacier properties and the hydrological cycle (e.g. Xu et al., 2009). In this context, the impact on snow reflectance (albedo) from black carbon (BC) aerosol particles is of particular interest. Being one of the most effective light-absorbing aerosols, BC enters the atmosphere by combustion of carbon-based fuels, including forest fires and anthropogenic burning of bio- and fossil fuels (Bond et al., 2013). Because of its negative effect on snow albedo, considerable effort has been made to globally quantify BC in snow (e.g. Doherty et al., 2010; Ming et al., 2008; Schmitt et al., 2015), as well as in ice cores (e.g. McConnell et al., 2007; Ruppel et al., 2014; Xu et al., 2009). In urban areas and in households using open fires, BC particles are also known to have adverse health effects, which make them interesting from a human health perspective as well (e.g. Shindell 2012).

The potential impact of LAI in snow and ice make the Himalaya a region of special interest. It contains numerous glaciers which are in a general state of recession, although contrasting patterns have been reported in different areas (e.g. Bolch et al., 2012; Kääb et al., 2012). Himalayan glaciers act as freshwater sources for several major rivers in Asia, including Indus, Ganges, Brahmaputra, Mekong, and Yangtze, thus having a vital part in millions of people's lives (e.g. Immerzeel et al., 2010). The glaciers are especially susceptible to BC emissions, since India and China located in close proximity, emit the most BC world-wide (Bond et al., 2007). A recent study by Ming et al. (2015) found a decreasing trend in albedo during the period of 2000-2011 on Himalayan glaciers, and suggested rising air temperatures and deposition of LAI to be responsible for the decrease. In light of the vast area of the Himalayas, there is a lack of in-situ measurements of LAI on glaciers, which are crucial for modeling work (Gertler et al., 2016). The lack of measurements is especially pronounced in the Indian Himalaya, since previous measurements of LAI in Himalayan snow and ice have largely been confined to China (e.g. Xu et al., 2006) and Nepal (e.g. Ginot et al., 2014; Kaspari et al., 2011; Kaspari et al., 2014; Ming et al., 2008).

At present, three primary methods are used to measure BC in snow and ice (see Qian et al., 2015, in which they are extensively presented). Out of the three methods, two utilize filters to collect impurities in a melted sample. The first filter method measures optically the spectrally resolved absorption by the impurities using an integrating sphere integrating sandwich spectrophotometer (ISSW) (e.g. Doherty et al., 2010; Grenfell et al., 2011). The second filter method is the thermal-optical analysis of filters (e.g. Forsström et al., 2009; Hagler et al., 2007). The third, non-filter-based method, uses laser-induced

incandescence with a single particle soot photometer (SP2) (e.g. McConnell et al., 2007; Schwarz et al., 2012).

Each measurement method has benefits and drawbacks. The SP2 is specific to refractory BC and is able to provide estimates on the size of the BC particles. However, the SP2 has a size range limitation (roughly 70–600 nm, depending on the instrument settings and nebulizer settup), which may result in the underestimation of BC mass since particles in snow have been reported to be larger (Schwarz et al., 2012; Schwarz et al., 2013). Moreover, the SP2 technique needs to have the liquid particles aerosolized, which may lead to additional particle losses (Schwarz et al., 2012). The use of filters, on the other hand, can provide a practical logistics advantage for the collection of LAI in remote locations because it is difficult to maintain the necessary frozen chain for the snow samples from the field to the laboratory for analysis. Filtering of liquid samples can be conducted in the field, and the substrates are more easily stored and transported to the laboratory. The ISSW method has the advantage that it measures light-absorbing constituents on the filter indiscriminately. Thus, the ISSW method is not specific to BC, and requires interpretation of the spectral response to determine the BC component. The thermal-optical method (TOM) provides an actual measurement of elemental carbon (EC) that is instrumentally defined. EC is assumed to be the dominant light-absorbing component of BC, and often EC and BC are used interchangeably in literature. The sampling efficiency of quartz filters used in TOM is not well characterized for small particles (Lim et al., 2014). However, smaller particles normally contribute little to total particulate mass (Hinds 1999). Thus, each method for measuring BC in snow has both advantages and disadvantages.

In addition to BC, other LAI may contribute significantly to the radiative balance of the cryosphere. Recent research has identified mineral dust and microbiology as having a more important role than previously thought in the current decline in albedo of the Greenland Ice sheet and other parts of the Arctic (e.g. Dumont et al. 2014, Lutz et al., 2016). Similarly, Kaspari et al. (2014) reported such high dust concentrations in the snow of Himalayan Nepal that the contribution of dust in lowering the snow albedo sometimes exceeded that of BC. The importance of dust has also been illustrated from other regions, for example the Colorado Rockies, US, where dust causes a significantly earlier peak in runoff (Painter et al. 2007). In the Arctic, Doherty et al. (2010) suggest that 30 to 50 % of sunlight absorbed in the snowpack by impurities is due to non-BC constituents. Evidently, dust has an important role in the cryospheric radiative balance. Differentiating between the different impurities in the snow is not trivial, however, and requires more than one analytical technique (Doherty et al., 2016). Traditionally, dust in snow has been quantified by gravimetrically measuring filters (e.g. Aoki et al., 2006; Painter et al., 2012). Other methods have consisted of using a transmitted light microscopy (Thevenon et al., 2009), a microparticle counter to measure the insoluble dust (Ginot et al., 2014), or mass spectrometry (using iron as a proxy for dust) (Kaspari et al., 2014).

Atmos. Meas. Tech. Discuss., https://doi.org/10.5194/amt-2017-186
Manuscript under review for journal Atmos. Meas. Tech.
Discussion started: 12 July 2017

Atmospheric Measurement Techniques Discussions

Here we present observations of LAI in snow from two glaciers in the Sunderdhunga valley in Indian Himalaya, which have not to our knowledge, been explored previously with respect to LAI in snow. Using a measuring approach whereby the TOM is combined with a custom-built particle soot absorption photometer (PSAP), we perform laboratory test to provide a correct interpretation of the results. Our Himalayan observations are further compared to samples from Arctic Finland for their LAI content.

2. Methodology

2.1 Snow sample collection and site characteristics

2.1.1 Himalayan India

Snow samples were collected in September of 2015, during the Indian post-monsoon season, from two adjacent glaciers in the Sunderdhunga valley (Figure 1). Bhanolti and Durga Kot glaciers (N 30º 12', E 79º 51') are located in the state of Uttarakhand, India. Facing northeast the glaciers cover an elevation range of about 4400-5500 m a.s.l. and are two small valley-type glaciers contributing to the Ganges hydrological basin. Since the glaciers are situated at a relatively low altitude, they are more likely to be exposed to BC than other Himalayan glaciers residing in higher altitude, as BC has been shown to decrease with altitude in other parts of the Himalaya (e.g. Kaspari et al., 2014; Ming et al., 2013; Yang et al., 2015). The Sunderdhunga area does not have any major local pollution sources. Regionally, however, the small towns of Bageshwar (~40 km S; population ~9000) and Almora (~70 km S; population ~34000), may play a role. On a larger scale, the Sunderdhunga area is affected by the large-scale emissions from the Indo-Gangetic Plain (IGP). Measurements of airborne BC and other aerosol particles at Mukteshwar, a distance of ~90 km southwards at an altitude of 2200 m a.s.l., have shown a clear seasonal pattern in atmospheric concentrations with emissions originating from the IGP (Hyvärinen et al., 2011; Raatikainen et al., 2017). With a peak during the pre-monsoon season (March-onset of monsoon), the BC loading has been reported to decrease by about 70 % at Mukteshwar during the monsoon (Hyvärinen et al., 2011). Similarly, dust concentrations in the air have been shown to peak during the pre-monsoon season at Mukteshwar (Hyvärinen et al., 2011). The pre-monsoon season, also known as the "dust-season" in India, brings air masses from the Thar Desert transporting dust to the Himalaya (Gautam et al., 2013). Dust from local sources have also been identified at Mukteshwar during this season (Hyvärinen et al., 2011).

At Durga Kot glacier four snow pits with varying depths were dug at different elevations, while at Bhanolti glacier one snow pit was dug (see table 1 for snow pits and sample details). Snow samples were collected with a metal spatula in Nasco whirl-pak bags, and thereafter brought to the designated base camp where the snow was melted and filtered. Since it was not possible to maintain the crucial frozen chain for the snow samples during transport back to the laboratory this approach of melting in the field was used for the glacier snow samples. The snow was melted gently over a camping stove in

Atmos. Meas. Tech. Discuss., https://doi.org/10.5194/amt-2017-186
Manuscript under review for journal Atmos. Meas. Tech.
Discussion started: 12 July 2017

Atmospheric Measurement Techniques Discussions

protected glassware to avoid contamination. The liquid samples were subsequently filtered through quartz fiber filters (Munktell, 55 mm, grade T 293), in accordance to previous work (e.g. Forsström et al., 2009; Svensson et al., 2013). The dried filters were then transported in petri dishes to the laboratory for analysis (described in section 2.2).

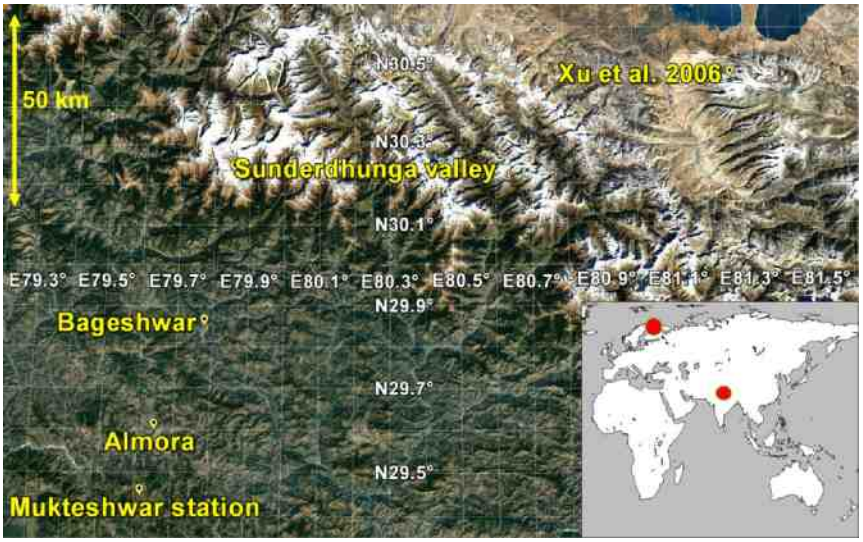

Figure 1. Google earth image of Indian sampling location, with sites discussed in text, as well as an overview map of measurement sites.

2.1.2 Arctic Finland

Snow samples collected in Finland originated from the seasonal snowpack of Sodankylä (N 67º 21' E 26º 37') and Pallas (N 67º 58' E 24º 06') c.f. Figure 1. The Pallas samples were gathered in March and April of 2015 (n=10) from an open mire and in March of 2016 (n=2) from an area above the tree line (in close proximity of the Pallas Global Atmosphere Watch Station). More details of the Pallas sampling area are provided in Svensson et al. (2013) where EC in the snow was previously investigated. The snow sampled was confined to the top layers of the snowpack. The Sodankylä samples (n=15) are from the Finnish Meteorological Institute Arctic Research Center, where weekly surface snow samples (0-5 cm) have been collected since 2009 (first part of time series is presented in Meinander et al., 2013; where details of area are provided). The samples used in this study originate from spring of 2013 and 2014. The snow samples from Pallas and Sodankylä were collected in Nasco whirl-pak bags and stored in a frozen state until filtration. Samples were then melted in a microwave oven at each site's respective

Atmos. Meas. Tech. Discuss., https://doi.org/10.5194/amt-2017-186
Manuscript under review for journal Atmos. Meas. Tech.
Discussion started: 12 July 2017

laboratory, and followed the same filtering procedure described above, according to e.g. Forsström et al. (2009) and Svensson et al. (2013).

2.2 Light-absorbing impurities analysis

To estimate the contribution to the reduction in transmission on the filter sample substrate due to minerals, we compared the light transmission through the filter using the PSAP before and after heating the sample as part of the TOM analysis. Since it is difficult to gravimetrically determine the dust content on quartz filters, we decided to use this combined instrument approach to estimate the dust content. A custom built PSAP (Krecl et al., 2007) was used for the optical measurements, and for the TOM a Sunset Laboratory OCEC-analyzer was used to determine EC. A brief description of the OCEC-analyzer and the PSAP is given below in sections 2.2.1 and 2.2.2, respectively.

The approach of measuring light transmission before and after heat treatment to estimate the different light-absorbing components has been previously used for airborne sampled aerosol (e.g. Hansen et al., 1993). In Hansen et al. (1993), filter samples were optically analyzed before and after being treated in a 600ºC furnace, in which the carbonaceous material was vaporized from the filter. These measurements enabled them to obtain an estimate of the dust content on the filter. Lavanchy et al. (1999) followed a similar optical and thermal approach to determine the BC and dust content of ice core samples. For the EC measurement they used a two-step combustion procedure by Cachier et al. (1989), and in between the thermal treatment they used a modified version of an aethalometer to measure the attenuation of light through the filter. Our experimental method is analogous to that of Lavanchy et al. (1999). However, as a Sunset Lab. OCEC-analyzer and a custom built PSAP were readily available to us, this instrument configuration was used in our study. Because results from this type of analysis may be very instrument specific, a series of laboratory tests (described in section 2.3) were conducted to confirm reliability of the method before ambient snow samples were measured. The analysis procedure for the filters (outlined further in section 2.3) was the same for the laboratory samples and the ambient samples.

2.2.1 Elemental carbon analysis

From a 10 cm^2 filter sample area, separate punches of 1 cm^2 were taken and analyzed for organic carbon (OC) and EC content using a Sunset laboratory OCEC-analyzer (Birch and Cary, 1996) with the EUSAAR_2 analysis protocol (Cavalli et al., 2010). First, in a helium atmosphere, the filter punch is heated at different temperature steps. In this phase OC is volatilized and detected by a flame ionization detector (FID). During the second stage, oxygen is introduced, and EC is released from the filter through combustion. To account for pyrolysis occurring (darkening of the filter) during the first step, a laser (at a 632 nm wavelength) measures the transmittance (or reflectance as an option for newer instruments) continuously of the filter punch, and when the original value of the transmittance is attained during the second step separation between OC and EC is done. The filters EC values reported here (referred to as

Atmos. Meas. Tech. Discuss., https://doi.org/10.5194/amt-2017-186
Manuscript under review for journal Atmos. Meas. Tech.
Discussion started: 12 July 2017

EC_{TOM}) are based on the transmittance correction for pyrolysis since the PSAP operates also on the basis of transmittance through the substrate. An additional EC value provided by the OCEC-analyzer from the analysis is an optical EC ($EC_{optical}$), which is based on the monitored transmittance and absorption coefficients of the OCEC-analyzer. For this study no special consideration was taken for carbon carbonate particles that can be present in the sample (Chow & Watson, 2002). Unless chemically removed before analysis, these particles will contribute to the OC fraction of the total particulate carbon content (e.g. Cavalli et al., 2010).

Uncertainties associated with the TOM method are mainly associated with the inefficiency of the filters to capture the small impurities, uneven filter loading, and loss of particles to filtering containers (Forsström et al., 2013). The artifact from samples with a high fraction of pyrolysis OC (Lim et al., 2014), and the interference of an accurate split point determination from filters containing a high dust load can also be considerable (Wang et al., 2012).

2.2.2 Absorption measurements

The PSAP use a single diode at 526 nm as light source. The light is split by two light pipes which illuminate two areas of 3.1 mm in diameter. The filter substrate is placed over these areas and individual detectors below the filter measure the transmitted light. During normal operations, when measuring BC in air, these two signals are used as sample and reference spots. The reference spot is exposed to particle free air and the sample spot is exposed to particles present in the ambient air. In this experiment both signals are used to measure the change in transmission by comparing the signal before and after the filter has been analyzed using TOM. The signal change is related to the transmission from a particle free filter (filtered using Milli-Q (MQ) water and dried).

The corrections required for the PSAP when used for air sampling is well documented (e.g. Bond et al., 1999; Virkkula et al., 2005), in particular this concerns enhanced absorption from the filter itself through multiple scattering effects from the filter fibers, and particle loading effects (shadowing and reduction in multiple scattering). However, these corrections are essentially uncharacterized for melted snow samples and the quartz fiber filters used. The fiber filters used are substantially thicker compared to what is normally used for PSAP measurements (Pallflex cellulose membrane filter) or the ISSW measurements (Nuclepore filter). Moreover, the filter substrate is very large in terms of surface area compared to the particles sampled. The geometry is very complex and in relation to a particle the substrate is more of a three dimensional web or sponge rather than a flat surface area on a filter. An example of a blank filter sample obtained by a scanning electron microscope is presented in Figure 2. The horizontal scale of 500 mm is for comparison, and the scale of 150 mm is to illustrate the relative thickness of the substrate.

Atmos. Meas. Tech. Discuss., https://doi.org/10.5194/amt-2017-186
Manuscript under review for journal Atmos. Meas. Tech.
Discussion started: 12 July 2017

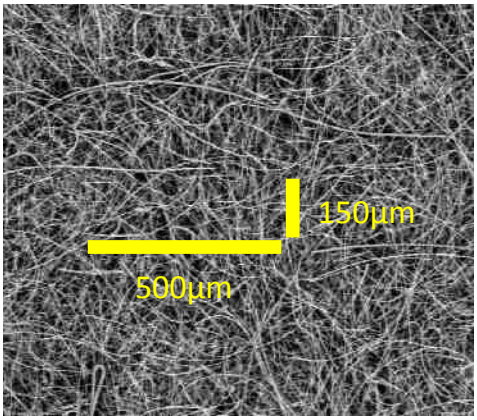

Figure 2. Electron microscope image of a blank quartz fiber filter used in this study.

The basis for the optical attenuation measurements is the exponential attenuation of light as it passes through some medium, often described by the Bouguer-Lambert-Beer-law (Eq. 1).

$$I = I_0\, e^{-\tau}\,, \qquad \text{(Eq. 1)}$$

where I_0 in our case is the light intensity through a clean filter and, I is the light intensity through a sample loaded filter. The exponent τ is the optical depth of LAI on the filter. For our study the multiple scattering absorption enhancement factor of the filter will be treated as a constant, but not given a numerical value. Due to the geometry of the filter, corrections for any enhanced absorption due to co-existing scattering particles, and the loading effect, are not specifically considered. Hence, we will assume a linear relation between the logarithmic change in transmittance (T_r) of a filter and the optical depth (Eq. 2).

$$ln(T_r) = \tau_{TOT}, \text{ (Eq. 2)}$$

where $T_r = \frac{I_0}{I}$ and τ_{TOT} is the combined effect of all light absorbing impurities. Our interest was to estimate the relative contributions of EC (τ_{EC},) and mineral dust (τ_D) particles to measured optical depth according to equation 3.

$$\tau_{TOT} = \tau_{EC} + \tau_D, \text{ (Eq. 3)}$$

From TOM we get the EC mass surface density (µg cm^{-2}). Thus, we can write τ_{EC} as the product of the EC mass surface density on the filter and an effective material specific mass absorption cross section $MAC_{eff,EC}$ of BC that includes the multiple scattering enhancement of the filter. Typically, MAC values are reported in units of m^2 g^{-1}.

Atmos. Meas. Tech. Discuss., https://doi.org/10.5194/amt-2017-186
Manuscript under review for journal Atmos. Meas. Tech.
Discussion started: 12 July 2017

2.3 Laboratory tests

Before initiating analysis of the field samples, a series of laboratory tests using the OCEC-analyzer and the PSAP combination were conducted. For this purpose, the following filter sets were created:

1. A set of filter samples (n=36) with different amounts of BC. Two types of soot (BC) were used and each was mixed (a minute amount of soot not weighed) with MQ water and a small amount of ethanol (to enable mixing of the BC particles in the liquid) in an ultra-sonic bath. One soot type was collected by chimney cleaners in Helsinki, Finland, originating from oil-based combustion, and has been used previously in soot on snow experiments (Svensson et al., 2016). The second type was a product from NIST (National Institute of Standards and Technology), which consists of diesel particle matter from industrial forklifts, NIST-2975. From the BC stock solutions, different amounts of solution were taken out and diluted with additional water for the same total volume of filtrate (ca. 0.5 L liquid). The newly created mixture solution was thereafter filtered using the same filter procedure as the ambient snow samples (described in 2.1.1).
2. The second set of filters (n=16) generated contained mineral dust only. Analogous to the soot mixtures, two types of mineral were used. The first mineral was SiC, Carborundum, mesh nr. 1200, corresponding to particles approximately < 1 µm in diameter. The amount of SiC added to the MQ water was measured using a digital scale (resolution of 10 µg) before filtration. With the known concentration of the mixture, we observed how much of the weighed mineral was deposited on the filter during filtration to estimate losses. By comparing the whole filters before and after filtration gravimetrically, these tests showed that 10 % or less of the mineral was lost during filtering. The second type of mineral consisted of stone crush from a site in Stockholm, Ulriksdal, likely to be mainly granite. A sieve mesh nr. of 400 was used for this material, which corresponds to mineral particles of approximately < 38 µm in diameter. Filters were prepared according to the procedure given above for the other mineral (SiC).
3. The last set of laboratory solutions made contained various mixtures of SiC mineral and chimney soot (n=30). These filters were treated in the same way as described above, with a soot stock solution and a mineral weighed solution being mixed into one solution.

The procedure to analyze all three sets of filters samples was identical. After the filter substrates had dried, one punch (1 cm^2) from the filter was put into the PSAP instrument to measure the transmission across the filter in relation to a blank filter. This punch was taken for analyses of OC and EC content using the OCEC-analyzer. After the TOM, and removal of the carbonaceous particles, this filter punch was again analyzed in the PSAP. Hence, we acquired the transmission through the filter before heating and after heating in comparison to a blank filter. We did tests where the same filter punch was used in the PSAP instrument as well as the OCEC-analyzer, and compared this to twin samples that were used

in separate instruments. Both procedures provided the same result. Furthermore, extensive tests were carried out using blank filters that had been subject to filtering of MQ water and treated the same way as prepared samples and the ambient snow samples. No measurable EC could be detected on these filters. It should be noted that part of the second set of the laboratory filters (stone crush mineral) were analyzed with a different, but identical, PSAP and OCEC-analyzer at a different laboratory (Stockholm University).

3. Results and discussion

3.1 Laboratory samples

The change in optical depth as a function of analyzed EC using our two standard types of BC particles (filter set nr. 1) is shown in Figure 3. Both materials behave optically similar and the slopes are within 15 % of each other, with chimney soot having a slope of 39.8 ± 1.5 $m^2 g^{-1}$ and NIST soot 34.4 ± 1.8 $m^2 g^{-1}$ (fits have been set to a fixed intercept at 0; ± refers to standard error of slope). Previous studies of atmospheric airborne BC aerosol and its MAC with different filter-based absorption photometers are numerous, while reported MAC values for BC in snow are very sparse. The MAC value of BC is dependent of many factors, such as particle size, density, and refractive index, mixing state (i.e. coating), thus many influences on it. Reported airborne BC MAC values are lower than what we found for the two soot standards (which were mixed in liquid solution to simulate similar conditions as for our ambient snow samples). However, the MAC of air sample usually takes into account the multiple-scattering correction factor (C_{ref}). For example for the commonly used aethalometer, its optical depth is divided by a C_{ref} somewhere in the range of 2.8-4.3 (Collaud Coen et al., 2010). If a C_{ref} of 5.2 was considered for our liquid originating BC data, similar MAC values would be found (e.g. Bond et al. (2013) reports freshly-generated BC with a MAC of 7.5 ± 1.2 $m^2 g^{-1}$ at λ = 550 nm). However, for our data set we have chosen not to take any C_{ref} into account as our samples are liquid instead of air based, and currently no C_{ref} exists for liquid samples.

Atmos. Meas. Tech. Discuss., https://doi.org/10.5194/amt-2017-186
Manuscript under review for journal Atmos. Meas. Tech.
Discussion started: 12 July 2017

Atmospheric Measurement Techniques Discussions

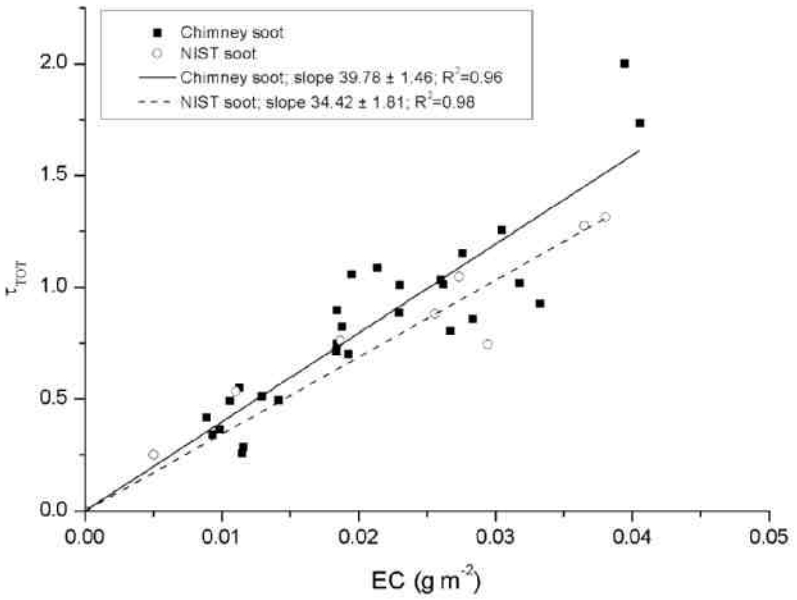

Figure 3. Comparison between the optical depth (at λ=526 nm) by Chimney and NIST soot as function of analyzed EC density by the OCEC-analyzer.

Figure 4 shows the analogous results as in Figure 3, but for the two mineral aerosol solutions (filter set nr. 2). The slope of the optical depth of SiC versus measured SiC amount is more than a factor of one hundred smaller (0.23 ± 0.008 $m^2 g^{-1}$) than the slopes for our BC standards. This is consistent with previously reported results for airborne mineral dust (e.g. Hansen et al., 1993). The stone crush material, an essentially white powder, yielded an even smaller slope of 0.02 ± 0.001 $m^2 g^{-1}$. Clearly, the slopes, or the MAC, for the mineral particles are very composition specific. For a few (n=5) of the mineral aerosol samples the optical depth was measured both before and after TOM. No EC was detected on these samples and no significant difference in τ could be observed before and after heating the sample, as one would expect since no BC was added to these filters.

Atmos. Meas. Tech. Discuss., https://doi.org/10.5194/amt-2017-186
Manuscript under review for journal Atmos. Meas. Tech.
Discussion started: 12 July 2017

Atmospheric Measurement Techniques Discussions

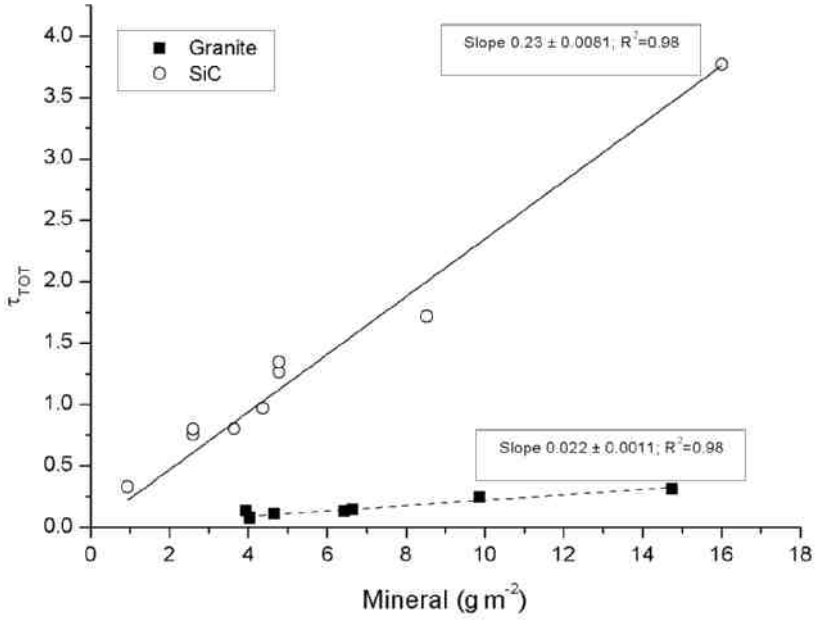

Figure 4. The optical depth as a function of the amount of minerals present on the filter.

From the analysis of chimney and NIST soot (Fig. 3) and SiC and stone crush dust (Fig. 4) the experiments were extended to comprise mixtures of soot and dust. Using the MAC of chimney soot (see Fig. 3), we estimate the EC content of the third set of filters, containing a mixture of SiC and chimney soot. The estimated EC (eEC) is based on the difference between the optical thickness before TOM analysis (τ_{TOT}) and the optical thickness after the analysis (τ_D). eEC is then compared to the amount of EC obtained in TOM, for the same filters. This comparison is presented in Figure 5. The data is rather scattered, but the slope of the linear regression is relatively close (17 %) to 1:1. Hence it shows that EC can be reproduced reasonably well based on the PSAP measurement even for a mixture of BC and minerals.

Atmos. Meas. Tech. Discuss., https://doi.org/10.5194/amt-2017-186
Manuscript under review for journal Atmos. Meas. Tech.
Discussion started: 12 July 2017

Atmospheric Measurement Techniques Discussions

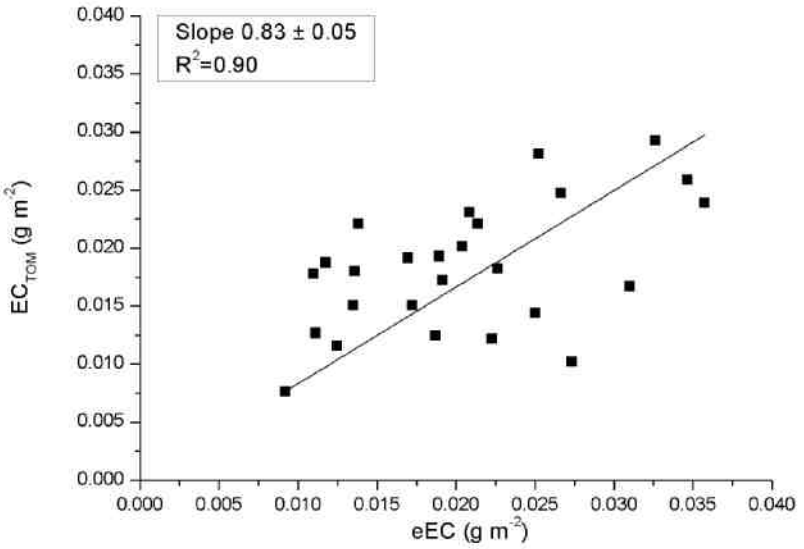

Figure 5. EC amount observed by the TOM (EC_{TOM}) for Chimney soot and SiC mixtures as a function of estimated EC (eEC), using a PSAP optical depth signal before and after heating the filter and using the $MAC_{eff,EC}$ of 39.8 m^2 g^{-1} from Figure 3.

In the context of this work it is further useful to compare our eEC content with the optical EC reported by the OCEC-analyzer. This comparison is presented in Figure 6, again for the third set of filters (Chimney soot+SiC). As observed, the two optically different derived EC amounts show a very consistent relation with nearly a slope of one. The good agreement between the two optically derived EC values suggests that much of the scatter seen in Figure 5 is due to the uncertainty in the analyzed content of EC using TOM (and FID).

Atmos. Meas. Tech. Discuss., https://doi.org/10.5194/amt-2017-186
Manuscript under review for journal Atmos. Meas. Tech.
Discussion started: 12 July 2017

Atmospheric Measurement Techniques Discussions

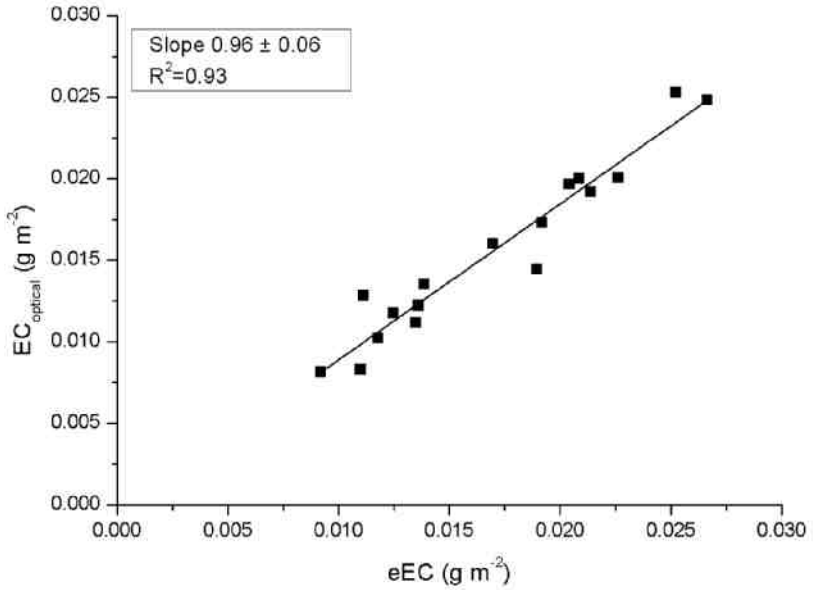

Figure 6. Comparison between the optically reported EC by the OCEC-analyzer and the derived EC surface amount on the substrate (using PSAP data and the relation in Figure 3). The data is for filters containing mixtures of Chimney soot and SiC.

In addition to chimney soot, the mineral SiC is the second absorbing component on the third set of filters. In Figure 7 the optically estimated SiC content, based on the SiC slope in Figure 4 and τ_D is compared to the known weighed amount of SiC before adding it to the liquid. Similarly, as in Figure 5, there is some scatter in the data, but the overall pattern indicates a consistency with a reliable optical measurement. There are two slopes presented, one including all of the data points (slope 1.02), and the second slope (0.88) excluding three data points with weighed SiC amounts exceeding 7.5 g m^{-2}.

Atmos. Meas. Tech. Discuss., https://doi.org/10.5194/amt-2017-186
Manuscript under review for journal Atmos. Meas. Tech.
Discussion started: 12 July 2017

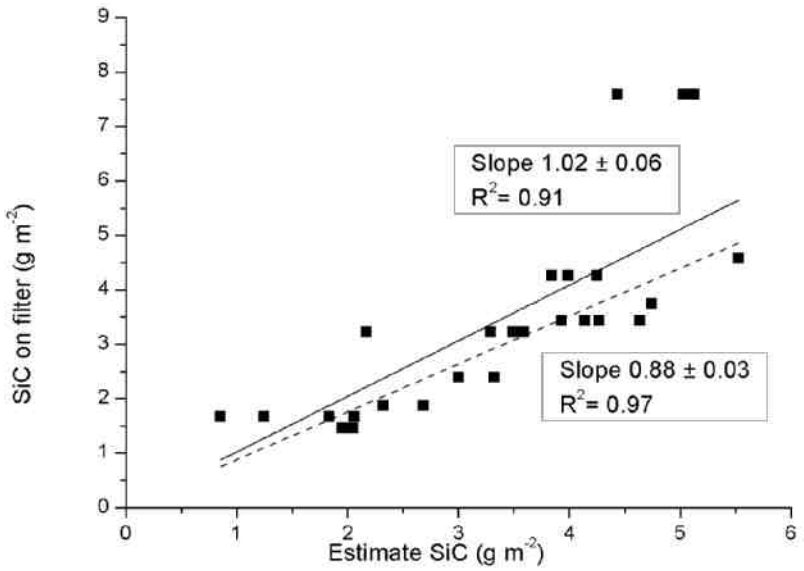

Figure 7. Comparison between the weighed SiC amounts added to the water and the optically derived SiC density on the substrate. The data is for Chimney soot and SiC mixtures, with two alternative slopes; one contain all data points (1.02), and one excluding three data point in the top right of graph (0.88).

Based on the relations established for EC and SiC individually in figures 3 and 4, respectively, it is possible to retrieve their separate concentrations from a mixture based on the change in filter transmission before and after heating the filter. The consistent results from these laboratory tests gives confidence in applying this method on our ambient samples from India and Finland.

3.2 Ambient snow samples

3.2.1 EC in snow

In all of the snow pits from Sunderdhunga a distinct layer with concentrated impurities was observed. These impurity layers always had the highest EC concentrations (exceeding 300 µg L^{-1}) of each pit (Table 1). For some of the samples from Sunderdhunga taken from the impurity concentrated layers, the substrates were actually too loaded with material that quantitative impurity values could not be determined (by not having an initial transmission value). Excluding these heavy impurity layers, the average and median EC concentration for the other snow samples were 141.3 and 101.9 µg L^{-1}, respectively. Surface samples taken above 4900 m a.s.l. had EC concentrations in the range of 13.2-

65.7 µg L^{-1}. Consisting of relatively fresh snow, fallen during the previous days (or weeks), these surface samples LAI content is likely to originate from the post-monsoon season.

Previous studies on BC in snow and ice from the Himalaya have shown seasonal variation. At Mera glacier in Nepal Ginot et al. (2014) showed that BC concentrations peak during the pre-monsoon in a shallow ice core. From the same glacier, Kaspari et al. (2014) observed similar seasonal peaks in BC concentration in snow and firn samples taken above the equilibrium line altitude, where the snow had not undergone any significant summer melt. Noteworthy, dust did not show the same strong seasonality as BC in their studies (Ginot et al., 2014; Kaspari et al., 2014).

Measurements of BC in snow taken closest to Sunderdhunga, reported in the literature, are from about 140 km east-north-east (78º heading), at a higher altitude between 5780-6080 m a.s.l. Gathered in the surface snow of Namunani glacier Xu et al. (2006) reported low EC concentrations in the range of 0.3-9.7 ng g^{-1}. The difference between Sunderdhunga and Namunani can probably be attributed to the difference in sampling altitude and different measurement techniques to determine the EC (Xu et al. used a two-step heating-gas chromatography, similar to method of Lavanchy et al.). The difference could also possibly be explained by the geographical location, with Namunani located on the northern flank of the Himalaya, and it is on the leeward side of the main sources of LAI to the south. Furthermore, it is not explicitly stated in Xu et al. during which season snow samples were collected, which likewise would affect EC concentrations.

For reference in relation to the comparison of the dust signal below in 3.2.2, the EC concentrations in the surface snow from the Finnish Arctic were in the range of 6.2-102 µg L^{-1}. Samples from Pallas had an average and median of 40.0 and 31.0 µg L^{-1}, respectively, whereas the samples from Sodankylä had an average of 23.7 µg L^{-1} and median of 13.1 µg L^{-1}. The higher concentration observed in Pallas is likely because a majority of the samples originated from later in the snow season compared to Sodankylä samples and EC has concentrated in the surface snow later in the season (e.g. Svensson et al., 2013). On a broader scale the concentrations are in the same magnitude as previous measurements of EC in snow (Forsström et al., 2013; Meinander et al., 2013; Svensson et al., 2013)

Our snow samples EC content is further compared in Figure 8, where the estimated EC content based on the optical depth measurement is plotted against the optical EC output from the OCEC-analyzer. The snow data presented in Figure 8 indicate the same relation between the two optical methods as presented in Figure 6 for the standard soot. That is, slopes near 1:1 line, namely 1.19, 1.02, and 1.11 for Sunderdhunga, Pallas, and Sodankylä samples, respectively. Hence, there is a strong consistency between the two optical approaches in the interpretation of the change in τ before and after the substrate has been analyzed with the EUSAAR-2 thermal protocol.

Atmos. Meas. Tech. Discuss., https://doi.org/10.5194/amt-2017-186
Manuscript under review for journal Atmos. Meas. Tech.
Discussion started: 12 July 2017

Atmospheric Measurement Techniques Discussions

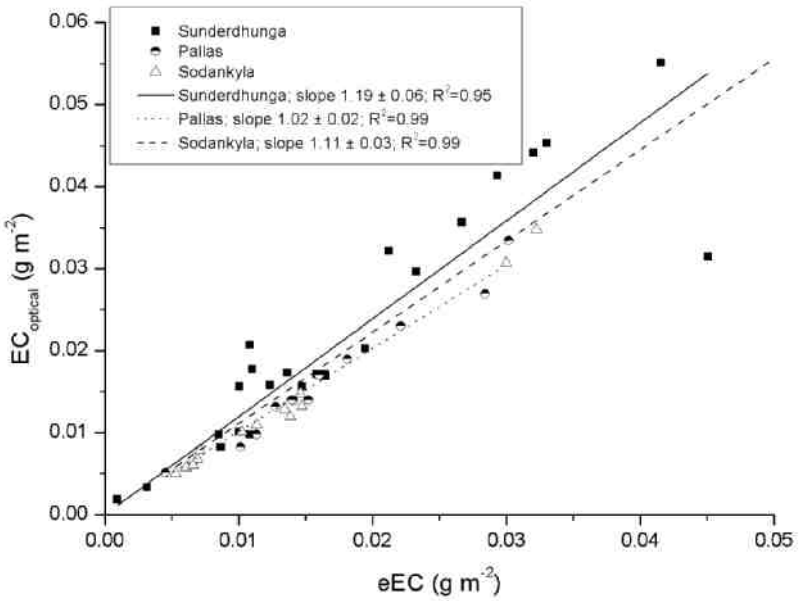

Figure 8. Comparison between the optical EC content given by the OCEC-analyzer and estimated EC (eEC) content using a PSAP and a $MAC_{eff,EC}$ of 39.8 m^2 g^{-1}, for the Arctic and Himalayan samples.

Although the EC content determined by the optical method of the TOM and the eEC content based on the PSAP and a MAC value (Figure 3) agree well, there is a significant difference in the site specific derived MAC values. In Figure 9 the optical depth of EC (τ_{EC}) is plotted as a function of the analyzed EC (with TOM) for all of the snow samples. The slopes for the three sampling sites are 21.0, 21.9 and 17.1 m^2 g^{-1} (Pallas, Sodankylä, and Sunderdhunga, respectively). These values are around half of what the laboratory standard BC tests show (Fig. 3), indicating less absorbing efficiency for the EC particles originating from the snow compared to the laboratory particles. This is unexpected, as any non-EC absorbing material or even scattering particles mixed with EC would tend to increase the MAC value compared to pure BC particles which we would expect to occur for our snow originating EC particles. A consequence of a lower MAC for the snow EC particles could be that the snow albedo reduction caused by the EC is inaccurate since the EC particles have less absorbing efficiency. Schwarz et al. (2013) previously reported a lower MAC value for BC particles in the snow compared to airborne BC particles due to a difference in mean size. The BC particles from the snow were observed to be larger compared to airborne BC particles, explaining the decrease in MAC for the snow originating particles.

The authors further showed how the BC effect in snow albedo reduction is currently overestimated due to the lower MAC for snow BC particles.

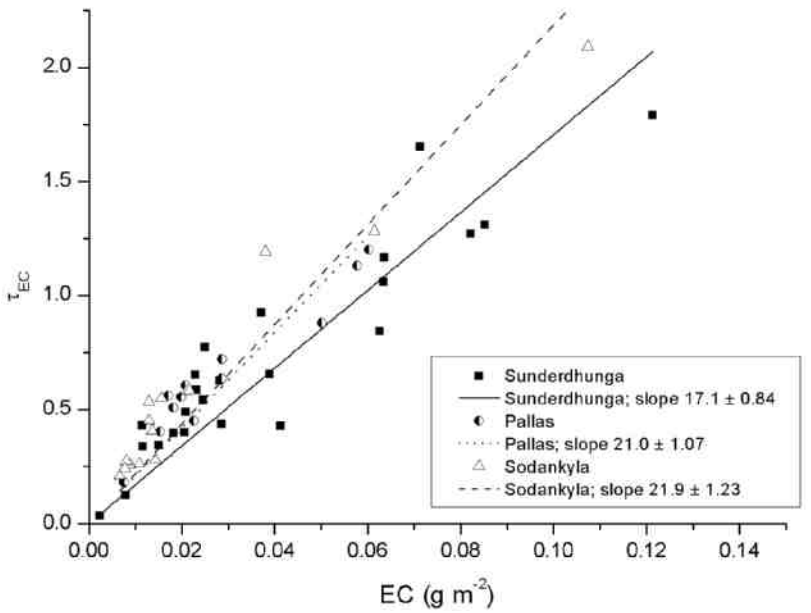

Figure 9. The optical depth τ_{EC} as function of the analyzed EC based on TOM, for the Arctic and Himalayan samples.

In our case, if the laboratory generated BC consist of smaller particles compared to the snow samples this could lead to a larger MAC value for the lab-standards. The size distribution of the BC particles in the filters are unknown to us, but as suggested by the modelled MAC curve, presented in Figure 10, this size dependence can play a role. The modelled MAC for theoretical BC particles demonstrate a decrease in MAC with particle size, particularly for particles larger than about 130 nm. The absorption efficiencies were calculated for λ = 526 nm by using the Mie code of Barber and Hill (1990) and for BC the same complex refractive index of 1.85 - 0.71i that was used by Lack and Cappa (2010) and a particle density of 1.7 g cm^{-3}.

Atmos. Meas. Tech. Discuss., https://doi.org/10.5194/amt-2017-186
Manuscript under review for journal Atmos. Meas. Tech.
Discussion started: 12 July 2017

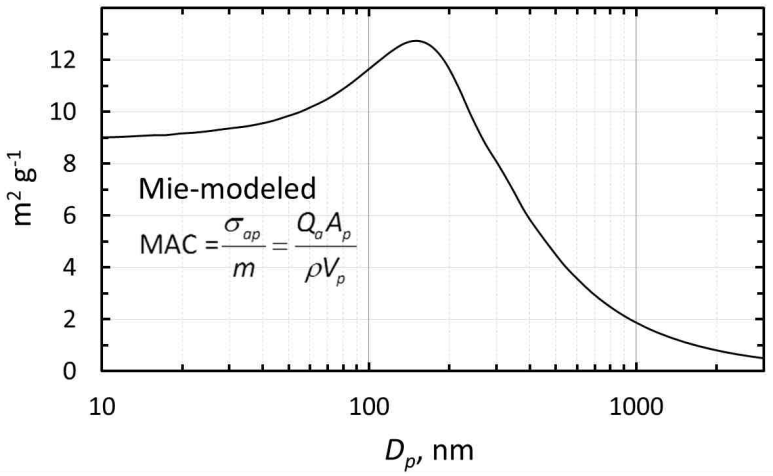

Figure 10. Modeled mass absorption coefficient (MAC) of single BC particles as a function of particle diameter at λ = 526 nm.

Another hypothesis is related to the fact that the samples are liquids and that the matrix is strongly light scattering and rather thick. It is likely that the liquid will embed the particles deeper into the filter than what is typical for air samples (e.g. Chen et al., 2004). In air and on filter surfaces, BC mixed with a scattering medium enhance the absorption. On the samples presented in Table 1, about 90 to 95% of the carbon is water insoluble organic carbon, whereas the laboratory BC were essentially free from OC. This difference could explain the lower MAC for the ambient samples if the net effect of the added OC actually made the BC less efficient absorber in this particular matrix. Further tests are required, however, to confirm this hypothesis.

3.2.2 Dust fraction of LAI in snow

Because the ambient mineral dust MAC value is unknown for our snow samples, it is not applicable to use the SiC or stone crush MAC values to estimate the dust content on the filters. Instead, we use the fraction of minerals (f_D) expressed in percent of the total optical thickness, $\left(\frac{\tau_D}{\tau_{TOT}}\ 100\ \%\right)$ to estimate the mineral aerosol contribution to the filter absorption. In our data set, there is a systematic difference between the two Arctic sites and the Himalaya site (Fig. 11). For Pallas and Sodankylä f_D is typically less than 20 %, whereas for Sunderdhunga f_D is typically much greater than that, with peaking fractions reached at both ca. 35 and 65 %. For the Arctic, the values are broadly in line with previous estimates on the amount of light absorption caused by other LAI than BC, i.e. 30-50 % (e.g. Doherty et al., 2010).

Atmos. Meas. Tech. Discuss., https://doi.org/10.5194/amt-2017-186
Manuscript under review for journal Atmos. Meas. Tech.
Discussion started: 12 July 2017

Studies from the Nepalese Himalaya concluded that dust may be responsible for about 40 % of the snow albedo reduction (Kaspari et al., 2014). Similarly, Qu et al. (2014) observed that the contribution of dust to albedo reduction can reach as high as 56 % on a glacier on the Tibetan plateau. Our dust estimate, as a fraction of the LAI on the filter, shows similar results or an even greater fraction of dust than these previous studies, highlighting the importance of dust (see also Fig. 12A) causing an albedo reduction in this region of the Himalaya.

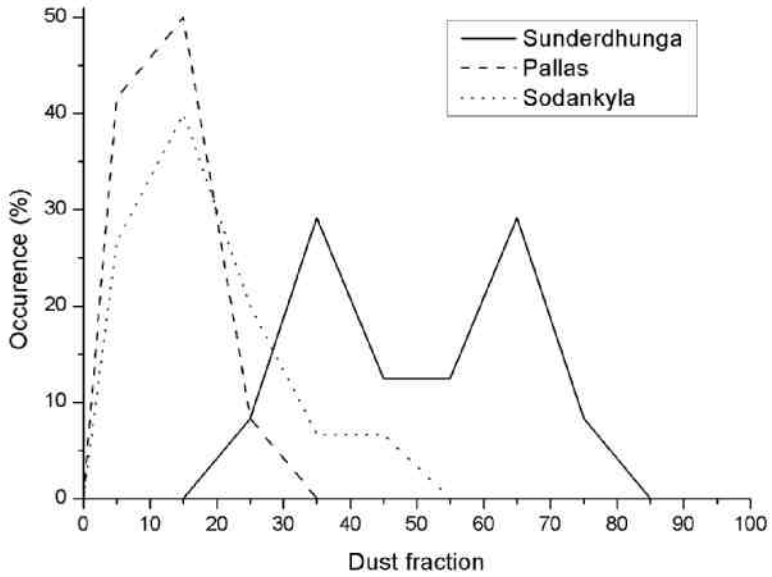

Figure 11. Frequency of occurrence for different derived dust fractions, f_D.

3.2.3 Vertical distribution of LAI in Sunderdhunga

A composite of the vertical profiles from pits C, D, and E are presented for EC and f_D in Figure 12A.

Atmos. Meas. Tech. Discuss., https://doi.org/10.5194/amt-2017-186
Manuscript under review for journal Atmos. Meas. Tech.
Discussion started: 12 July 2017

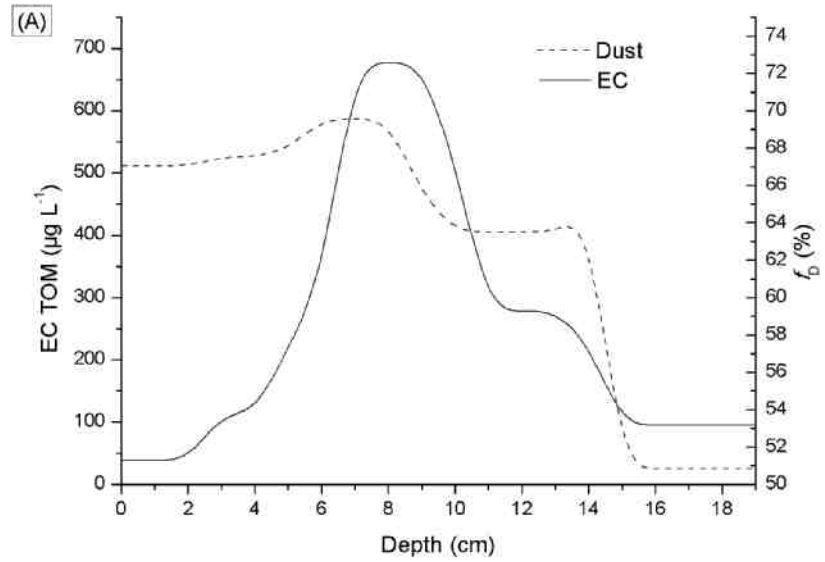

Figure 12. (A) Profile displaying average EC concentration and dust fraction from snow pits C and D (Durga Kot glacier), and snow pit E (Bhanolti glacier); (B) Complete vertical profile E, taken at Bhanolti glacier.

Atmos. Meas. Tech. Discuss., https://doi.org/10.5194/amt-2017-186
Manuscript under review for journal Atmos. Meas. Tech.
Discussion started: 12 July 2017

Atmospheric Measurement Techniques Discussions

The variables plotted in Figure 12B display layers of enhanced amounts of both dust and EC, located between ice layers, and additionally evidently high values at the top of the core above the first ice layer. These layers are interpreted as indicators for seasonal variation at this location, with altering melt and refreezing periods marked by the ice layers. Since the ice layers and the enhancements in LAI are interleaved it suggest that the impurities were deposited on the glacier mainly in-between the melt and refreeze periods. In addition, the melting seems to take place in a relative shallow layer at the surface and does not protrude deeply, which would cause the annual layers to mix. The observed variation in EC and dust values could correspond to the findings of Ginot et al. (2014) and Kaspari et al. (2014) that showed annually peaking BC concentrations in the pre-monsoon in Himalayan ice cores. However, for instance, between the ice layers at ca. 65 and 85 cm, no clear peak is observed in EC or dust values (Fig. 12B), which could either indicate that no peak occurred during that particular year, or an ice layer formed at ca. 65 cm in the middle of the year, similarly as potentially at ca. 105 cm.

The snow pit covers at best ca. five years of snow accumulation which is certainly a too short time period to make any conclusions on a temporal trend of LAI variations at the site. However, an evident increase in LAI is present, especially in the top 20 cm. Due to the time span of the snow pit we cannot know for certain whether this increase presents a short term pollution event or indicates increasing LAI at the site over a longer time period. We have two hypothesis for the observed increase in EC concentrations and the fraction of dust occurring in the top layer of the snow pit. The higher values may be a consequence of increased ambient EC and dust concentrations in the area, causing increased dry and wet deposition fluxes of these impurities to the glacier, even when assuming constant precipitation. Moreover, as it is f_D that increases, the deposition of dust would have had to increase proportionally more than EC and OC. This could be a result from larger areas in the region being free of snow or changes in the wind characteristics (e.g. stronger winds and/or change in direction). On the other hand, local changes in the net snow mass balance due to a larger fraction of the snow being sublimated in the time period covered by the top 20 cm in comparison to the deeper layers, may partly explain the increased EC and dust absorption values at the top of the pit. Both these basic scenarios can be in effect at the same time.

Interestingly, while the EC and OC concentrations and f_D are peaking at the top of the snow pit and potentially decrease very slightly towards the bottom of the snow pit, the absorbing efficiency of EC seems to be decreasing towards the top of the snow pit. We illustrate this in Figure 13 by plotting the ratio between the optical EC from the OCEC-analyzer and the analyzed EC based on TOM, and scale this ratio with the MAC value of 39.8 derived in Figure 3. While the EC concentrations in the snow are the highest at the top of the pit, it appears that at the same time this EC is a less potent light absorber per unit mass (Fig. 13) than in deeper snow layers.

Atmos. Meas. Tech. Discuss., https://doi.org/10.5194/amt-2017-186
Manuscript under review for journal Atmos. Meas. Tech.
Discussion started: 12 July 2017

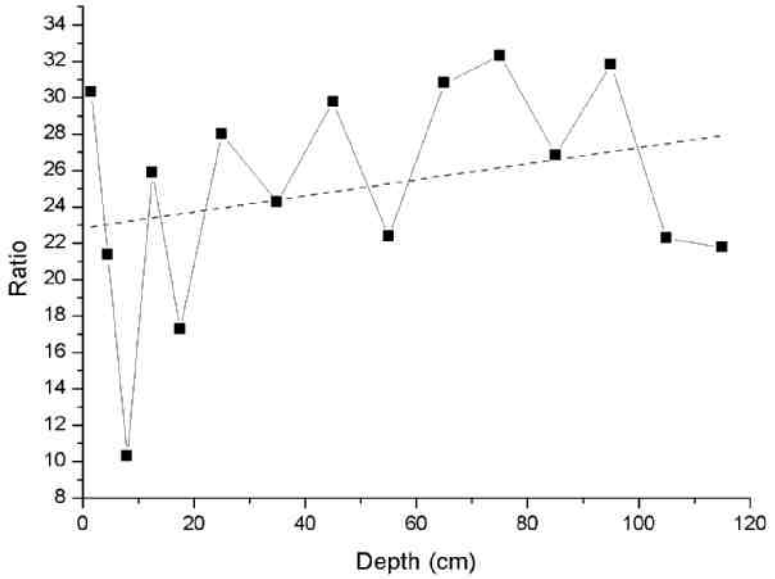

Figure 13. The ratio between the optical EC content and analyzed EC content (TOM method) as measured by the OCEC-analyzer using the EUSAAR-2 thermal protocol. The ratio is scaled by the effective MAC value of 39.78 $m^2 g^{-1}$ derived in Figure 3.

4. Conclusions

Here, first observations of LAI in snow originating from two glaciers in the Indian Himalaya are presented with a method not used widely before to determine LAI in snow. Consisting of a custom built PSAP and an OCEC-analyzer, the attenuation of light is studied on quartz filters, providing estimates on the fraction of light-absorbance caused by non-EC constituents in LAI. Himalayan data display a much greater light-absorbance by dust in the LAI compared to filter samples originating from the seasonal snowpack of Arctic Finland. The role of dust in reducing the snow albedo in this part of Himalayan glaciers needs to be further evaluated, as our results suggest that it might be the dominating LAI in the snow. Our measurements further reveal that the optical properties of EC are different for laboratory generated soot compared to EC originating from snow. With a MAC value off about half of the laboratory EC for the ambient EC particles, it can have potential implications on the snow albedo reduction caused by EC. Over the last approximately five year period in the Himalaya, EC concentrations in the snow are elevated in the top part of the snow pit compared to deeper layers, while at the same time its light absorbing potential is decreasing towards the highest EC-laden layers.

Consequently, additional work on the optical properties of EC in snow are needed to enable more accurate estimates of albedo reduction caused by EC in snow, both spatially and temporally.

Acknowledgments

This work has been supported by the Academy of Finland projects: Absorbing Aerosols and Fate of Indian Glaciers (AAFIG; project number 268004) and Greenhouse gas, aerosol and albedo variations in the changing Arctic" (project number 269095). The Academy of Finland Center of Excellence program (project number 272041), as well as the Nordic research and innovation initiative Cryosphere-Atmosphere Interactions in a Changing Arctic Climate have also supported this work. Jonas Svensson is thankful for the support from Svenska kulturfonden. We would like to thank the providers of the soot Consti Taloteknikka, and Göran Lidén at SU luftlab for the mineral samples. The ACES department at Stockholm University, is part of the Bolin centre for climate research. Finally we would like to thank the participants of the AAFIG 2015 expedition, including Sherpas and guides from Real adventure, for their work during the expedition.

References

AMAP: The Impact of Black Carbon on Arctic Climate. Arctic Monitoring and Assessment Programme (AMAP), Oslo, Norway, 72 pp, 2011.

Aoki, T., Motoyoshi, H., Kodama, Y., Yasunari, T. J., Sugiura, K., and Kobayashi, H.: Atmospheric aerosol deposition on snow surfaces and its effect on albedo. SOLA, 2, 13–16, doi: 10.2151/sola.2006-004, 2006.

Barber, P. W. and Hill, S. C.: Light scattering by particles: Computational methods, World Scientific Publishing, Singapore, 1990.

Birch, M. E., and Cary R. A.: Elemental carbon-based method for monitoring occupational exposures, to particulate diesel exhaust, Aerosol. Sci. Technol., 25, 221– 241, 1996.

Bolch, T., Kulkarni, A., Kääb, A., Huggel, C., Paul, F., Cogley, J. G., Frey, H., Kargel, J. S., Fujita, K., Scheel, M., Bajracharya, S., and Stoffel, M.: The State and Fate of Himalayan Glaciers, Science, 336, 310–314, doi:10.1126/science.1215828, 2012.

Bond, T. C., Anderson, T. L., and Campbell, D.: Calibration and Intercomparison of Filter-Based Measurements of Visible Light Absorption by Aerosols, Aerosol Sci. Technol. 30:582–600, 1999.

Bond, T. C., Doherty, S. J., Fahey, D. W., Forster, P. M., Berntsen, T., DeAngelo, B. J., Flanner, M. G, Ghan, S., Kärcher, B., Koch, D., Kinne, S., Kondo, Y., Quinn, P. K., Sarofim, M. F., Schultz, M. G., Schulz, M., Venkataraman, C., Zhang, H., Zhang, S., Bellouin, N., Guttikunda, S. K., Hopke, P. K., Jacobson, M. Z., Kaiser, J. W., Klimont, Z., Lohmann, U., Schwarz, J. P., Shindell, D., Storelvmo, T., Warren, S. G., and Zender, C.S.: Bounding the role of black carbon in the climate system: A scientific assessment, J. Geophys. Res. Atmos., 188, 5380–5552, doi: 10.1002/jgrd.50171, 2013.

Bond, T., Bhardwaj, E., Dong, R., Jogani, R., Jung, S., Roden, C., Streets, D. G., and Trautmann, N.: Historical emissions of black and organic carbon aerosol from energy-related combustion, 1850–2000, Global Biogeochem. Cy., 21, doi:10.1029/2006GB002840, 2007.

Cachier, H., Bremond, M.P., and Buat-Ménard, P.: Determination of atmospheric soot carbon with a simple thermal method, Tellus Ser.B, 41B, 379-390, 1989.

Cavalli, F., Viana, M., Yttri, K.E., Genberg, J., and Putaud, J-P.: Toward a standardised thermal-optical protocol for measuring atmospheric organic and elemental carbon: the EUSAAR protocol, Atmos. Meas. Tech. 3, 79–89, doi:10.5194/amt-3-79-2010, 2010.

Chen, L.-W. A., Chow, J. C., Watson, J. G., Moosmüller, H., and Arnott, W. P.: Modeling reflectance and transmittance of quartz-fiber filter samples containing elemental carbon particles: Implications for thermal/optical analysis, J. Aerosol Sci., 35, 765–780, 2004.

1 Chow, J. C., & Watson, J. G.: PM2:5 carbonate concentrations at regionally representative Interagency
2 monitoring of protected visual environment sites. J. Geophys. Res., 107(D21), 8344,
3 doi:10.1029/2001JD000574, 2002.
4 Collaud Coen, M., Weingartner, E., Apituley, A., Ceburnis, D., Fierz-Schmidhauser, R., Flentje, H.,
5 Henzing, J. S., Jennings, S. G., Moerman, M., Petzold, A., Schmid, O. and Baltensperger, U.:
6 Minimizing light absorption measurement artifacts of the Aethalometer: evaluation of five correction
7 algorithms, Atmos. Meas. Tech., 3, 457–474, 10.5194/amt-3-457-2010, 2010.
8 Doherty, S. J., Warren, S. G., Grenfell, T. C., Clarke, A. D., and Brandt, R. E.: Light-absorbing
9 impurities in Arctic snow, Atmos. Chem. Phys., 10, 11647–11680, doi: 10.5194/acp-10-11647-2010,
10 2010.
11 Doherty, S. J., D. A. Hegg, J. E. Johnson, P. K. Quinn, J. P. Schwarz, C. Dang, and Warren, S.G.:
12 Causes of variability in light absorption by particles in snow at sites in Idaho and Utah, J. Geophys.
13 Res. Atmos., 121, 4751-4768, doi:10.1002/2015JD024375, 2016.
14 Dumont, M., Brun, E., Picard, G., Michou, M., Libois, Q., Petit, J.-R., Geyer, M., Morin, S., and Josse,
15 B.: Contribution of light-absorbing impurities in snow to Greenland's darkening since 2009, Nat.
16 Geosci., 7, 509–512, doi:10.1038/ngeo2180, 2014.
17 Forsström, S., Ström, J., Pedersen, C. A., Isaksson, E., and Gerland, S.: Elemental carbon distribution
18 in Svalbard snow, J. Geophys. Res. Atmos., 114, D19112, doi:10.1029/2008JD011480, 2009.
19 Forsström, S., Isaksson, E., Skeie, R. B., Ström, J., Pedersen, C. A., Hudson, S. R., Berntsen, T. K.,
20 Lihavainen, H., Godtliebsen, F., and Gerland, S.: Elemental carbon measurements in European Arctic
21 snow packs, J. Geophys. Res. Atmos., 118, 13614–13627, doi:10.1002/2013JD019886, 2013.
22 Gautam R., Hsu, N. C., Lau, W. K.-M., and T. J. Yasunari, T. J.: Satellite observations of desert dust-
23 induced Himalayan snow darkening, Geophys. Res. Lett., 40, 988–993, doi:10.1002/grl.50226, 2013.
24 Gertler, C.G., Puppala, S.P., Panday, A., Stumm, D., Shea, J.: Black carbon and the Himalayan
25 cryosphere: a review. Atmos. Environ. 125, 404–417, doi.org/10.1016/j.atmosenv.2015.08.078, 2016.
26 Ginot, P., Dumont, M., Lim, S., Patris, N., Taupin, J.-D., Wagnon, P., Gilbert, A., Arnaud, Y., Marinoni,
27 A., Bonasoni, P., and Laj, P.: A 10 year record of black carbon and dust from a Mera Peak ice core
28 (Nepal): variability and potential impact on melting of Himalayan glaciers, The Cryosphere, 8, 1479–
29 1496, doi:10.5194/tc-8-1479-2014, 2014.
30 Grenfell, T. C., Doherty, S. J., Clarke, A. D., and Warren, S. G.: Spectrophotometric determination of
31 absorptive impurities in snow, Appl. Opt., 50(14), 2037–2048.
32 Hagler, G. S. W., Bergin, M. H., Smith, E. A., Dibb, J. E., Anderson, C., and Steig, E. J.: Particulate
33 and water-soluble carbon measured in recent snow at Summit, Greenland, Geophys. Res. Lett., 34,
34 L16505, doi:10.1029/2007GL030110, 2007.
35 Hansen, A.D. A., Kapustin, V. N., Kopeikin, V. M., Gillette, D. A., and Bodhaine, B. A.: Optical
36 absorption by aerosol black carbon and dust in a desert region of central Asia, Atmos. Environ., Part ,4,
37 27,4, 2527-2531, 1993
38 Hinds,W. C.: Aerosol Technology,Wiley-interscience, 1999.
39 Hyvärinen, A.-P., Raatikainen, T., Brus, D., Komppula, M., Panwar, T. S., Hooda, R. K., Sharma, V.
40 P., and Lihavainen, H.: Effect of the summer monsoon on aerosols at two measurement stations in
41 Northern India – Part 1: PM and BC concentrations, Atmos. Chem. Phys., 11, 8271-8282,
42 doi:10.5194/acp-11-8271-2011, 2011.
43 Immerzeel, W. W., van Beek, L. P. H., and Bierkens, M. F. P.: Climate Change Will Affect the Asian
44 Water Towers, Science, 328, 1382–1385, doi:10.1126/science.1183188, 2010.
45 Kaspari, S., Painter, T. H., Gysel, M., Skiles, S. M., and Schwikowski, M.: Seasonal and elevational
46 variations of black carbon and dust in snow and ice in the Solu-Khumbu, Nepal and estimated radiative
47 forcings, Atmos. Chem. Phys., 14, 8089–8103, doi:10.5194/acp-14-8089-2014, 2014.
48 Kääb, A., Berthier, E., Nuth, C., Gardelle, J., and Arnaud, Y.: Contrasting patterns of early 21st century
49 glacier mass change in the Himalaya, Nature, 488, 495–498, doi:10.1038/nature11324, 2012.
50 Krecl, P., Ström, J., and Johansson, C.: Carbon content of atmospheric aerosols in a residential area
51 during the wood combustion season in Sweden, Atmos. Environ., 41, 6974–6985, 2007.
52 Lack, D. A. and Cappa, C. D.: Impact of brown and clear carbon on light absorption enhancement,
53 single scatter albedo and absorption wavelength dependence of black carbon, Atmos. Chem. Phys., 10,
54 4207-4220, doi:10.5194/acp-10-4207-2010, 2010.

Lavanchy, V. M. H., Gäggler, H. W., Schotterer, U., Schwikowski, M., and Baltensperger, U.: Historical record of carbonaceous particle concentrations from a European high-alpine glacier (Colle Gnifetti, Switzerland), J. Geophys. Res., 104, 21227–21236, doi:10.1029/1999JD900408, 1999.

Lim, S., Faïn, X., Zanatta, M., Cozic, J., Jaffrezo, J.-L., Ginot, P., and Laj, P.: Refractory black carbon mass concentrations in snow and ice: method evaluation and inter-comparison with elemental carbon measurement, Atmos. Meas. Tech., 7, 3307-3324, doi:10.5194/amt-7-3307-2014.

Lutz, S., Anesio, A.M., Raiswell, R., Edwards, A., Newton, R.J., Gill, F., and Benning, L.G.: The biogeography of red snow microbiomes and their role in melting arctic glaciers. Nat. Commun. 7: 11968, doi: 10.1038/ncomms11968, 2016.

Meinander, O., Kazadzis, S., Arola, A., Riihelä, A., Räisänen, P., Kivi, R., Kontu, A., Kouznetsov, R., Sofiev, M., Svensson, J., Suokanerva, H., Aaltonen, V., Manninen, T., Roujean, J.-L., and Hautecoeur, O.: Spectral albedo of seasonal snow during intensive melt period at Sodankylä, beyond the Arctic Circle, Atmos. Chem. Phys., 13, 3793-3810, doi:10.5194/acp-13-3793-2013, 2013.

McConnell, J. R., Edwards, R., Kok, G. L., Flanner, M. G., Zender, C. S., Saltzman, E. S., Banta, J. R., Pasteris, D. R., Carter, M. M., and Kahl, J. D. W.: 20th century industrial black carbon emissions altered arctic climate forcing, Science, 317, 1381–1384, doi:10.1126/science.1144856, 2007.

Ming, J., Cachier, H., Xiao, C., Qin, D., Kang, S., Hou, S., and Xu, J.: Black carbon record based on a shallow Himalayan ice core and its climatic implications, Atmos. Chem. Phys., 8, 1343– 1352, doi:10.5194/acp-8-1343-2008, 2008.

Ming, J., Xiao, C., Du, Z., and Yang, X.: An Overview of Black Carbon Deposition in High Asia Glaciers and its Impacts on Radiation Balance, Adv.Water Resour., 55, 80–87, 2013.

Ming, J., Wang, Y., Du, Z., Zhang, T., Guo, W., Xiao, C., Xu, X., Ding, M., Zhang, D., and Yang, W.: Widespread albedo decreasing and induced melting of Himalayan snow and ice in the early 21st century. PLoS One 10(6):e0126235. doi:10.1371/journal.pone.0126235, 2015.

Painter, T. H., Barrett, A. P., Landry, C. C., Neff, J. C., Cassidy, M. P., Lawrence, C. R., McBride, K. E., and Farmer, G. L.: Impact of disturbed desert soils on duration of mountain snow cover, Geophys. Res. Lett., 34, L12502, doi:10.1029/2007GL030284, 2007.

Painter, T. H., Skiles, S. M., Deems, J. S., Bryant, A. C., and Landry C.C.: Dust radiative forcing in snow of the Upper Colorado River Basin: 1. A 6 year record of energy balance, radiation, and dust concentrations. Water Resources Research, 48, doi: 10.1029/2012wr011985, 2012.

Qian,Y., Yasunari, T. J., Doherty, S. J., Flanner, M. G., Lau, W. K., Ming, J., Zhang, R.: Light-absorbing particles in snow and ice: measurement and modeling of climatic and hydrological impact. Adv. Atmos. Sci. 32(1),64–91, doi: 10.1007/s00376-014-0010-0, 2015.

Qu, B., Ming, J., Kang, S.-C., Zhang, G.-S., Li, Y.-W., Li, C.-D., Zhao, S.-Y., Ji, Z.-M., and Cao, J.-J.: The decreasing albedo of the Zhadang glacier on western Nyainqentanglha and the role of light-absorbing impurities, Atmos. Chem. Phys., 14, 11117-11128, doi:10.5194/acp-14-11117-2014, 2014.

Ruppel, M. M., Isaksson, E., Ström, J., Beaudon, E., Svensson, J., Pedersen, C. A., and Korhola, A.: Increase in elemental carbon values between 1970 and 2004 observed in a 300-year ice core from Holtedahlfonna (Svalbard), Atmos. Chem. Phys., 14, 11447-11469, doi:10.5194/acp-14-11447-2014, 2014.

Raatikainen, T., Brus, D., Hooda, R. K., Hyvärinen, A.-P., Asmi, E., Sharma, V. P., Arola, A., and Lihavainen, H.: Size-selected black carbon mass distributions and mixing state in polluted and clean environments of northern India, Atmos. Chem. Phys., 17, 371-383, doi:10.5194/acp-17-371-2017, 2017.

Schmitt, C. G., All, J. D., Schwarz, J. P., Arnott, W. P., Cole, R. J., Lapham, E., and Celestian, A.: Measurements of light-absorbing particles on the glaciers in the Cordillera Blanca, Peru, The Cryosphere, 9, 331-340, doi:10.5194/tc-9-331-2015, 2015.

Schwarz, J. P., Doherty, S. J., Li, F., Ruggiero, S. T., Tanner, C. E., Perring, A. E., Gao, R. S., and Fahey, D. W.: Assessing Single Particle Soot Photometer and Integrating Sphere/Integrating Sandwich Spectrophotometer measurement techniques for quantifying black carbon concentration in snow, Atmos. Meas. Tech., 5, 2581–2592, doi:10.5194/amt-5-2581-2012, 2012.

Schwarz, J. P., Gao, R. S., Perring, A. E., Spackman, J. R., and Fahey, D.W.: Black carbon aerosol size in snow, Nat. Sci. Reports, 3, 1356, doi:10.1038/srep01356, 2013.

Shindell, D., Kuylenstierna, J. C. I., Vignati, E., van Dingenen, R., Amann, M., Klimont, Z., Anenberg, S. C., Muller, N., JanssensMaenhout, G., Raes, F., Schwartz, J., Faluvegi, G., Pozzoli, L., Kupiainen,

K., Höglund-Isaksson, L., Emberson, L., Streets, D., Ramanathan, V., Hicks, K., Oanh, N. T. K., Milly, G., Williams, M., Demkine, V., and Fowler, D.: Simultaneously Mitigating Near-Term Climate Change and Improving Human Health and Food Security, Science, 335, 183–189, doi: 10.1126/science.1210026, 2012.

Svensson, J. Ström, J., Hansson, M., Lihavainen, H., and Kerminen, V.-M.: Observed metre scale horizontal variability of elemental carbon in surface snow, Environ. Res. Lett., 8, 034012, doi:10.1088/1748-9326/8/3/034012, 2013.

Svensson J., Virkkula A., Meinander O., Kivekäs N., Hannula H.-R., Järvinen O., Peltoniemi J.I., Gritsevich M., Heikkilä A., Kontu A., Neitola K., Brus D., Dagsson-Waldhauserova P., Anttila K., Vehkamäki M., Hienola A., de Leeuw G. & Lihavainen H. 2016: Soot-doped natural snow and its albedo — results from field experiments. Boreal Env. Res. 21: 481–503.

Thevenon, F., Anselmetti, F. S., Bernasconi, S. M., and Schwikowski, M.: Mineral dust and elemental black carbon records from an Alpine ice core (Colle Gnifetti glacier) over the last millennium, J. Geophys. Res., 114, 102, doi: 10.1029/2008JD011490, 2009.

Virkkula, A., Ahlquist, N. C., Covert, D. S., Arnott,W. P., Sheridan, P. J., Quinn, P. K., and Coffman, D. J. (2005). Modification, Calibration and a Field Test of an Instrument for Measuring Light Absorption by Particles, Aerosol Sci. Technol. 39:68–83.

Warren, S. G., and Wiscombe, W. J.: A model for the spectral albedo of snow. II: Snow containing atmospheric aerosols, J. Atmos. Sci., 37, 2734–2745, 1980.

Wang, M., Xu, B., Zhao, H., Cao, J., Joswiak, D., Wu, G., and Lin, S.: The Influence of Dust on Quantitative Measurements of Black Carbon in Ice and Snow when Using a Thermal Optical Method, Aerosol Sci. Technol., 46, 60–69, doi:10.1080/02786826.2011.605815, 2012.

Xu, B., Yao, T., Liu, X., and Wang, N.: Elemental and organic carbon measurements with a two-step heating-gas chromatography system in snow samples from the Tibetan Plateau, Ann. Glaciol., 43, 257–262, 2006.

Xu, B., Cao, J., Hansen, J., Yao, T., Joswiak, D.R., Wang, N., Wu, G., Wang, M., Zhao, H., Yang, W., Liu, X., and He, J.: Black soot and the survival of Tibetan glaciers. Proc. Nat. Acad. Sci. USA, 106, 22114–22118, doi:10.1073/pnas.0910444106, 2009.

Yang, S., Xu, B., Cao, J., Zender, C. S., and Wang, M.: Climate effect of black carbon aerosol in a Tibetan Plateau glacier, Atmos. Environ., 111, 71–78, doi.org/10.1016/j.atmosenv.2015.03.016 1352-2310, 2015.

Atmos. Meas. Tech. Discuss., https://doi.org/10.5194/amt-2017-186
Manuscript under review for journal Atmos. Meas. Tech.
Discussion started: 12 July 2017

Atmospheric Measurement Techniques Discussions
Open Access
EGU

1 Table 1. Snow pit filter samples from Sunderdhunga 2015. Durga kot glacier snow pits are A-D and Bhanolti glacier snow pit E.

Snow pit ID and elevation (m a.s.l.)	Sample interval (cm)	τTOT	τD	τEC	EC TOM (g m^{-2})	EC optical (g m^{-2})	eEC (g m^{-2})	Total C (g m^{-2})	EC (µg L^{-1})	F_D
A, 4869	0-2	3.94	2.63	1.31	0.09	0.05	0.03	1.75	362.18	66.68
	2-5	-	-	-	0.25	0.00	-	0.25	1010.62	-
	5-10	-	-	-	0.30	0.01	-	11.11	1030.84	-
B, 4921	0-2	0.69	0.26	0.43	0.01	0.01	0.01	0.15	40.33	37.64
	2-6	-	4.79	-	0.13	0.04	-	4.24	398.60	-
C, 4921	0-3	0.29	0.16	0.13	0.01	0.00	0.00	0.21	35.71	56.62
	3-6	1.76	1.32	0.44	0.03	0.02	0.01	1.24	55.15	75.12
	6-9	-	5.19	-	0.15	0.00	-	4.88	1095.79	-
	9-13	2.20	1.35	0.84	0.06	0.03	0.02	0.76	381.63	61.57
D, 4950	0-5	0.11	0.07	0.04	0.00	0.00	0.00	0.06	13.20	66.65
	5-10	-	-	-	0.07	0.01	-	6.70	327.14	-
	10-20	1.37	0.94	0.43	0.04	0.02	0.01	0.64	220.21	68.63
	20-30	1.15	0.66	0.49	0.02	0.02	0.01	0.34	78.58	57.36
E, 5008	0-3	1.81	1.41	0.40	0.02	0.02	0.01	1.27	65.73	77.87
	3-6	3.25	1.97	1.27	0.08	0.04	0.03	1.45	272.57	60.77
	6-10	5.88	4.09	1.79	0.12	0.03	0.05	3.58	607.83	69.55
	10-15	2.94	1.77	1.17	0.06	0.04	0.03	0.97	233.21	60.32
	15-20	0.98	0.32	0.66	0.04	0.02	0.02	0.30	111.42	33.05
	20-30	1.06	0.52	0.54	0.02	0.02	0.01	0.23	140.71	49.15
	30-40	1.04	0.41	0.63	0.03	0.02	0.02	0.21	105.55	39.61
	40-50	1.03	0.38	0.65	0.02	0.02	0.02	0.21	98.15	36.71
	50-60	2.10	1.04	1.06	0.06	0.04	0.03	0.66	269.67	49.53
	60-70	2.75	1.10	1.65	0.07	0.06	0.04	0.49	179.30	39.90
	70-80	1.21	0.44	0.77	0.02	0.02	0.02	0.19	93.00	36.12
	80-90	0.91	0.33	0.59	0.02	0.02	0.01	0.15	72.80	35.81

Atmos. Meas. Tech. Discuss., https://doi.org/10.5194/amt-2017-186
Manuscript under review for journal Atmos. Meas. Tech.
Discussion started: 12 July 2017

Atmospheric Measurement Techniques Discussions

90-100	1.65	0.73	0.92	0.04	0.03	0.02	0.31	143.80	43.95	
100-110	0.57	0.17	0.40	0.02	0.01	0.01	0.15	79.31	29.54	
110-120	0.46	0.12	0.34	0.02	0.01	0.01	0.15	56.91	25.68	

FINNISH METEOROLOGICAL INSTITUTE
Erik Palménin aukio 1
P.O. Box 503
FI-00101 HELSINKI
tel. +358 29 539 1000
WWW.FMI.FI

FINNISH METEOROLOGICAL INSTITUTE
CONTRIBUTIONS No. 140
ISBN 978-952-336-038-9 (paperback)
ISSN 0782-6117
Erweko
Helsinki 2017

ISBN 978-952-336-039-6 (pdf)
Helsinki 2017